REPAIR WORKS FOR UPLIFT AND SEEPAGE CONTROL IN EXISTING CONCRETE DAMS

Fina Report
by

José O. Pedro
Abel T. Mascarenhas
Luís R. Sousa
Luís F. Rodrigues
Henrique S. Silva
António T. Castro

August 1989

United States Army
EUROPEAN RESEARCH OFFICE OF THE U. S. ARMY
London England

CONTRACT NUMBER DAJA 45-87-C-0022

LABORATÓRIO NACIONAL DE ENGENHARIA CIVIL
Lisbon Portugal

UNCLASSIFIED

SECURITY CLASSIFICATION OF THIS PAGE

REPORT DOCUMENTATION PAGE

Form Approved
OMB No 0704 0188
Exp Date Jun 30 1986

1a REPORT SECURITY CLASSIFICATION Unclassified	1b RESTRICTIVE MARKINGS
2a SECURITY CLASSIFICATION AUTHORITY	3 DISTRIBUTION/AVAILABILITY OF REPORT Approved for public release; distribution unlimited.
2b DECLASSIFICATION/DOWNGRADING SCHEDULE	
4 PERFORMING ORGANIZATION REPORT NUMBER(S)	5 MONITORING ORGANIZATION REPORT NUMBER(S) R&D 5513-EN-01
6a NAME OF PERFORMING ORGANIZATION Laboratorio National de Engenharia Civil (LNEC) 6b OFFICE SYMBOL (If applicable)	7a NAME OF MONITORING ORGANIZATION USARDSG(UK)
6c ADDRESS (City, State, and ZIP Code) Av. do Brasil, 101 1799 Lisboa Codex Portugal	7b ADDRESS (City, State, and ZIP Code) Box 65 FPO NY 09510-1500
8a NAME OF FUNDING/SPONSORING ORGANIZATION USAE Waterways Experiment Station 8b OFFICE SYMBOL (If applicable) WES-CW	9 PROCUREMENT INSTRUMENT IDENTIFICATION NUMBER DAJA45-87-C-0022
8c ADDRESS (City, State, and ZIP Code) P.O. Box 631 Vicksburg, MS 39180-0631	10 SOURCE OF FUNDING NUMBERS PROGRAM ELEMENT NO: 61102A PROJECT NO: 1L161102BH57 TASK NO: 01 WORK UNIT ACCESSION NO:

11 TITLE (Include Security Classification)

(U) Repair Works for Uplift and Seepage Control in Existing Concrete Dams

12 PERSONAL AUTHOR(S)
Jose O. Pedro

13a TYPE OF REPORT	13b TIME COVERED	14 DATE OF REPORT (Year, Month, Day)	15 PAGE COUNT
Final	FROM 06/87 TO 08/89		

16 SUPPLEMENTARY NOTATION

17 COSATI CODES			18 SUBJECT TERMS (Continue on reverse if necessary and identify by block number)
FIELD	GROUP	SUB-GROUP	
13	02		

19 ABSTRACT (Continue on reverse if necessary and identify by block number)

ABSTRACT

This report aims at contributing to the study of the problems involved in the control of the deterioration of the rock foundations of concrete dams. The analysis of case histories on deterioration of rock mass and repair works of Portuguese dams is the main objectiv

Three case histories in Portuguese arch dams are presented. For each case the following is referred to: main characteristics of the works and main features of their design; relevant aspects of site studies, namely geological and geotechnical studies, and studies on materials; models and the experimental and numerical methods used in their analysis developed to support design and safety control during operation; main features of the observation system and the most important results observed, with particular reference to the hydromechanical behaviour; detection of abnormal behaviour; main aspects of the repair works; and finally behaviour after repair. The three arch dams have different characteristics, namely as

20 DISTRIBUTION/AVAILABILITY OF ABSTRACT	21 ABSTRACT SECURITY CLASSIFICATION	
☒ UNCLASSIFIED/UNLIMITED ☒ SAME AS RPT ☒ DTIC USERS	Unclassified	
22a NAME OF RESPONSIBLE INDIVIDUAL Jerry C. Comati	22b TELEPHONE (Include Area Code) +441-402-7331	22c OFFICE SYMBOL AMXSN-UK-RD

DD FORM 1473, 84 MAR 83 APR edition may be used until exhausted
All other editions are obsolete

SECURITY CLASSIFICATION OF THIS PAGE

19.ABSTRACT (continued)

regards the geotechnical properties of the foundation, the shape and the year of construction; however, in the three cases similar methods were used in the repair works, particularly by using polymers. Excepting for one case still in progress, satisfactory results were obtained with the repair works carried out in the other two cases.

PREFACE

This report includes part of a study developed at Laboratório Nacional de Engenharia Civil (LNEC, Lisbon, Portugal) and sponsored by the European Research Office of the U.S. Army (contract number DAJA - 87 - C - 0022, Repair Works for Uplift and Seepage Control in Existing Concrete Dams).

Mr. J. Oliveira Pedro conducted the work as principal investigator, being associate investigators Mr. A. Torres Mascarenhas, Mr. L. Ribeiro e Sousa, Mr. L. Fialho Rodrigues, Mr. H. Santos Silva and Mr. A. Tavares de Castro. Mr. Ricardo Oliveira, Deputy Director, represented LNEC on contractual matters.

Mention should be made of some papers prepared for the ISRM Symposium "Rock Mechanics and Power Plants" and for the 3rd Portuguese Meeting on Geotechnics. LNEC research reports were prepared by Mr. H. Santos Silva and Mr. A. Tavares de Castro, as part of their work to obtaining the degree of Assistant Research Officer of LNEC.

ELECTRICIDADE DE PORTUGAL EDP, owner of the structures reported, deserve our best thanks for allowing us to publish the information, for supplying data and for their co-operation.

CONTENTS

REPAIR WORKS FOR UPLIFT AND SEEPAGE CONTROL IN EXISTING CONCRETE DAMS

1. INTRODUCTION

1.1 - Preliminary considerations

1.1.1 - Studies on the deterioration of dams are usually concerned with the accidents and incidents occurring in the dam body and foundation, appurtenant works, downstream slopes of the dam and reservoirs, in the lifetime of the works. In the present report, we are mainly concerned with the deterioration occurring in the rock mass foundation of concrete dams, though the behaviour of whole dam--foundation complex has to be taken into account.

Concrete dams have different structural types (gravity, arch, buttress and multi-arch) and different shapes, each one demanding the contribution of the rock mass foundation in a specific way. We may classify these different cases into two basic ones:

- those corresponding to thick dams, which distribute the loads applied by the structure on a large area of the foundation surface and create relatively small gradients between the water levels, upstream and downstream; and
- those corresponding to thin dams, which concentrate the loads applied by the structure in a small area of the foundation surface and create very large gradients between the water levels, upstream and downstream.

Concrete dams are designed to prevent potential deterioration (accidents and incidents) which are likely to occur in their lifetime. Accidents are associated with violations of the safety requirements for the works, and imply important losses of human lives and property; and incidents are associated with violations of the serviceability requirements for the works, and may bring about a break or a limitation of the exploration conditions and require the execution of repair works.

1.1.2 - Different cases of deterioration of the foundation of concrete dams are reported in the work of the ICOLD Committee on the Deterioration of Dams and Reservoirs (ICOLD 1984). These cases clearly illustrate the relative importance of the deteriorations associated with the rock mass foundation of concrete dams.

Considering the total number of cases of deterioration in concrete dams and their foundations, 28% are due to foundations; and as regards accidents, 83% of the cases are associated with foundations.

Among the deterioration associated with foundation, the hydraulic behaviour (percolation, internal erosion, grouting curtains and other watertight systems, drainage systems, etc.) is responsible for 70% of the cases; the mechanical behaviour (deformation and land subsidence, shear strength, initial state of stress, tensile stress at the upstream toe, strengthening treatment, etc.) is responsible for 25% of the cases; and the remaining cases are associated with deterioration of the foundations of the appurtenant works (ICOLD 1984, Silveira et al. 1984).

Estimates of the probability of occurrence of accidents and incidents in the foundation of concrete dams have been made (Kaloustian 1984). These estimates, considering the period 1900 to 1978 (approximately the same covered by the data assembled by the Committee on the Deterioration of Dams and Reservoirs), indicate 0.24% for the probability of accident and 2.26% for the probability of incident.

Concerning Portuguese concrete dams we have not had to report important accidents up to now. However, mention should be made of some incidents due to external and internal actions.

1.2 - Design and performance criteria

1.2.1 - According to Portuguese practice, the main scenarios of deterioration associated with the rock mass foundation of concrete dams which are usually taken into account in the design, construction and operation of the works are as follows:

- cracking and movements of the rock mass associated with the joint systems and faults, upstream and downstream, as well as possible occurrence of slidings affecting significant volumes of rock under the dam foundation, namely along those joint

systems and faults;

- displacements of the foundation surface, absolute and relative (relative movements of adjacent blocks) which may affect the grout curtains and other watertight systems, conditions of operation of equipment, etc.; and
- seepage through the dam and mainly through the foundation, in order to control the flow of the water and the distribution of the water pressures inside the foundation.

To fulfil the safety and serviceability requirements for the above scenarios, different measures are usually considered (CSOPT 1987).

1.2.2 - At the design stage, estimates of the hydraulic and mechanical behaviour are made for design situations which are expected to involve the different situations likely to occur in the lifetime of the works, related with actions (due to construction, filling and operation of the reservoir and environment conditions) and with structural properties (geometrical, mechanical, hydraulic, thermal, etc.).

For the design situations associated with normal operation conditions the following is required:

- the displacements and stresses in the rock mass near the foundation surface should be relatively small, therefore an approximately elastic behaviour (only small local ruptures) being likely to occur; and
- the seepage conditions through the foundation of the dam should be such that the drained flow would be less than 1 liter per minute and per meter length of the principal drainage gallery along the foundation surface, and the maximum uplift would be about 1/3 to 1/4 of the maximum upstream hydraulic head, at the upstream drainage surface.

For the design situations associated with extreme conditions (one extreme exceptional action or structural property superimposed to operation conditions) the following is required:

- equilibrium should exist in wedges defined by joints and faults of the rock mass near the foundation surface and for which movement is possible; and

- the expected displacements and hydraulic behaviour of the rock mass foundation near the dam-foundation interface should be such that out-of-control seepage of the water is not likely to occur.

1.2.3 - At the construction and operation stages measures are also taken to improve the mechanical and hydraulic properties of dam and foundation materials and to control their evolution in course of time. The following measures have been taken:

- use of concretes with high strength and small permeability, as well as drainage systems (galleries, porous concrete, etc.) near the upstream face of the dam; and
- treatment of the foundation (consolidation and reinforcement, watertightening - use of grout curtains and other watertight systems - and use of drainage systems).

To control the behaviour of dams and their foundations, during and after construction, it is commom practice in Portugal:

- to plan, execute and operate an observation system;
- to perform periodic inspections to the works;
- to perform tests for the characterization of the works; and
- to use quantitative analyses and numerical models.

1.3 - Dams selected for the study

1.3.1 - Dams of the different structural types have been built in Portugal (see Fig.1). Most of them were designed and constructed by Portuguese firms after the 2nd World War (Pedro 1987).

As referred to above, no important accidents have occurred up to now with Portuguese concrete dams. However, some incidents have happened, mainly associated with the rock mass foundations, those of Varosa, Bouçã and Venda Nova dams being among the most important ones.

Varosa and Bouçã dams are of thin double curvature, arch type, the first being a relatively young structure (it was completed in 1976) and the latter being a structure almost forty years old (it was completed in 1955). Venda Nova dam is of arch-gravity type and was completed in 1951.

Fig.1 - Main concrete dams of Portuguese hydraulic schemes.

The incidents in the rock mass foundation of Varosa, Bouçã and Venda Nova dams were detected during their operation period, but in the case of Varosa dam deficient behaviour was observed during the first filling of the reservoir.

In all the three cases malfunctions of the watertight and drainage systems were observed, associated with the development of abnormal uplift and seepage; reservoirs were emptied and repair works were performed in the foundations.

1.3.2 - The cases of Varosa, Bouçã and Venda Nova dams (Fig.2) will be presented in this report. For each case, the following aspects will be reported:

- main features of the design and construction of the works;
- monitoring systems and main results of observation, considering the first filling of the reservoir, the detection of the abnormal behaviour and the control of the repair works;
- evaluation of safety conditions, by means of structural and hydraulic models using physical and numerical techniques;
- description and justification of the repair works; and
- structural and hydraulic behaviour after the repair works.

Fig.2 - Siting of Varosa, Bouçã and Venda Nova dams.

2. VAROSA DAM

2.1 - General characteristics of the dam and foundation

2.1.1 - Varosa dam is sited on the river Varosa, a left bank tributary of river Douro (Fig.2). This dam creates a reservoir with 14.46 million cubic meters of capacity essentially used for power production. The power house is located two kilometers downstream and is equipped with two turbines of 20 MW.

Varosa arch dam (Fig.3) is defined by parabolic arches, its main dimensions being approximately (in meters):

- maximum height above foundation 76
- crest length 213
- crest thickness 3.5
- thickness at the base of the central cantilever 12

The dam is composed of 13 blocks defining parabolic arches; the blocks on the right abutment support a surface spillway. The dam has a span-height ratio of about 2.5 and a volume of concrete of about 81,000 cubic meters.

The dam incorporates a bottom discharge, and a surface spillway (with 1,200 cubic meters per second of maximum discharge capacity).

The designer of the dam was Companhia Hidroeléctrica do Norte de Portugal (CHENOP 1969) with the support of Bureau Stucky (Lausanne, Switzerland).

The construction of the dam extended from the end of 1974 until the middle of 1976 and the first filling of the reservoir occurred between November 1976 and December 1977.

2.1.2 - The basin of the river Varosa, limited in the South by the horst that separates the basins of the rivers Douro and Tagus (Fig. 2), is essentially composed of rock masses of schistous, graywackoid and granitic types.

The region is crossed by some faults, with the general orientation NNE - SSW, but the seismic activity is relatively small (the seismic

Fig.3 - Varosa dam. Geometrical characteristics.

risk map for the Portuguese territory indicates the peak acceleration of 0,07g for a return period of 1,000 years (LNEC 1976).

The reservoir, with the approximate area of 700 thousand square meters, is essentially formed of schistous rocks except in the vicinity of the dam, on the right bank, where granites occur (Fig.4). Only small faults were detected in the area of the reservoir.

The site of the dam, in granitic rocks, was studied by means of boreholes (RODIO 1965) and by observation and tests in galleries (LNEC 1971a). Three different zones were defined in the dam foundation with different degrees of weathering (Fig.4):

- the bottom of the valley and the lower part of the left bank, composed of fresh rock (W_1 according to ISRM classification);
- the upper part of the left bank, composed of slightly weathered rock (W_1 to W_2 according to ISRM classification); and
- the right bank, composed of moderately wheathered rock (W_3 according to ISRM classification).

The rock mass foundation of the dam is crossed by several faults, sets of joints and fractures. The main set of joints and faults, for the three zones above referred to, are indicated in Fig.4. It can be seen that sets of horizontal joints occur mainly in the banks, sets of vertical joints occur through the whole foundation and sets of inclined joints occur mainly in the right bank.

The spacing of the joints is classified as F_3 and F_4 (respectively 0.6 to 0.2 and 0.2 to 0.06 meters, according to the ISRM classification).

2.1.3 - The mechanical properties of the rock mass and of the joints were determined by means of field and laboratory tests.

The following field tests were carried out: deformability tests, by means of large flat jacks (Rocha 1970, Pinto 1983) carried out in the three galleries indicated in Fig.3; wave propagation tests, by the seismic method (LNEC 1971b); and tests on samples of joints taken from the three galleries, with an area of one square meter, to evaluate the

Fig.4 - Varosa dam. Geologic conditions of the reservoir and of the site.

shear strength.

In laboratory, the following tests were carried out: on rock samples to characterize the deformability, uniaxial compression failure strength, the quality index (apparent porosity) and ultrasonic wave propagation.

The main results of the tests to evaluate the mechanical properties of the rock mass and of the joints are summarized in Fig.5. These results show that:

- the deformability of the rock mass in both abutments is about twice the deformability at the bottom of the valley, and the latter is not smaller than that of the concrete (velocity of the longitudinal wave propagation over 2,500 m/s); and
- although the strength of the rock is high, the shear strength along the joints is not so high, namely in the left bank (where low values of apparent cohesion and angles of internal friction with average and minimum values of about 30 and 20 degrees were obtained).

The hydraulic properties of the rock mass were evaluated by means of Lugeon tests performed in lengths of 5 meters along the boreholes used for sampling and treatment, under pressures of 1 MPa.

The main results of tests to evaluated the hydraulic properties are also indicated in Fig.5:

- in the upper part of the figure, the lines of equivalent permeability (taken from the results obtained in the exploration phase) indicate relatively high permeabilities near the surface zone; of the rock mass, particularly in the right bank; and
- in the lower part of the figure, the results of Lugeon tests performed during the foundation treatment (namely the lines of the equivalent permeability and type of flow - Chézi or Darcy laws - and the diagrams of water absorption along boreholes), indicate higher water absorption and a Darcy flow in the right bank, which is more weathered and therefore where the presence of soil mterials is likely to occur in joints and fractures.

Fig.5 - Varosa dam. Main results of mechanical and hydraulic tests conducted during exploration studies and foundation treatment.

2.1.4 - Foundation treatment was made by cement grouting, aiming at improving its mechanical and hydraulic properties (namely along the dam-foundation surface and inside the rock mass until depths from 10 to 20 meters in weathered zones); and at building a grout curtain. This grout curtain was performed from the drainage gallery of the dam, 1/10 inclined to upstream in relation to the vertical and reaching depths from 35 to 60 meters.

The grout pressures ranged from 0.5 MPa to 3 MPa. Deep treatment was initially made, followed by the construction of the grout curtain and finally by the dam-foundation surface treatment (Stucky 1973, TECNASOL 1973).

Fig.6 presents some results of the foundation treatment, namely the weights of grout cement (Stucky 1977). It may be seen that higher weights of cement were grouted under the abutment blocks and also in the bottom of the valley, under blocks 7 and 8, during the construction of the grout curtain.

The total amount of cement grouted into the foundation along 8,500 meters of drill was about 700 tons; about 300 tons were spent only for the construction of the grout curtain, along 3,400 meters of drill, and covering inside the rock foundation an estimated area of 11 thousand square meters.

After the foundation treatment, a drainage system was made, formed of 5 subhorizontal drains in each bank reaching lengths of about 35 meters. However, in the sequence of the first filling of the reservoir which showed high uplift under the blocks of the bottom of the valley, 8 new drains were drilled from the drainage gallery.

2.2 - Monitoring the behaviour

2.2.1 - A monitoring system was installed providing data related with water (hydrostatic pressure, uplift and hydrochemical actions), temperature variations, displacements, movements of joints, strains and seepage. This system has been operated by a team, usually every week, the data being processed in a computer.

First the monitoring system consisted of three plumb-lines with 10 measuring bases, 18 rockmeters, 61 joint meters (electrical and mechanical), 68 strain gauges, 31 electrical thermometers, 27

Fig.6 - Varosa dam. Initial foundation treatment and weights of injected cement.

piezometers, one limnimeter and one air thermograph; subsequently in 1985, it was complemented by means of a geodetical observation network, one rockmeter, 21 mechanical joint meters and 34 piezometers (Fig.7).

2.2.2 - The first filling of the reservoir began in November 1976, and proceeded until December 1977; inspections and analyses of the behaviour having being performed at levels 230 and 240 meters.

In February 1977 (which will be called hereinafter situation 1) with water level (254.5 m), small horizontal displacements were measured in the left bank section corresponding to block 4, and in the central cantilever (block 7); such displacements were more important in the right bank section corresponding to block 10, where movements to downstream and towards the bank itself could be observed (Fig.8). One year later, in January 1978, with the water level (259.8 m) (situation 2) displacements reached higher values (Fig.8). A nearly symmetrical behaviour could be observed, although there is a slight tangential displacement towards the right bank. The same figure presents displacements measured in the foundation with reliefs in the foundation being observed, particularly at the base of the central cantilever upstream and reaching about 5 meters deep.

Fig.9 shows cumulated seepage following the downward direction of banks, for situations 1 and 2. For the latter (at the beginning of 1977 the piezometers had not yet been set into operation) the distribution of uplift along the drainage gallery is presented as well as the corresponding piezometric head percentages - in three upstream-downstream sections.

Drained flows are reduced in both situations. In the situation 2, however, uplifts reach high values in the left bank and particularly in the bottom of the valley where hydraulic head percentages of about 100% are obtained, which extend to downstream with values exceeding 80%

This behaviour revealed that relief in the rock mass produced considerable increase in the hydraulic conductivity of joints.

This situation was improved after the installation of eight drains in the foundation of the central zone (between blocks 5 and 9) in March 1978. Fig.9 shows conditions, before and after construction of

Fig.7 - Varosa dam. Monitoring system.

Fig.8 - Varosa dam. Dam horizontal displacements (plumb-lines) and foundation displacements (rockmeters) during the first filling of the reservoir.

Fig.9 - Varosa dam. Uplift and cumulated seepage into the foundation after the first filling of the reservoir.

the drains, uplifts decreasing in the bottom zone, and obviously seepage increasing there.

2.2.3 - The behaviour of the dam between 1978 and 1987 is shown in Figs.10, 11 and 12, which represent the displacement of the dam and foundation as well as seepage and uplifts in the foundation.

The main actions resulted from water (hydrostatic pressure, uplift and physical-chemical actions) and temperature variations, which are much influenced by the operation of the reservoir comprising important emptying each summer.

As a result of relief the close neighbourhood and of the exposure of the dam to solar radiation, the structure presents higher temperatures on its rightside (Fig.13).

The displacements observed in the structure (Fig.10) follow a regular pattern fully consistent with variations of the main actions (water and temperature). Only the displacements of section 3 (left bank) show a slight progress downstream.

Displacements observed in the foundation with rockmeters (Fig.11) show also a regular trend in conformity with the variation of actions. The largest displacements are observed upstream and occur in the upper five meters of the central zone foundation (section 1) and from five to eight meters in the left bank (section 3). Downstream the observed displacements have small values.

After drainage was improved in 1978, uplifts show a tendency to decreasing at the bottom of the valley (section 1) and keep a regular pattern in the banks (sections 2 and 3) in conformity with variations in actions and relatively high water pressures.

Seepage (overall total and total for each bank) behaves consistently with the variations of actions (Fig.12).

Fig.14 presents the dam-foundation displacements in March 1978 (water level 263.5 m) and in May 1983 (water level 263.8 m). It may be observed that there are no significant permanent displacements and that the behaviour of the dam is nearly symmetrical.

2.2.4 - In April 1983, when water level in the reservoir raised again, seepage in the bottom drains (particularly in block 7) increased to

Fig.10 - Varosa dam. Time evolution of the horizontal displacements, measured by plumb-lines.

Fig.11 - Varosa dam. Time evolution of the displacements measured by rockmeters.

Fig.12 - Varosa dam. Time evolution of uplift and seepage into the foundation.

Fig.13 - Varosa dam. Isothermals (°C) at surfaces 1 m deep from the faces, in winter (February) and in early summer (May).

Fig.14 - Varosa dam. Horizontal displacements of the dam (plumb-lines) and displacements in foundation (rockmeters) in 1978 and 1983.

never before recorded values (Fig.12); these values tend to increase with the reservoir stabilized at the highest levels.

Nevertheless there is no significant change in the uplift behaviour as compared to that precedingly observed.

Fig.15 presents uplifts and seepage recorded on May 2nd, 1983, with the water level (263.8 m) and ten days later with the water level (260.2 m).

The decrease of 3.6 meters in the water level produced a reduction of seepage and a small reduction of uplift. In all the other monitoring apparatus, no significant changes were detected.

The water pressure relief at the bottom of the valley (section 1, Fig.15) is associated with the increase of hydraulic conductivity also observed.

Tests for the determination of the percolation conditions were conducted in the bottom drains. As can be seen (Fig.16), the highest hydraulic conductivities were recorded in the foundation of block 7, near the dam-foundation interface.

Chemical analyses for checking the quality of drained water indicated low contents of salts incorporated along the seepage paths, which varied in inverse relation to the corresponding rates of flow. This reveals that the highest values of seepage correspond to waters travelling only a short distance within the rock mass and at high percolation velocity.

The tests above indicated make it possible to identify the deteriorated zones of the foundation as well as the phenomena therein associated. The hydraulic behaviour deteriorates due to the setting up of tensile stresses at the upstream base, which brought about the opening of the most superficial system of joints and the corresponding disorders in the grout curtain. The most affected zones could mainly be found in the foundation of the central blocks along an upstream stretch less than one meter deep.

Owing to this situation, the decision was taken to carry out works for improving the hydromechanical conditions of the dam foundation.

Fig.15 - Varosa dam. Uplift and cumulated seepage observed in 1983 increase.

Fig.16 - Varosa dam. Hydraulic inspection inside drainage boreholes.

2.3 - Model analysis

2.3.1 - The design of the dam was based on analysis by the trial-load method (CHENOP 1969). Later on, at the repair works design stage, further analyses by the trial-load method were developed by the owner (EDP 1983).

The trial-load analyses essentially differ in the number of components of deformation fitting the arches and cantilevers (three in the initial analysis and five in the more recent ones), besides the use of different meshes (at the EDP analysis five arches and ten cantilevers were used).

The main design assumptions were as follows:

- Moduli of elasticity and Poisson's ratios in concrete and in foundation: E_c = 20 GPa, E_r = 10 GPa, and $\nu_c = \nu_r = 0.22$.
- Actions considered, namely: i) dead weight of concrete (W), assuming independent cantilevers and 24.5 KN per cubic meter for the unit specific weight of concrete; ii) hydrostatic pressure (HP), for water levels (265), (260), (250) and (240) respectively HP (0), HP (5), HP (15) and HP (25); iii) uplift (UP), evaluated through a triangular diagram whose upstream value equals water load; iv) temperature variations for cold season (DT) or hot season (UT), the temperature variations inside the concrete being estimated from the air temperatures (mean annual value of 14.5°C, and amplitude of 19°C) and from water temperatures (equal to air temperature variation at the surface and decaying with depth) and assuming a diffusivity coefficient of 0.094 m^2/day for concrete; and v) earthquake (S), with a uniform 0.1g acceleration, a pseudo-static approach being used.

Nine different load combinations were considered, as follows: W + UT; HP(0); HP(0) + UP; W + HP(0) + UP; W + HP(0) + UP + S; W + HP(5) + UP; W + HP(15) + UP; W + HP(25) + UP; W + HP(0) + UP + DT. These design situations are associated with: emptying of reservoir by hot summer; water effects due to hydrostatic pressure and uplift; winter, spring and autumn conditions; and filling of reservoir.

2.3.2 - The analytical studies developed at the design stage were

2.3.2 - The analytical studies developed at the design stage were supported by tests of three-dimensional plaster-diatomite models, carried out at LNEC (1971c).

The models were built in a scale of 1/200. The foundation was reproduced to a depth through suitable, and its deformability was simulated in the models by removing foundation material through a set of boreholes (Fig.17).

The effects of the water pressure at the levels already mentioned were analysed, the water pressure being simulated by means of mercury. Displacements were measured by 0.001 mm deflectometers, installed in such a way that their rods were normal to the model surface, at the measuring points; and strains were measured by strain gauges, glued on both faces. Principal stresses were determined on basis of the principal strains (the elastic constants of the model material having been determined on prisms).

Displacements and stresses as determined by the model tests, due to the water pressure at elevation (265 m) are shown in Figs.18 and 19; values therein presented are the mean of the values obtained with two different models.

Fig.20 shows the principal stresses along the dam-foundation interface under the dead weight and hydrostatic pressure at elevation (265 m). It may be observed that the tensile stresses are not very high, both in the upstream face (at the insertion of the arch into the foundation) and in the downstream face (at points of the central zone of the arch and of the insertion of the arch into the socket).

2.3.3 - Finite element models, developed by LNEC (Pedro et al.1984) and by EDP (1983), were also used for the design of the repair works. The main assumptions of these models were:

- they consider the actions of the dead weight of concrete, water loads and temperature variations;
- dam elastically supported by the foundation following the Vogt coefficient technique (USBR 1956), LNEC's one being a shell model (Fig.21) whereas the EDP's model used a three-dimensional mesh of isoparametric elements;
- linear elastic behaviour of dam and foundation (both homogeneous

Fig.17 - Varosa dam. Upstream face of 3D scale model.

Fig.18 - Varosa dam. Radial displacements of the upstream face due to hydrostatic pressure at level 265 m.

Fig.19 - Varosa dam. Principal stresses at the faces due to hydrostatic pressure at level 265 m.

Fig.20 - Varosa dam. Principal stresses along the dam-foundation interface due to dead weight and hydrostatic pressure.

Fig.21 - Varosa dam. Division into shell finite elements and model of temperature actions.

and isotropic), the elastic characteristics being identical to those adopted in design;

- dead weight simulated in the LDP's model in accordance with stages of concreting of the dam, eleven successive stages having been considered with variable characteristics along the sequence of the process.

In the analysis of the construction sequence opening and closure of joints are indicated for each stage by comparing pairs of points that are connected in closing conditions.

In the model developed by LNEC, temperature variations were analysed; air and water temperature variations were represented by harmonic functions for a one-year period as shown in Fig.21.

Some typical results are given below.

- Dead weight of concrete

The joint movements (opening and closing) were computed along the construction sequence. As a rule it was found that the joints are closed in the upper zone of the dam, excepting for those nearer to the central zone. Some are closed in their total extent; in general, however, the lower part remains open.

Fig.22 shows cantilever stresses at the base of the central blocks (6, 7 and 8) in the course of the construction sequence, which are in satisfactory agreement with the assumption of independent cantilevers.

- Water loads and temperature variations

As concerns displacements, Fig.23 illustrates the values obtained respectively for the tangential, radial and vertical components at the crown of the crest and at the base of the central cantilever, for which the influence of each elementary action is indicated. Of note are the great influence of temperature variations over displacements when compared with that of water pressure at maximum reservoir level and the contribution of uplift for vertical displacements.

Fig.24 presents cantilever stresses at the upstream and downstream faces and mean shear stresses through the thickness of the base of the central cantilever, due to water loads, temperature variations and dead weight of concrete.

Fig. 22 - Varosa dam. Cantilever stresses due to dead weight at the base of the central blocks.

Fig.23 - Varosa dam. Displacements for water and temperature actions.

Fig.24 - Varosa dam. Cantilever stresses at the base of the central cantilever.

2.3.4 - For the LNEC's finite element model above referred to, different comparisons between computed and observed data were made. Some results are presented below.

In order to analyse the effects of the variation of the water level two pairs of observation dates were considered, which correspond to sudden variations of water level associated with small temperature variations:

- the first pair (November 30th and December 14th, 1978), representing an increase of the water level (from 233.6 to 260 m); and
- the second pair (April 25th and May 15th, 1979), representing a decrease of the water level (from 263.4 to 238.7 m).

The small thermal variations were considered through the corresponding linear equivalent distribution (mean temperature and mean gradient), together with the difference between the real distribution and the linear equivalent distribution.

Fig.25 shows good agreement between stresses at the central cantilever as computed by finite elements and determined from the observation (quantitative interpretation analysis); it may be seen that although the temperature changes were small, their influence on stresses cannot be disregarded.

Displacements were also observed at the three blocks close to those indicated above for stresses; they agree with displacements computed by finite elements, as shown in Fig.26 for the central cantilever.

In order to analyse the effects of periodic temperature variations (Fig.21) the best fit of the observed annual air and water waves by harmonic functions with a one-year period was first considered. These waves cause also harmonic temperature variations into the body of the dam determined by Fourier's equation (Pedro et al. 1984) and these temperature variations give origin to displacements and stresses also with harmonic variations, determined by the finite element model. The results obtained at the central cantilever are represented in Fig.27, for radial displacements, and in Fig.28 for hoop and cantilever stresses; a good agreement was obtained, by comparing the functions computed with those derived from the observed displacements and

Fig.25 - Varosa dam. Hoop and cantilever stresses at central cantilever due to variations of the water level.

Fig. 26 - Varosa dam. Radial displacements due to variations of water level.

Fig.27 - Varosa dam. Radial displacements due to annual thermal waves.

Fig.28 - Varosa dam. Hoop and cantilever stresses due to annual thermal waves.

strains.

2.3.5 - The assessment of the stability conditions of the dam foundation was based on the LNEC model above referred to, previously calibrated for normal operation conditions of the dam.

Scenarios of failure along discontinuity surfaces of the rock mass in the neighbourhood of the insertion of the dam were considered (LNEC 1984a). In the stability analyses for these scenarios, the stress distributions on the foundation surface determined by elastic analyses were initially considered (Fig.29). This figure presents normal and shear forces ($N'_{y'}$, $T'_{xy'}$, T'_{yz}) in the neighbourhood of the insertion surface, due to dead weight and hydrostatic pressure for water level (265 m).

Concerning the stresses installed by the construction of the dam, the simplifying assumption which consists in applying the concrete dead weight simultaneously throughout the structure, supposed to be continuous, was adopted. This assumption led to an evaluation by default of the stabilizing action of the dead weight at the base of the highest cantilevers.

Concerning water actions, the hydrostatic pressure on the upstream face and the uplift were considered. The uplift is important for stability analyses though it only produces small stresses in sections of the dam near to the insertion surface.

Concerning seasonal temperature variations, they induce tensile and compressive compensated forces at the dam-foundation interface with a roughly harmonic variation over the year. Important normal tensile forces in the central block will develop due to cooling in the cold season; however, in stability analyses, temperature variations were not taken into account, since a very unfavorable assumption had been adopted for assessing the structural effects of dead weight.

Fig.29 shows that: i) three zones can be distinguished, namely the two banks (with shear forces T'_{xy} directed to upper elevations and large compression forces N'_{y}), and the central zone (with nearly linear forces T'_{xy}, anti-symmetrical, and reduced forces N'_{y}); ii) there is an asymmetry of behaviour due to the spillway in the right bank; iii) forces T'_{yz} have nearly symmetrical distributions, the

Fig.29 - Varosa dam. Normal and shear forces near the dam-foundation interface due to dead weight, hydrostatic pressure and uplift (water at level 265 m).

highest values being found in the central zone.

In accordance with the computed stresses local failures should be expected in the bottom of the valley, given the existence of several sets of joints in this zone, mainly set H_1 (Fig.4), subhorizontal. However, the stability analysis on rigid wedges, defined by the joint sets in the abutments, indicated that no instability should occur.

As the studies carried out evidenced the possibility of local failures in the rock mass near the base of the dam, it was sought to investigate how this scenario of local failures might evolve, in order to be sure that it would not degenerate into scenarios of overall failure. The point was whether the rock mass would be able to redistribute stresses without producing further tensile or compression forces that would overcome strengths. A non-linear model was thus considered, able to represent extension and shear failures of rock wedges in the neighbourhood of the dam-foundation interface, through a joint with adequate characteristics of deformability and strength.

The main scenarios of potential failure were as follows: i) in the left bank, wedges defined by horizontal joints (H_1), vertical plane tangent to the upstream surface and vertical fault or radial vertical joints (V_1); ii) in the bottom of valley and deep zone of the right bank, wedges defined by joints H_1, vertical plane tangent to the upstream surface, and vertical faults; and iii) in the remaining of right bank, including spillway, wedges with high angles of shear since horizontal joints are not present.

The resistant characteristics of the foundation zones above referred to are indicated in Fig.30. Since it was not likely that the most unfavorable conditions would occur simultaneously in the three zones, four different hypotheses were adopted (LNEC 1984a); for one of these hypothesis Fig.31 presents the distributions of stresses in sections of the dam-foundation interface. The calculations made lead to the following conclusions:

- The horizontal joints open in the vicinity of the dam-foundation interface, along a considerable extent; however, the maximum compressive and shear stresses remain within acceptable limits.

Fig.30 - Varosa dam. Resistant characteristics of the foundation zones.

Fig.31 - Varosa dam. Stresses distributions in cross-sections of the dam-foundation interface.

- For all the assumptions studied as regards jointing surfaces, equilibrium is possible.
- Assuming that movements are possible on the planes tangent to the dam-foundation interface, displacements are obtained in that interface with significant vertical components, similar to those observed in the dam.

2.4 - Repair Works

2.4.1 - Repair works were carried out in 1984 and 1985; they mainly consisted of the consolidation of the foundation rock mass, in the left bank, and its watertightening in the bottom of the valley.

Cement grouting was used for the consolidation of the left bank. The work was made along boreholes directed to the foundation of the dam and drilled from downstream (Fig.32), in accordance with the following general criteria: packer grouting by 5 - meter stages, the maximum grout pressure in each stage depending on the minimum overlay; grouting proceeded following zones at increasing elevations and following profiles also of increasing order; water level in the reservoir did not exceed 250 m; before consolidation grouting, a set of anchorages was applied (about 60 m long, subhorizontal, sealed in the last 45 m, with a small load in their initial 15 m).

The use of anchorages was intended to prevent possible displacements of the rock blocks. Subsequently concrete surfacing and retaining walls were built.

Although there was no evidence of defective behaviour in the right bank, it was decided to clean out the slope surface and consolidate it, taking advantage of the presence of technicians and equipment on site.

Works for improving the watertightness of the foundation rock mass were carried out in the bottom of the valley, between blocks 3 and 10, including the zones where abnormalities in the hydraulic behaviour had been detected.

Grouting of acryclic resin was also carried out in four holes drilled in the foundation of block 11, in order to improve watertightness in that zone, owing to increasing weathering and alteration

Fig.32 - Varosa dam. Consolidation works of the left bank.

of the rock mass there. The resin was grouted in holes 1.5 meters apart, down to the depth of 10 meters, the holes being drilled between the earlier grout curtain and an upstream cut-off curtain formed of cement grout (Fig.33). These cut-off curtain was meant to avoid escape of acrylic resin to upstream through the rock mass joints, a measure that was justified on account of the high cost of resin and its low viscosity.

Grouting of the cut-off curtain was done with the reservoir water level below 220 m (which corresponds to less than 40% of the maximum hydrostatic pressure at the base of the central cantilever). On the contrary, acrylic resin grouting was carried out with high water levels in the reservoir (about 80% of the maximum hydrostatic pressure at the base of the central cantilever), in order to relief the rock mass at the base of the dam and to improve its capacity to being injected.

Highest grout absorption occurred in the upper zones of the foundation, near the dam-foundation interface. Between blocks 5 and 9, absorption in the foundation generally exceeded one hundred liters of resin per linear meter of hole. A total of 19,300 liters of resin were injected, as shown in Fig.33.

The acrylic resin is a hydrogel (Siprogel 110/25 - Rhone Poulenc) that results from the polymerization of two basic components in presence of water, the time of reaction being controlled through the volume variation of a catalyser. This resin has high deformability and ability to swell in presence of water and to shrink failing it; therefore, it is particularly suitable for adjusting itself and filling the voids of the rock mass at every moment, making the rock mass impervious.

2.4.2 - Further to the works above referred to, drainage was improved in the foundation of the dam and in the left bank slope. In the foundation of the dam, 19 aditional drains were drilled (the total number increased to 38, which corresponded to 3.5 drains in average per block in general, and 4.4 drains per block in the central zone).

Holes used for resin grouting (a total of 74) were not capped later, so that they may serve as regulators of the hypometric variations of the resin induced by changes in the state of stress of

Fig.33 - Varosa dam. Treatment of the foundation.

the foundation rock mass.

2.5 - Behaviour after repair

2.5.1 - As already said, repair works were performed in the course of 1984 and early in 1985.

After the upstream retaining curtain was constructed, improvement of the rock mass watertightness was already noticeable during the rise of the water level in the reservoir to levels not exceding (250 m).

Later the acrylic resin grouting brought about a striking reduction of water percolation and thus of uplift and drained seepage.

As can be seen in Fig.12, seepage through the foundation was drastically reduced at the end of this phase, and the same occurred with uplift, particularly in the bottom of the valley.

Fig.34 shows the cumulated seepage along the drainage gallery and the uplift observed after the repair works. Whereas at the bottom, uplift was strongly reduced at the left bank (section 3) there still remain significant hydraulic heads although less than 30% for high levels of hydrostatic pressure; and at the right bank (section 2), uplift seems to be influenced by with rainwater infiltration.

The analysis of results obtained with rockmeters (Figs.11 and 35) indicates that displacements in the foundation have a narrower range of variation after grouting, particularly in the bottom of the valley. This points to a decrease of the rock mass deformability due to cement-filling of joints.

2.5.2 - As concerns the behaviour of the structure, the apparent decrease of the foundation deformability seems to have slightly reduced the amplitude of rotation at the base of the dam. This fact, already detected by rockmeters, seems to occur also with radial horizontal displacements observed by means of plumb-lines (Figs. 10 and 35).

Displacements along the joints of the dam (particularly opening and closing movements) are very small, as a rule less than 0.1 millimeter near the base, than 0.3 millimeter at the crest in the central zone, and than 0.5 millimeter at the crest in the abutments.

Fig.34 - Varosa dam. Uplift and cumulated seepage after treatment of the foundation.

Fig. 35 - Varosa dam. Horizontal displacements of the dam (plumb-lines) and displacements in the foundation (rockmeters) after treatment works.

It is difficult to detect short-term tendencies with so small values; however, there seems to be a very slight restraint in the amplitude of these movements.

2.5.3 - Geophysical tests of the foundation (LNEC 1986) were carried out by measuring the velocity of propagation of elastic longitudinal waves (LV) along and between boreholes; in laboratory ultrasonic propagation tests were made on core samples (VV).

Results obtained (Fig.36) led to the following conclusions: i) in general the foundation rock mass has good mechanical properties with LV > 3,000 m/s and velocity ratios (LV/VV) exceeding 0.6; ii) in the right bank, one finds a wider range of propagation levels than in the left bank owing to larger heterogeneity; and iii) at the bottom of the valley the rock mass is more homogeneous, with LV > 5,000 m/s and LV/VV about 1, which points to sound rock mass with low degree of jointing.

Fig.36 - Varosa dam. Seismic longitudinal wave velocities in the foundation after treatment works.

3. BOUÇÃ DAM

3.1 - General characteristics of the dam and foundation

3.1.1 - Bouçã dam was built in the river Zêzere, in the central region of Portugal (Fig.2); it is a thin double curvature arch dam (Fig.37), with a concrete volume of 70,000 cubic meters and the following main dimensions (in meters):

- maximum height above foundation 70
- crest length 171
- crest thickness 0.9
- thickness at the base of the central cantilever 7.5
- maximum thickness at the socket base 13.5

The hydraulic scheme, integrated in a system including others dams upstream and downstream, is mainly intended for power production. The capacity of the reservoir is 49 million cubic meters, and the power station, equipped with two 28 MW sets, is located in the right bank.

The dam is provided with a overflow spillway which develops in two levels, without gates and can discharge more than 2,200 m^3/s, as well as with a bottom outlet (through a tunnel in the right bank) designed for a discharge of 200 m^3/s.

3.1.2 - The river basin of Zêzere, which is a right bank tributary of the river Tagus, lies in the Central Iberian paleogeographic zone that consists of Paleozoic and Precambrian rock formations.

Precambrian formations consist mainly of a thick sequence of phyllites and graywackes, with intrusions near the contact with Paleozoic intrusive granites. The Paleozoic formations are formed of: calc-alkalic granites from a later phase of the Hercynian orogeny; Ordovician quartzites; and series of Silurian flysch which cross-bed the other formations.

In the Zêzere river basin upstream of the dam, there are not tectonic accidents of regional scope, with detected recent activity; downstream of the dam, at about 10 Km to West, lies the western

Fig.37 - Bouçã dam. Geometrical characteristics.

boundary of the central Iberian region, a zone of contact with mesozoic formations where recent tectonic activity has been noticed. Concerning the seismic activity in the region of Bouçã dam there have been some earthquakes of small magnitude. Studies of seismic risk for the Portuguese territory, based on the series of recorded earthquakes since the beginning of the century, indicate maximum probable accelerations of about 0.1g for 1,000 years return period.

The reservoir is located in a flat area about 1.9 Km^2 and is surrounded by Precambrian formations intensively folded and jointed mostly consisting of series of alternate layers of phyllite and graywacke (Fig.38); hornfels intrusions can be found close to the contact with intrusive granites. At the site of the dam there occur formations of the same type as those of the reservoir (Fig.38).

The foundation of the dam mainly consists of granite and hornfels (Neiva 1982). The granite belongs to the calc-alkalic series, and contains quartz, feldspars (represented by microcline, microperthite and chiefly oligoclase-andesine) and mica (in which biotite prevails over muscovite) as essential minerals; and mainly apatite, titanite and onfacite as accessory minerals. The dam rests on hornfels in the right bank and on granite in the left bank (Fig.38).

Veins of quartz, aplite and pegmatite cross throughout the rock mass. Associated with these veins intense mineralization of pyrite generally occurs.

Several folds are found, and the schistosity, which is hardly detected in hornfels, has the mean attitude of N 45°W, 68°S. There is intensive fracturing of the rock mass evidenced by the large number of local faults, in the NNE - SSW direction, whose inclination generally exceeds 50° for the SE sector (Fig.38). Some faults reach openings of about 1.5 m with clayey milonitic filling due to crushing of granite and hornfels.

Jointing is also very intense particularly in granitic zones (in the left bank and in the bottom of the valley) (Fig.38). Joints have varied inclinations and spacings (smaller than 1.5 m), which produces a random mesh with blocks of small dimension (the largest size being less than 0.6 m, and the most frequent being less than 0.2 m). Joint surfaces in general have little roughness and variable degree of weathering (some of the most open being clayfilled and presenting

Fig.38 - Bouçã dam. Geologic conditions of the reservoir and of the site.

pyrite mineralizations).

3.1.3 - In the phase of the geotechnical exploration Lugeon tests were carried out in boreholes by lengths of 5 m with pressures of water from 0.2 to 1 MPa (RODIO 1954a). The definition of the apparent permeabiliy of the rock mass was based on the absorption recorded for pressure levels equal to or lower than 0.5 MPa, to avoid changing the pattern on the system of conductive joints.

As can be seen (Fig.39), rock mass permeabilities exceed 10^{-7} m/s until depths about 30 m in the slopes and 40 m at the bottom of the valley, presenting values 20 x 10^{-7} m/s near the surface.

Lugeon tests were also carried out after construction of the dam in order to optimize the foundation watertightening works. These tests indicate significant reduction of the rock mass permeability, as well as the influence of the state of stress induced by the weight of the structure in the reduction of permeability.

Unconfined compression tests and joint sliding tests were carried out on cores removed from boreholes and exploration galleries (LNEC 1955a, 1984b). In two of these galleries - one driven in the hornfels of the right bank, the other in the granite of the left bank - in situ deformability tests were made with hydraulic jacks for pressure stages up to 2 MPa. The tests with hydraulic jacks let to moduli of 18 GPa in the right bank hornfels and 16 GPa in the left bank granite; the tests on cores led to moduli of elasticity exceeding 25 GPa (Fig.39).

The mean values of cohesion and of the friction angle are 0.09 MPa and 31° for hornfels and 0.11 MPa and 40° for granites, respectively (however, these values significantly decrease in clayfilled joints).

Geophysical tests (LNEC 1983) led to elastic wave velocities in the foundation ranging from 1,350 to 4,500 m/s (Fig.40).

3.1.4 - The initial treatment of the foundation rock mass consisted of cement grouting for establishing a grout curtain, contact grouting at the dam-foundation interface and grouting for consolidation of crushed zones (Fig.41) (RODIO 1954b).

Fig.39 - Bouçã dam. Permeability, deformability and strenght of the foundation by the exploration studies.

Fig.40 - Bouçã dam. Seismic longitudinal wave velocities by tests conducted in 1983.

Fig.41 - Bouçã dam. Initial foundation treatment and cement absortion rates.

The grout curtain (with slope of 20° in the central zone and 60° in the abutments) was made by grouting 204 tons of cement into holes with a total length of 1,590 m. The absorption was in average 128 Kg/m, with higher values along the left bank (Fig.41).

Contact grouting started from upstream and reached the depth of 3 m in holes 3 m apart; 26 tons of cement were used in holes with a total length of 1,414 m, the mean absorption being 18 Kg/m.

Consolidation of crushed zones, particularly at the bottom of the valley, was carried out by means of cement and bentonite grouting; 24 tons were applied with a mean absorption of 96 Kg/m. In the stilling basin consolidation grouting was made to the depth of 8 m, and sealing at 2.5 m, 5 m long anchorages being installed.

A drainage system was built, which consists of 37 drains runing downstream towards the stilling basin and beginning at the drainage gallery, along the socket near the downstream face of the dam.

3.2 - Monitoring the behaviour

3.2.1 - A monitoring system was installed during construction of the dam to control the main actions, the structural properties and the structural responses (LNEC 1954).

As regards the observation of the dam the system consisted of (Fig.42): i) one limnigraph and one thermograph for water level and air temperature measurements; ii) 33 thermocouples for measuring temperatures at the surface and inside concrete (the latter was also measured by strain gauges, stress meters and electrical joint meters); iii) 179 strain gauges in 48 groups, and 9 stress meters for measuring stresses in concrete; iv) 139 joint meters, 49 of which are electrical and 90 mechanical; v) 6 pore pressure meters for concrete and 6 moisture content meters; and vi) a system for measuring horizontal displacements by geodetical methods.

Observation of the foundation was initially based on measurement and analysis of seepage of 44 drains drilled from the drainage gallery. Subsequently, in 1984, as the need was recognized for thorougher knowledge about the hydromechanical behaviour of the foundation, the monitoring system was complemented by means of 8

Fig. 42 - Bouçã dam. Monitoring system.

piezometers and 16 rockmeters (Fig.42).

3.2.2 - The first filling of the reservoir occurred from September 1955 to January 1956 (dates 1 and 4, Fig.43).

Displacements measured by the geodetical method in course of the first filling and for the period following the first filling are shown in Fig.43. As can be seen, the structure behaved initially in a practically symmetrical way, but a slight asymmetry was noticed afterwards. An asymmetry of the temperature distribution on the upstream face was also observed (Fig.44) thought to derive from the different exposure of the banks to sun radiation.

In general, displacements are larger in the right bank than in the left bank, in accordance with the somewhat different conditions of initial deformability in the two banks (Fig.39).

Fig.45 represents the radial and tangential components of horizontal displacements measured at observation dates 2, 3, 4 and 9 (see Fig.43).

Fig.46 indicates the stress variations calculated from the measured strains between observation dates 1 and 3, with moduli of elasticity of concrete ranging from 20 to 29 GPa (Rocha et al. 1960); temperature variations through the thickness of the dam between those dates are also represented and they increased through the thickness from downstream to upstream. The largest compressive stress (3.7 MPa) was determined near the abutment downstream and the largest tensile stress (2.8 MPa) was found near the base of the dam upstream.

Immediately after the first filling the reservoir was emptied in January 1956 and filled again two months later (March 1956). By this occasion grouting of contraction joints was completed.

Displacements of the dam associated with reservoir emptying and re-filling are also shown in Fig.43. With reference to the initial period there is not full recuperability of displacements (this may be associated to cooling of the structure and to the adjustment of the rock mass foundation).

3.2.3 - During the normal operation of the work, satisfactory behaviour was observed until the recent years, i.e. the observed

Fig.43 - Bouçã dam. Horizontal displacements (geodetic methods) during the first filling and after 1956's re-filling of the reservoir.

Fig.44 - Bouçã dam. Isothermals (°C) at surfaces 1 m deep from the faces before and during the filling of the reservoir.

Fig.45 - Bouçã dam. Horizontal displacements before and after reservoir's emptying occurred in 1956.

Fig.46 - Bouçã dam. Stress and temperature variations during the first filling of the reservoir.

behaviour was, in general, relatively close to the model forecasts.

As a rule, the water level in the reservoir remained above level H = 174 m, excepting for short periods in 1958, 1963, 1982 and 1983, in which the water level decreased to about H = 168 m. On the other hand the air annual temperature remained approximately constant between 1961 and 1975, no records being available for the period 1975-1985.

Fig.47 represents the thermal state on the faces of the dam in a winter period and in a summer period, for full reservoir condition. In both situations temperatures are higher in the right bank than in the left, and the downstream face is warmer than the upstream face.

The quantitative analysis of the horizontal displacements in the structure, measured between 1956 and 1983 with the water at elevations H=174 m to H=175 m, made it possible to evaluate the radial displacements associated with the time effect. They reach values of about 20 mm at the crown of the arch, and decrease to the abutments and to the bottom (Fig.48). The thermal displacements derived from the same analysis are also indicated in Fig.48, the maximum values being recorded at the crest of the central cantilever, and not exceeding 8 mm.

The displacements associated with the time effects (creep, ageing, local ruptures, etc.) markedly decreased between 1968 and 1978; but after this period, they show a tendency to increasing again.

Drained seepage as recorded since 1961 and uplifts measured since 1984 are indicated in Fig.49. The maximum total seepage observed up to 1981 was 68 l/min in 1961 and a clear tendency to progressive decrease has been evident since then (from 1982 to 1984 readings were not taken because the drainage gallery was flooded).

The total seepage measured in the right bank always exceeded the values obtained in the left bank (in 1961 total seepage in the right bank reached a value three times that of the left bank, whereas in 1981 it was a little less than twice). Progressive reduction of seepage was also more significant in the right bank than in the left bank.

As shown in Fig.50, concerning seepage cumulated along the abutment zones and the bottom of the valley, the seepage measured in

Fig.47 - Bouçã dam. Isothermals (°C) at surfaces 1 m deep from the faces after the first filling of the reservoir.

Fig.48 - Bouçã dam. Radial displacement due to time efect and temperature variations between 1956 and 1983 and horizontal displacements measured in 1980, 1982 and 1986.

Fig.49 - Bouçã dam. Time evolution of uplift and seepage.

Fig.50 - Bouçã dam. Cumulated seepage observed in 1?.1's summer and winter.

the bottom blocks specially downstream of blocks HI and IJ are those which give the major contributions to total seepage. In fact seepage drained comes only from the foundation of the bottom blocks, below joint E in the right bank, and from the foundation of blocks LM, JK and IJ in the left bank.

Winter and summer periods correspond to the extreme thermal conditions in the structure. There seems to be little influence of thermal annual variations in the percolation regime (Fig.49).

Since 1985 the distribution of seepage along the drainage system keeps the same characteristics as indicated above (Fig.51). This figure shows seepage drained and uplifts in the foundation for two dates of 1986 with different thermal conditions - March and October - and with full reservoir condition; it may be seen that the influence of temperature on the seepage is not considerable: about 10 l/min for total seepage in the right bank and 4 l/min for the left bank.

Uplift presents higher values in the bottom zone (blocks HI, IJ and JK) with values that reach 70% of the total head in March for block JK; these values are lower in October, which points to the influence of the annual temperature variation. However, seepage does not show a tendency to increasing during the thirty years' life of the structure.

3.2.4 - In 1981 owing to progressive decrease of seepage that may be resulted from clogging of the drainage system due to a process of foundation deterioration the following measures were taken:

i) hydromechanical and geochemical characterization of percolated water and of transported sediments;

ii) further geological exploration of the foundation rock mass;

iii) mechanical characterization of the rock mass through geophysical tests (direct seismic method) and laboratory joint sliding tests; and

iv) improvement of the monitoring system by placing piezometers and rockmeters in the foundation.

Fig.51 - Bouçã dam. Uplift and cumulated seepage in March and October 1986.

The hydrochemical analysis of drained water conducted by EDP indicated that the specific mean rates (increase of concentration of the ion or ions of the drained water with reference to the reservoir water for a discharge of 1 l/min) of dissolution of the calcium from the foundation grouting cements were about 3.6 Kg/year in 1981 and 3.7 Kg/year in 1984; as to the total dissolved salts these rates were about 24.6 Kg/year in 1981 and 20.9 Kg/year in 1984. These values are rather low and do not reveal an unfavourable evolution from 1981 to 1984. The geochemical analysis on sediments collected in the drains reveal that in all drains the granite minerals are present particularly quartz, feldspar (more orthoclase than albite) and muscovite; though rather unfrequently clay minerals and some chlorite occur. These minerals evidence a process of mechanical wear of the joint surfaces and of the milonite infilling of some faults.

Permeability tests of the modified Lugeon type, carried out in boreholes drilled in the foundation under the blanket and the stilling basin (TECNASOL 1983), made it possible to define laws of permeability variation with depth, of the type $k = k_o . e^{-\alpha z}$ where: K_o is the coefficient of permeability at the base of dam ($z = 0$); α is a constant; and z is the depth in meters.

The following mean values of k_o and α were respectively obtained: 14.4×10^{-7} m/s and 2.1×10^{-4} for the left bank; 18×10^{-7} m/s and 4.8×10^{-4} for the zone at the bottom of the valley; and 26.8×10^{-7} m/s and 3.3×10^{-4} for the right bank. These high permeabilities remain at large depths, according to the small values of α.

Permeability tests conducted in holes drilled for rockmeters, close to the grout curtain, showed values of permeability about four times lower than those mentioned, which was explained by the influence of the state of stress and of the grout curtain.

The results of the mechanical characterization (LNEC 1984b) were already referred to and presented in Fig.39. They show a comparatively low friction angle under joint sliding, which points to weathering of surfaces and/or clay-filling. Both situations were detected in geological study from boreholes.

During 1982 and 1983 the drainage gallery was full of water which made the measure of seepage impossible. After the drains had been cleaned out in 1984, considerable increase of seepage was recorded

(Fig.49). The total drained seepage reached 164 l/min in the first trimester of 1985; later it decreased to about 60 l/min in 1986. The seepage in the left bank exceeded that of the right bank, mainly due to drain P7 whose cleaning allowed full contact with water cumulated downstream. Drain P7 was closed by the end of 1985, the total seepage from the left bank decreased to 12 l/min.

The piezometers installed between the grout curtain upstream and the drainage system downstream indicated uplifts at the bottom (4 to 40% in 1984), lower values in the left bank and practically zero in the right bank (Fig.49). Subsequent evolution reveals an increase of the corresponding hydraulic head percentages, as a result of self-clogging of drains. This tendency to clogging is more intense in drains of the bottom, towards the right bank (blocks HI and IJ).

Displacements measured at the base of the dam by means of the rockmeters installed in 1984 are represented in Fig.52. Vertical displacements are maximum at the bottom, progressively decreasing to the banks. Emptying of the reservoir in 1987, by producing rock mass compression upstream and relief downstream, induced rotation of the base of the dam.

3.3 - Model analysis

3.3.1 - In the design of the dam by Hidroeléctrica do Zêzere (HEZ) calculations were made assuming: independent horizontal arches for analysis of the hydrostatic pressure and temperature effects; and independent cantilevers for analysis of the dead weight (EDP 1984a).

Other assumptions adopted were as follows: i) the grouting temperature for contraction joints was considered equal to 16°C; ii) the moduli of elasticity adopted for the foundation and for the dam were in the same value; iii) air temperature was expressed by a sinusoidal law with the origin of time on 15th May, annual mean temperature (16°C), half-range of annual variation (8°C) and delay of 44 days; and iv) water temperature was established by comparison with values measured in other reservoirs and considered in phase with air temperature at all elevations, the mean temperature and the half-range of annual variation being: 16°C and 8°C for elevation 173 m; 12°C and 5°C for elevation 160 m; 9°C and 2°C for elevation 145 m; 8°C

Fig.52 - Bouçã dam. Time evolution of the displacements (in mm) at the dam-foundation interface (rockmeters).

and 0°C for elevation 130 m; and 7°C and 0°C for elevation 115 m.

The largest stresses due to dead weight were about 7 MPa for compression at the abutments of the lower arches and 1 MPa for tension at cantilevers, in what concerns the action of dead weight. Stresses due to dead weight at the base of the cantilevers are indicated in Fig.53; and stresses due to hydrostatic pressure and temperature variations, at the crown and abutments of several arches, are summarized in Fig.54.

3.3.2 - The design of the dam was also supported by tests of physical models, carried out at LNEC. Four different models at the scale of 1/200, were built and tested, the material used being a plaster-diatomite-water mix. Two models were used for the first study (Rocha 1960) and the other two models, slightly different from the former ones by the shape of the crest (LNEC 1955b) were used for the second study. The foundation was represented in the models to a suitable depth and its modulus of elasticity was assumed to be equal to that of concrete (Fig.55).

Tests for the hydrostatic load (applied by means of mercury contained in a rubber bag fitting perfectly the upstream face of the models) were made for water levels at 150, 165, 175 and 177.5 m in the reservoir. Strains were measured by strain gauges, radial displacements were measured by 0.01 mm mechanical deformeters and tangential and vertical displacements of the middle surface of models as well as rotations were measured by 1 micron spring deformeters.

Fig.56 (a) shows the directions of the principal stresses at the faces of the dam as indicated by the brittle coat method, for maximum water level in the reservoir (177.5 m); it also indicates that the same directions were obtained in scale models tests. The principal stresses at the faces of the dam for level 175 m, (mean values observed in the tests of the four models) are indicated in Fig.56 (b), as well as the principal stresses for the maximum hydrostatic pressure and dead weight (assuming the blocks to be separated by joints).

Fig.57 shows radial displacements at the middle surface of the dam for maximum water level, and displacements at the central cantilever for several levels.

One of the models of the dam was tested up to rupture. A loading

Fig.53 - Bouçã dam. Stresses due to dead weight at the base of the cantilevers.

Fig.54 - Bouçã dam. Stresses due to hydrostatic pressure and temperature variations in several arches.

Fig.55 - Bouçã dam. Downstream view of 3D scale model.

Fig.56 - Bouçã dam. Principal stresses at the faces due to dead weight and hydrostatic pressure.

Fig.57 - Bouçã dam. Radial displacements due to hydrostatic pressure.

system by means of hydraulic jacks was used that allowed progressive increase of the action (hydrostatic pressure and dead weight) in such a way as to simulate a general decrease of the concrete strength. The rupture test indicated that the dam would fail for concrete strengths about 1/10 of the usual strength of the concrete used in dam construction. The rupture process begins by the occurrence of cracks along the insertion of the dam into the foundation, but the collapse only occurs by crushing of the arches. Rupture tests were also conducted under thermal shocks (daily wave and sun radiation) in an attempt to investigate their influence on the safety of the dam (LNEC 1969). In this case use was made of a mortar model in the scale 1/200. The device adopted for heating and cooling the surface of the model is presented in Fig.58; this device was able to impose quick temperature variations at the downstream face of the model, which was previously deformed up to a state close to rupture.

Results of failure tests are indicated in Fig.59; the curves plotted limit plastified zones (deformations exceeding 2×10^{-3}) for different pressures and for models of mortars of two different types. It may be seen that in both cases rupture occurs as the arch crushes, at the crown or at the haunches. The tests with thermal shocks were conducted under increasing load levels (Fig.60). These tests led to the general conclusion that the temperature variation imposed on the face of model (from 22 to 52°C) brought about only 15% decrease of the forces that produced rupture and thus of the safety coefficient.

3.3.3 - Throughout the operation phase, finite element models were developed at LNEC to support the safety control of the dam (Pedro 1977). The main assumptions of these models were the following: i) dam represented by a thin shell elastically supported by the foundation (Vogt's coefficients); ii) linear elastic and thermal behaviour of the concrete with modulus of elasticity 20 MPA, Poisson's ratio 0.2 and coefficient of thermal expansion 10^{-5} $°C^{-1}$.; iii) linear elastic behaviour of the foundation which was assumed to be of the half-space type and of the quarter-space type; iv) temperature and water load variations, the latter acting on the dam and in the foundation.

Fig.58 - Bouçã dam. Devices for heating and cooling the surface of the model in the thermal shock tests.

Fig.59 - Bouçã dam. Curves limiting zones with deformations exceading 2 x 10^{-3} under different forces.

Fig.60 - Bouçã dam. Deformations in the central zone of the arch at level 165 m, due to temperature.

The finite element mesh is represented as a perspective projection in Fig.61.

Fig.62 represents displacements at the central cantilever and principal stresses due to the hydrostatic pressure at levels 155, 165 and 177.5 m. The displacements were observed in the dam (by the geodetical method) and were estimated by finite elements; and stresses were determined through scale model tests and finite elements for the level 177.5 m.

Other situations were analysed, by the finite element model such as the following:i) the rising of the water level from 127.5 m to 172.5 m that occurred between 1956.03.03 and 1956.03.14; ii) the temperature variation between summer (1955.09.02) and winter (1956.02.04) with the reservoir nearly empty.

For the situation denoted by i), Fig.63 represents variations of hoop and cantilever stresses, at the central cantilever, and normal stresses at two cross-sections of the dam between the two dates in the two hypotheses assumed for the foundation; agreement is found between stresses observed and those calculated assuming a foundation of the quarter - space type. For the situation denoted by ii), Fig.64 represents variations of hoop and cantilever stresses at the central cantilever and normal stresses at two cross-sections of the dam, as well as the temperature variations measured between the two dates; agreement is found since the stresses calculated by the shell model (thus assuming linear distribution through the thickness) are corrected by the local temperature effect.

Finite element analyses were also developed at LNEC (1987) for studies on the behaviour of the dam up to rupture. In these analyses hazard scenarios are associated to the concrete deterioration, in a way similar to that considered in the rupture model tests. Fig.65 illustrates the principal stresses at the faces of the dam near the collapse of the structure, for which a safety factor of 10.4 was obtained (for ductile material under unconfined compression, the tensile strenght and the compressive strenght being respectively 2 and 35 MPa - friction angle of 50° and cohesion equal to 5.0 MPa) the same safety factor was determined by the scale model tests (see 3.3.2).

The models developed at LNEC were also used to estimate the maximum allowable displacements of the base of the blocks during the

Fig.61 - Bouçã dam. Finite element mesh and instrumented cross-section for stresses measurements.

Fig.62 - Bouçã dam. Displacements and principal stresses due to water pressures.

Fig.63 - Bouçã dam. Stresses at the central cantilever due to water pressures.

Fig.64 - Bouçã dam. Stresses at the central cantilever due to a cooling.

Fig.65 - Bouçã dam. Principal stresses at the faces in model *analysis up to rupture* (near rupture conditions).

foundation treatment above referred to.

3.3.4 - For assessing the deterioration conditions of the dam foundation, analyses by the finite element method were performed by EDP (1984). A tridimensional model of the dam elastically supported by the foundation (Fig.66) was used. The discretization was aimed to answer several purposes, particularly accurate representation of the structure and different groups of elastic properties corresponding to several concreting stages.

Calibration of the foundation mathematical model was done by iteration, starting from the moduli of elasticity indicated by tests; the initial and the final characterization of these moduli is shown in Fig.67. After deterioration phenomena moduli of deformability of the foundation and of the dam were obtained, which sought to express the tendency to deterioration (Fig.67).

The actions considered were as follows:

- Dead weight of concrete (W), simulating the sequence of construction by means of 12 successive phases. In each phase, opening and closure of joints were considered by comparing dual points in contact (Fig.66).
- Hydrostatic pressure (HP) for full reservoir and maximum flood conditions (respectively 174.5 m and 179.8 m upstream and 122 m and 136 m downstream).
- Uplift (UP), a trapezoidal diagram being adopted for taking into account the influences of water upstream and downstream.
- Temperature variations (VT), three distinct approaches being followed: i) integration of the Fourier equation through the thickness of the dam, based on air and water temperatures assumed to be in phase, the actual diagrams being latter replaced by their trapezoidal equivalent; ii) a composite method based on the dam temperatures determined by joint meters; and iii) a composite method, proposed by LNEC, that sought to express the superposition of an annual wave and of other for half the period. The results obtained with these three methods show that the differences are of the same order of magnitude as the errors of measurement. Grouting temperatures were taken for

Fig.66 - Bouçã dam. 3D finite element model.

Fig.67 - Bouçã dam. Foundation deformabilities of the model.

1955.08.24.

- Earthquakes (S), an equivalent static analysis for an acceleration of 0.1 g (100 years return period) being considered.

Different combinations of actions (normal - N, extraordinary - E and work - T) were considered. Fig.68 illustrates the hypotheses adopted, among which the following are stressed: NW (normal winter, calc. 18); NS (normal summer, calc. 19); EW (extraordinary winter with flood, calc. 26); RS (repair in summer, calc. 29). The hypothesis first mentioned correspond to the initial situation of the dam and its foundation whereas those mentioned in second place correspond to the situation before the repair works.

Fig.69 presents displacements at the crown of the arches for the combinations (NW, NS, EW, LS) and for the two situations mentioned, a clear change in the elastic curve being evident when one passes from one situation to the other. Fig.70 gives a general view of displacements at the dam-foundation interface and Fig. 71 presents stresses and the relation between normal and tangential forces on the dam-foundation interface.

The foundation treatment was also simulated by considering a generalized increase of the modulus of elasticity of the foundation. Significant variations were not found similarly to what occurred in other analyses, used to simulate the action of grouting pressure in foundation treatment.

3.4 - Repair works and behaviour after repair

3.4.1 - Repair works aiming at the improvement of hydraulic and mechanical properties of the foundation began in 1987. These works were mainly intended to reduce the rock mass permeability and subsidiarily to consolidate the most superficial zones with a dense pattern of open joints (EDP 1984b, PNCOLD 1985).

The foundation zone to be treated was limited by two cut-off curtains, upstream and downstream, carried out by cement grouting, and reaching depths above 25 meters.

Fig.68 - Bouçã dam. Combinations of actions.

Fig.69 - Bouçã dam. Displacements at the crown of the arches for different combinations of actions.

Fig.70 - Bouçã dam. Displacements at the dam-foundation interface.

Fig.71 - Bouçã dam. Normal stresses, shear stresses and sliding coefficients.

The scheme devised included grouting with a cement and fly - ash mix (Fig.72) aiming at: i) building a vertical curtain from upstream, to reach depths of about 50 meters at the bottom of the valley; and ii) building a vertical curtain downstream that separates the dam from the stilling basin and reach depths of about 10 meters.

Between these two grout curtains and the corresponding upstream and downstream cut-off curtains, complementary cement grouting was carried out for watertightening and superficial consolidation of ground.

Use was made of a mix of blast-furnace cement (60-80) and ashes for consolidation grouting, in cut-off curtains and in primary holes of the main grout curtain. In some cases bentonite was also used for cavity grouting. The secondary holes of the main grout curtain were filled with a high deformability mineral product, easy to inject, which results from the reaction of a silicate (HYDROSIL - RODIO) strongly ionized with potentially reactive calcium, in presence of water.

Grouting pressures were chosen taking into account the characteristics of the rock mass and the dam-foundation interaction.

The second phase of the planned repair works is still under way; it includes improvement of watertightness (Fig.72), as well as possible local improvements in zones with high hydraulic conductivity.

During the first phase the following approximate quantities of materials were injected into the foundation: 864 tons of cement, 139 tons of fly-ashes, 3 tons of bentonite and 46,000 liters of HYDROSIL - RODIO.

Fig.73 shows grout distribution along the foundation. The largest absorptions for consolidation were recorded at the bottom of the valley and in the left bank, whereas the largest absorptions for watertightening occurred in the abutments (primary holes) and at the bottom of the valley (secondary holes).

The largest volumes injected (following the decreasing order of quantities) were recorded at the foundation cf blocks JK, KL, GH, HI, FG and MN. These zones roughly correspond to those where the largest absorptions were recorded during the initial treatment of the foundation (Fig.41) and where later the highest values of seepage and

Fig. 72 - Bouçã dam. Foundation treatment.

Fig.73 - Bouçã dam. Absorption of the injected products during foundation treatment until January 1988.

uplift were observed.

Complementary to grouting, improvement was introduced in the existing drainage system that runs towards the stilling basin, by constructing a drain per block approximately at mid-thickness.

The uplift measuring system of the foundation was provided with a further piezometer in each block, at the downstream base, making it possible to observe upstream-downstream radial profiles.

3.4.2 - Taking advantage of the emptying of the reservoir, repair and maintenance works were carried out in the power house equipment. When these works finished, it was decided to fill the reservoir. Some results were obtained on the behaviour of the dam after repair, but it must be taken into account that the treatment of the foundation is not yet completed.

Horizontal displacements of the structure (Fig.74), measured in April, evidence characteristics of dam deformation of the same order of magnitude as what was observed before the foundation repair works. On the other hand both through the analysis of horizontal and vertical displacements measured at the base of the dam and through results of geophysical tests, a small improvement of the mechanical characteristics of the foundation rock mass can be observed.

As regards the hydraulic behaviour of the foundation it is difficult to make before and after repair comparison; this difficulty arises from the fact that drainage conditions in the rock mass changed due to the installation of drains upstream of the earlier drainage curtain and very close to the piezometers installed downstream of the grout curtain (Fig.72). As it seems, uplift in the central zone foundation significantly decreased; the seepage due to the new drainage holes is high (Fig.75).

Development of repair works is expected to ensure small uplift as well as a reduction of the seepage.

Fig.74 - Bouçã dam. Horizontal displacements (geodetic method) before and after foundation treatment.

Fig.75 - Bouçã dam. Uplift and seepage before and after foundation treatment.

4. VENDA NOVA DAM

4.1 - General characteristics of the dam and foundation

4.1.1 - Venda Nova Dam is located on the river Rabagão, a left bank tributary of river Cávado (Fig.2). It is an arch-gravity dam completed in 1951 (Fig.76); it is formed of 22 blocks and its main dimensions are as follows (in meters):

- maximum height above foundation: 97
- crest length 345
- crest thickness 5
- thickness at the base of the central cantilever 32

The dam has a concrete volume of 228,000 cubic meters, a vertical upstream face and a downstream face sloping at 40%.

Between contraction joints F and M (Fig. 76), a perimetral joint was placed upstream, which was intended to decrease tensile forces in the upstream part of the foundation.

The dam creates a reservoir with a capacity of 95 millions of cubic meters, mainly intended for power production. The dam is provided with a bottom outlet at the base of block HI, (discharge capacity of 130 cubic meters per second); and with a ski-jump spillway which develop in two channels on the blocks NO and OP (maximum discharge capacity of 1,500 cubic meters per second).

4.1.2 - The river Rabagão basin comprises Paleozoic formations consisting of igneous and metamorphic rocks (Fig.77). The former are composed of granites of different types; the latter occupy the major part of the basin and are formed of schists with layers of quartzite schists (crossed by numerous aplite and pegmatite veins).

The reservoir is 4 million square meters in area, it occupies essentially schistous formations and no significant tectonic accidents were found.

The largest earthquake recorded in the region (on 1941.04.24) had the magnitude (M = 4.4) and its epicenter was about 15 Km far from the dam site. The seismic risk studies for the Portuguese territory, based on continental and Atlantic zones of earthquake generation (LNEC

Fig.76 - Venda Nova dam. Geometrical characteristics.

Fig.77 - Venda Nova dam. Geologic conditions of the reservoir and of the site.

1976) point to maximum acceleration of about 0.06g on the dam site, for a 1000 years return period.

The dam is founded on a rock mass consisting of two-mica, medium to coarse grain granite essentially biotitic, with feldspar crystals that give it a pitic facies. At the right bank phyllite occurs with metagraywacke inserts (Fig.77). These two formations, separated by a hornfels belt, are crossed by aplite and pegmatite dykes and veins. Rock is sound, with slightly weathered layers, in the upper zone of the right bank.

Fracturing in the rock mass made it possible to define several sets of joints (spacings from some decimeters to some meters) and five local faults in general milonite-filled (Neiva 1981) (Fig.77).

4.1.3 - During the geologic survey Lugeon tests were made (RODIO, 1946). These tests showed considerable permeability in the upper zones of the banks, particularly in the right bank.

Tests carried out in 1979 (TECNASOL 1984), when the dam was in operation, showed relatively low permeabilities (in general smaller than 5 Lugeon) at the upstream zone of the foundation. As a rule the highest values are found in a length of the rock mass about five meters deep under the base of the dam.

Tests in holes at the downstream zone of the foundation showed higher permeabilities down to depths of about seven meters. The largest values (about 50 Lugeons) were recorded in the right bank under block DE and in the left bank under block MN, decreasing to the bottom of the valley.

Association of some faults, namely faults A and B (Fig.77), with subhorizontal joints originates favourable conditions for appearance of local zones with large permeability.

At the design phase tests on cores removed from boreholes were made for determining the deformability of the rock (LNEC 1949a). The moduli of elasticity obtained were as follows: at the right bank, 10 GPa; at the bottom of the valley, 8 to 10 GPa; and at the left bank, 16 to 20 GPa. For the rock mass, although considering larger deformabilities owing to jointing, the left bank was assumed to have a deformability half that of the right bank and the bottom of the valley.

4.1.4 - The initial treatment of the foundation, for which a brief report only is available (TEIXEIRA DUARTE 1950), consisted of a vertical grout curtain and contact grouting at the dam-foundation interface (Fig.78). For the grout curtain it was required that cement grouting should reach the depth corresponding to 1 Lugeon water absorption, within a maximum of 50 meters; and cement grouting at the dam-foundation interface should reach the depth of 3 meters.

After the reservoir was filled, water resurgences were noticed and it was decided to carry out the following works from the drainage gallery: i) grouting of the dam-foundation interface near the upstream face; and ii) improvement of the grout curtain. These works were made in 1964 with water at level 650 m (about 50% of maximum head).

Simultaneously with the works above indicated a drainage system was drilled and piezometers were installed (Fig.78).

The drainage system consisted of 87 drains, of which 32 from the drainage gallery and directed to downstream whereas 55 from downstream and directed to upstream.

Seven piezometers were installed in three upstream - downstream profiles, one for the right bank, and two for the bottom of the valley.

4.2 - Monitoring the behaviour

4.2.1 - The monitoring plan of Venda Nova dam (LNEC 1949a) define a monitoring system installed during construction (Fig.79) with the main characteristics as indicated below.

For observing the main actions, - water pressure and temperature variations - there are: one limnimeter for measuring water level in the reservoir; one thermohygrograph for measuring air temperature and humidity; and 71 resistance thermometers for measuring temperature in the concrete.

For observing the structural responses, there are: 3 direct plumb-lines, with 16 measuring points for horizontal displacements inside the structure; a geodetical network for measuring displacements at 18 points of the downstream face; a precision geometrical levelling system at 15 points of the crest; 75 contraction joint meters applied

Fig.78 - Venda Nova dam. Drainage system and initial foundation treatment.

Fig.79 - Venda Nova dam. Monitoring system.

along the galleries inside the dam; and 138 acoustical strain meters for measuring strains in concrete.

In 1964 7 piezometers were installed for measuring foundation uplifts in three upstream-downstream cross-sections.

4.2.2 - The first filling of the reservoir occurred from September 1950 to December 1951.

Geodetical measurement of horizontal displacements was carried out for the first time in November 1950, only points of the down - stream face below elevation 660 m having been observed.

Fig.80 indicates the horizontal and vertical displacements observed during the first filling (LNEC 1961). Except for points near the dam-foundation interface, horizontal displacements are approximately radial. An asymmetric variation is observed with reference to the central cantilever, both as regards horizontal and vertical displacements, which is related with the asymmetric insertion of the dam into the valley. As the water level raised from elevations 686 m to 700 m between (1951.11.14) to (1952.03.15) the crest raised in 5 millimeters at the central zone. This value points to marked pressure relief in the lower zone of the dam and to opening of the perimetral joint (openings of 0.3 mm were recorded in the same period).

By that time, apparatus for measuring vertical displacements were not available in the foundation, as well as drains or piezometers to observe its hydraulic behaviour. Vibrating-wire strain meters were installed in the rock foundation, near the base of the dam, but they could only indicate small pressure reliefs in the rock mass.

Until 1964 (the year when Alto Rabagão dam, upstream of Venda Nova, began to operate) the regime of Venda Nova reservoir could be characterized by annual variations of the water level from 15 to 20 meters below full reservoir level; the structural behaviour was very much influenced also by the annual temperature variations at the site.

Fig. 81 represents the thermal state of the structure at points one meter distant from the faces, in a cold period (January) and in a hot period (September). The larger ranges of variation reaching 13°C occur in the right bank, due to its longer exposure to the sun

Fig.80 - Venda Nova dam. Horizontal and vertical displacements (geodetic methods) during the first filling of the reservoir.

Fig.81 - Venda Nova dam. Isothermals (°C) at surfaces 1 m deep from the faces in summer and winter with full reservoir.

radiation.

The cyclic forces applied by the dam on its foundation combined with a possible defective operation of the perimetral joint, gave rise to increasing resurgences in the foundation rock mass (downstream and in grout holes). This situation suggested that high uplift should exist in the foundation, as evidenced by the subsequent drilling of drains and installation of piezometers. In fact, maximum seepage of about 200 litres per minute and uplifts of about 0.7 MPa (about 80% of maximum head) were recorded at the bottom of the valley.

4.2.3 - After the repair works described in 4.1.4, the filling of the reservoir in 1965 led the foundation to hydraulic behaviour conditions similar to those earlierly observed, though more favourable. This fact points to the marked influence of the dam behaviour over its foundation, namely by opening the subhorizontal joints (more frequent in the left bank and at the bottom of the valley) and the faults, thus originating the intense seepage observed.

As the diagram of Fig.82 shows, the temperature variations should be accounted for the largest variations of seepage. In February and March (when the structure reaches its lower annual temperature) seepage impressively increased, particularly in the left bank; in summer, seepage practically vanished despite water in the reservoir being kept at high levels.

In 1978 raisings were observed for the rate of increase of seepage and for the uplift (Fig.83). Therefore, it was decided to increase drainage of the foundation as it was concluded that cement grouting would not be an effective solution; in fact the tensile stresses upstream would disturb again the new grout curtain.

Seepage increased when the new drains were drilled (Fig.82) but uplifts reduced to values half those observed in 1978 (Fig.83, Fig.84), particularly at the bottom of the valley. Part of the total seepage from the right bank was transferred to the left bank, as drains at the bottom of the valley captured those flows; and as observed above there is a clear influence of temperature variation on the seepage in the foundation.

Though no significant changes in the uplift values were recorded subsequently, drained seepage increased in the left bank at a mean

Fig.82 - Venda Nova dam. Time evolution of seepage.

Fig.83 - Venda Nova dam. Time evolution of the hydraulic head percentage in the foundation (piezometers).

Fig.84 - Venda Nova Dam. Uplift and cumulated seepage before and after 1979's drainage improvement.

rate of about 100 litres per year (LNEC 1985). In 1983, seepage reached about 1000 litres per minute, the largest individual contributions coming from 4 drains of the left bank (M2, M3, M4 and PSE14) drilled in the foundation of blocks IJ, JK, KL and LM in 1979.

Another important feature observed in the evolution of seepage between 1979 and 1983 was the increase (at a mean rate of about 40 litres per year) of the minimum annual seepage from the left bank. This was associated with the washing off of the materials sealing the joints of the rock mass, i.e. their natural filling (mylonite and clay) and of cement grouts.

Concerning the behaviour of the dam no significant changes were detected. In particular, the observed displacements remained within acceptable values in accordance with the model previsions.

Fig.85 shows horizontal displacements of the downstream face, which were measured in 3 of the 41 geodetical observation dates, between 1951 and 1983; measurements in May 1963, May 1973 and March 1983 are represented, with water level in the reservoir at elevations 700.6 m, 699.0 m and 698.0 m respectively. As can be seen, no significant changes of displacements are noticed.

4.2.4 - The results of the observation above referred to revealed an unfavourable hydraulic behaviour of the foundation.

Chemical analysis of seepage water and X-ray diffractometric identification of the materials washed off from the rock mass and deposited at the outlet of drains (LNEC 1985) led to the conclusion that a physical-mechanical deterioration of fillings and surfaces of joints and a chemical deterioration of grout cements and rock matrix was in course.

The chemical analysis of the water (conducted by EDP) was intended to investigate and quantify the main ions in solution (namely Ca^{2+}, Na^{+}, K^{+}, Mg^{2+}, Fe^{2+}, HCO_3^{-}, CO_3^{2-}, Cl^{-} and SO_4^{2-}).

The mineralization of drained water (total of dissolved salts, TDS) showed an average value of 115 milligrammes per litre, while the TDS of the reservoir water was only about 22 milligrammes per litre. The difference between the mineralization of the reservoir and drained waters indicated how much foundation material was being dissolved, an

Fig.85 - Venda Nova dam. Horizontal displacements (geodetic method) measured in 1963, 1973, and 1983.

approximated budget being possible to establish by considering the amount of the drained seepage.

Fig.86 presents the mean values of the mineralization for the water analysed at the foundation of each block; only values of TDS and calcium are reported since they are the most representative of the overall deterioration of the rock mass, and of the deterioration of the cement of the grout curtain.

In the same figure the cases of deposition of sediments at the outlet of drains are indicated: detrital crystalline materials correspond to processes of mechanical rubbing away and subsequent physical deposition; and non-detrital colloidal or crystalline materials correspond to processes of dissolution and subsequent chemical deposition.

By associating the two above approaches the deterioration phenomena in progress were identified and the zones most affected were defined (LNEC 1985).

Chemical deterioration reached higher values at the foundation of blocks GH, IJ, LM, NO and OP (bottom of the valley and left bank); physical-mechanical deterioration was most intense at the foundation of blocks EF and FG (right bank) and of blocks KL and MN (left bank). Low chemical and physical-mechanical deteriorations are determined for the foundation of block JK. As in this zone the rate of seepage is very large, the seepage velocities through cracks are such that the chemical action of water is not important as compared with its physical-mechanical action but the latter is not observed through deposition and collection of materials at the outlets of drains on account of the velocity of the water.

Further to these analyses, tests were conducted for determining seepage conditions in the foundation (TECNASOL 1984). As shown by these tests, the main hydraulic conductivities could be found: i) in the left bank, from the dam-foundation interface down to 5 meters; and ii) in the right bank, at variable depths in general not larger than 10 meters (LNEC 1985).

Fig.86 - Venda Nova dam. Hydrogeochemical tests in drain-water (1983).

4.3 - Model analysis

4.3.1 - The design of the dam was supported by mathematical and physical models.

Mathematical models were made following the trial-load method, approaching the dam behaviour by a system of 4 arches and 3 cantilevers, only radial displacements being adjusted. The valley was assumed to be symmetrical and the rock mass to have the same modulus of elasticity as the concrete (COYNE-BELLIER 1947).

The simplified trial-load analysis was complemented by tests of 3D scale models: in a first phase, stresses and displacements were determined on a first shape of the dam (LNEC 1949b) and of the spillway zone (LNEC 1950a); in a second phase, the final shape of the dam, including the insertion of the joint upstream was tested (LNEC 1950b).

4.3.2 - In the first phase of the Venda Nova experimental study, a plaster-diatomite model in the scale of 1/100 was built with parallelipiped units, 10 cm thick. The ground was modelled by horizontal layers, joints being carefully filled with plaster. The model foundation represented the heterogeneity of the rock mass (Fig.87), the different materials being obtained by varying the proportions of the mixture.

The hydrostatic pressure for water level at 660 m, 680 m and 700 m (crest level) was analysed. Displacements (radial, tangential and vertical) were measured with 0.002 mm deformeters; and strains were measured on the faces with strain gauges and mechanical strain meters.

Stresses due to dead weight were not determined by means of the scale model because the blocks forming the dam were supposed to be built independently, therefore the corresponding action being easily calculated by analytical methods.

Figs.88 and 89 illustrate the behaviour of the dam in terms of radial displacements and principal stresses in both faces for the maximum level of the water. Maximum tensile stresses reached 4.3 MPa near the left bank haunch and the maximum compressions are 5.5 MPa at the crown of the crest arch.

Fig.87 - Venda Nova dam. 3D model (1ª phase of the tests).

Fig.88 - Venda Nova dam. Radial displacements due to hydrostatic pressure

Fig.89 - Venda Nova dam. Principal stresses due to hydrostatic pressure.

Analytical calculations supplied values of normal stresses in arches and cantilevers. In Figs.90 and 91, these values are compared with those obtained in the scale model, large differences being observed. These differences may be justified by the different simplifying assumptions adopted in both analyses, namely by the fact that the rock mass was assumed to be heterogeneous only in the physical model.

Fig.92 presents the principal stresses along the upstream zone of the dam-foundation interface, due to dead weight and hydrostatic pressure for level 700 m. It can be seen that large tensile stresses remained (3.2 and 2.2 MPa, respectively in the left bank and in the right bank). These tensile stresses were not considered permissible, since they would cause important cracks to occur. Therefore a proposal was advanced for their elimination by changing the dam shape near the insertion into the foundation, and by constructing a horizontal joint upstream.

The scale model made it possible (LNEC 1950a) to analyse stresses using the model already referred to in which the shapes of the spillway zone were reproduced in the vicinity of the spillway openings.

4.3.3 - In the second phase of the Venda Nova experimental study different scale models in the scale 1/300 (Fig.93) were built and tested (LNEC 1950b).

The study concerned the action of hydrostatic pressure at the crest level, applied by a set of hydraulic jacks, which loaded different areas of the upstream face through load-distributing plates.

For studying the effect of the opening of the joint upstream, a cut was made in the model by means of a half-circular hole, 2 cm in radius as shown in Fig.94. As the joint reproduced in the model has a different shape of the joint built in the prototype studies were made through a bakelite model in the scale of 1/500; initially a cut was performed with the same shape as in the prototype and subsequently this cut was enlarged up to the size of the model joint. It was then possible to estimate the stresses in the dam represented in Fig.95.

In overall terms, the improvement of the dam shape and opening of the joint upstream decreased the maximum compressive and tensile

Fig.90 - Venda Nova dam. Arch stresses.

Fig.91 - Venda Nova dam. Cantilever stresses.

Fig.92 - Venda Nova dam. Principal stresses at the upstream face of the dam-foundation interface, due to dead weight and hydrostatic pressure.

Fig.93 - Venda Nova dam. 3D scale model (2nd phase of the tests).

Fig.94 - Venda Nova dam. Bakelite model for the study of the effect of the opening of the joint upstream.

Fig.95 - Venda Nova dam. Principal stresses due to dead weight and hydrostatic pressure - model with open joint.

stresses due to the action of hydrostatic pressure.

4.4 - Repair works

4.4.1 - In 1984, taking advantage of the emptying of the reservoir for the improvement of the hydromechanical equipment, measures were taken (EDP, 1984c) in order to: i) improve the foundation rock mass and its hydraulic behaviour, namely its watertighteness; and ii) stop the development of eventual deterioration processes.

In a first phase (that took place between July and October 1984, with the reservoir emptied), the rock mass was consolidated in the downstream zone of the foundation up to depths of about 15 m, and an upstream grout curtain was built. This curtain was made with blast furnace cement 60/80, reached depths of about 25 m and was intended to form a barrier for the grout products to be injected in the second phase. Fig.96 schematically shows the works carried out.

In the second phase (that took place from February to May 1985, with the reservoir filled again to 70% of maximum head), the main grout curtain was performed by using an acrylic resin. This resin (RODIO 1986) is an hydrogel (Siprogel 110/25 - Rhone Poulenc) and results from the polymerization of two monomers in presence of water. It has low viscosity before polymerization reactions begin, thus being easily injectable. The final product is a material with high deformability, which swells in presence of water and shrinks failing water. These characteristics make it particularly suitable to fit the joints and cracks in the foundation of hydraulic structures.

The amount of materials injected during these works is the following:

- for consolidation, 22 tons of cement in 870 m drilling;
- for previous grouting, 36 tons of cement in 1,533 m drilling; and
- for joint grouting and for grout curtain, 63,752 litres of acrylic resin in 2,755 m drilling.

Fig.97 gives a graphical representation of the distribution of those amounts per block (Silva and Bravo 1987). The following

Fig.96 - Venda Nova dam. Foundation treatment.

Fig.97 - Venda Nova. Quantities of the injected products in the foundation treatment.

conclusions may be derived from the analysis of Fig.97:

- cement absorption increases from the bottom of the valley to the banks, giving evidence of progressive relief of the rock mass as the elevation increases;
- when preliminary grouting was performed with the reservoir empty, cement absorptions were practically null at the bottom of the valley as a result of joint closure due to the weight of the dam; and
- in the left bank the largest absorptions of cement and resin were recorded up to depths of about 5 meters, whereas absorption in the right bank went to larger dephts, the most significant rates being recorded up to 15 m depth.

These results confirmed the conclusions drawn from the studies concerning the deterioration processes of the foundation.

4.4.2 - The monitoring system was also improved by means of the following new equipment (EDP 1984d): i) 8 rockmeters, for measuring displacements of the foundation; ii) 9 electrical joint meters and 14 mechanical joint meters; and iii) renewal of the geodetical system for measuring displacements.

After the second phase of the foundation treatment, along the drainage gallery 28 new piezometers were installed (subvertical and directed to downstream).

Foundation drainage remained essentially based on the already existing draining system, to which should be added the drills for geophysical observation (one per block) and the grout holes for the acrylic product (which form a primary drainage system that develops in the plane of the grout curtain).

4.5 - Behaviour after repair

4.5.1 - The effectiveness of the treatment is shown by the diagrams in Fig.82, 83 and 98; as seen seepage and uplift significantly decreased after treatment.

Maximum drained seepage before repair with water at level 698.7 m was 1,046 litres per minute (on 1983.02.28). During re-filling of

Fig.98 - Venda Nova dam. Cumulated seepage and uplift before and after the foundation treatment with full reservoir.

the reservoir with water at level 697.6 m, the maximum drained seepage raised to 1,300 litres per minute (on 1985.01.29). However, at this time, drilling had already started, and thus the larger number of draining holes justifies increase of flow. After completion of the 2nd phase of treatment, the maximum drainage seepage with the water at level 699.9 m was 11.5 litres per minute (on 1986.02.24) (Silva and Bravo 1987).

Diagrams in Fig.98 represent conditions before, during and after treatment as regards uplift and seepage drained from the foundation.

To appreciate the meaning of the reduction of the drained seepage fully it is worth mentioning that the 114 holes of the grout curtain form a primary drainage system which augments in about 2,500 m the prior drainage system.

Uplift in the foundation is small (as can be seen in Fig.98 for all the piezometers now installed along the drainage gallery) with the following two exceptions:

- at the base of blocks GH and HI, this fact being explained by the occurrence of a fissure in concrete at the base of the gallery which prevented the foundation in this zone from being perfectly grouted;
- at the upper part of the left bank which was not concerned by treatment; a further treatment programme in this zone is advisable.

Vertical displacements of the base of the dam recorded with rockmeters during re-filling of the reservoir (Fig.99) show considerable relief in the foundation rock mass.

Horizontal displacements measured by geodetical methods (Fig.100) and with plumb-lines (Fig.101) evidence a behaviour similar to that previously observed.

Fig.101 illustrates also the important effect of temperature variations over displacements; in July (the hot season) although with the reservoir 3 meters above the level recorded in January (cold season) the structure displaced towards upstream.

A comparison is made in Fig.101 between the radial displacements measured after repair works with plumb-lines and those calculated with

Fig.99 - Venda Nova dam. Time evolution of the displacements (in mm) at the dam-foundation interface (rockmeters).

Fig.100 - Venda Nova dam. Horizontal displacements of the crest (geodetic method) after re-filling of the reservoir (1985).

Fig.101 - Venda Nova dam. Radial displacements observed (plumb-lines) and computed after the foundation treatment.

a model calibrated with results of the observation before the repair works. The comparison of the dam behaviour before and after treatment leads to the conclusion that the foundation rigidity slightly increased as a result of repair works.

Geophysical tests were carried out after the treatment (direct seismic method). These tests pointed to velocities of elastic wave propagation of about 4,000 to 5,000 m/s at the upper zone of the foundation and 5,000 to 6,000 m/s in depth (Fig.102). At the right bank (between the abutment and block EF) and at the left bank (foundation of blocks LM and OP) the lower velocities reach larger depths. These results make it possible to zone the foundation (Fig. 102).

Permeability tests were also carried out after treatment (RODIO 1986). These tests pointed to mean permeabilities of about 0.1 Lugeon (with maximum values of 0.5 Lugeon) all grout curtain holes having been considered. As a general conclusion, the behaviour observed after repair indicates that the main purposes in view (restore satisfactory conditions of the hydraulic behaviour into the foundation and stop the deterioration processes) were fulfilled.

Fig.102 - Venda Nova dam. Seismic longitudinal wave velocities measured after treatment works.

5. CONCLUSIONS

Rock mass foundation deterioration of Portuguese concrete dams is examplified in this report through 3 case histories. The cases selected - Varosa, Bouçã and Venda Nova dams - are arch dams integrated in hydroelectric schemes. The three dams are supported on granitic rocks, Varosa and Bouçã are thin shell dams and Venda Nova is an arch-gravity dam; Varosa is a structure a little more than 10 years old (concluded in 1976) whereas Bouçã and Venda Nova are more than 30 years old (concluded, respectively in 1955 and 1951). For each case, the general characteristics of the dam and foundation were referred to, as well as monitoring the behaviour and model analysis of the dam and foundation, before, during and after repair.

The examples presented point to the following general conclusions:

- There are a small number of cases of rock mass foundation deterioration among Portuguese concrete dams of different types. The most important cases, presented in this report, concern arch dams (which are also the highest structures). Others repair works have been made in dams more than 30 years old most of which should be considered as maintenance works.
- The deterioration cases that have occurred have been detected in due course, making it possible to adoption of adequate measures for the operation of the dams until the execution of the repair works.
- To support the design, construction and monitoring of the works, different types of models have been used (deterministic, statistic-numerical and experimental).
- The repair works in the foundation of Venda Nova and Varosa dams (Bouçã dam has not yet been completed) proved to be effective; however, it must be taken into account that those works were made only four years ago.

The above conclusions show that the design criteria, the construction practices, the monitoring techniques and the models used for safety evaluation have, in general, been adequate.

6. FINAL NOTE

Thanks are due to ELECTRICIDADE DE PORTUGAL, EDP, owner of the works reported, for allowing publication, of information supplying data and co-operation.

REFERENCES

CHENOP 1969. "Project of expansion of river Varosa hydroelectric scheme (in Portuguese)", Internal report, Porto.

COYNE-BELLIER 1947. "Barrage de Venda Nova. Note de calcul complementaire", HICA, Internal report, Paris.

CSOPT 1987. "Dams Safety Regulations (in Portuguese)", Lisbon.

EDP 1983. "Varosa dam (in Portuguese)", Internal report, Porto.

EDP 1984a. "Bouçã dam. Analysis of structural behaviour (in Portuguese)", Internal report, Porto.

EDP 1984b. "Bouçã dam. Repair project (in Portuguese)", Internal report, Porto.

EDP 1984c. "Venda Nova dam. 1984 repair (in Portuguese)", Internal report, Porto.

EDP 1984d. "Grout curtain (2nd phase). Design of monitoring system (in Portuguese)", Internal report, Porto.

EDP 1988. "Bouçã. Foundation Treatment. Grout absorption recorded (in Portuguese)", Internal report, Porto.

ICOLD 1984. "Committee on Deterioration of Dams and Reservoirs", Final Report.

Kaloustian, E.S. 1984. "Statistical analysis of distribution of concrete dam rock foundations failures", International Conference on Safety of Dams, Coimbra.

LNEC 1949a. "Monitoring plan of Venda Nova dam (in Portuguese)", Internal report, Lisbon.

LNEC 1949b. "Experimental study of Venda Nova dam (in Portuguese)", Internal report, Lisbon.

LNEC 1950a. "Model study of stresses developed in the spillway zone of Venda Nova dam (in Portuguese)", Internal report, Lisbon.

LNEC 1950b. "Experimental study of Venda Nova dam in accordance with the modified design (in Portuguese)", Internal report, Lisbon.

LNEC 1954. "Plan of observation of Bouçã dam (in Portuguese)", Internal report, Lisbon.

LNEC 1955a. "Determination of the mechanical properties of Bouçã dam (in Portuguese)", Internal report, Lisbon.

LNEC 1955b. "Experimental study of Bouçã dam (in Portuguese)", Internal report, Lisbon.

LNEC 1961. "Observation of Venda Nova dam. Final report (in Portuguese)", Internal report, Lisbon.

LNEC 1969. "Experimental study of the influence of temperature variations on the factor of safety against failure of arch dams (in Portuguese)", Internal report, Lisbon.

LNEC 1971a. "Experimental study of Varosa dam (in Portuguese)", Internal report, Lisbon.

LNEC 1971b. "Study of Varosa dam foundation (in Portuguese)", Internal report, Lisbon.

LNEC 1971c. "Geophysical exploration on Varosa dam site (in Portuguese)", Internal report, Lisbon.

LNEC 1974. "Plan of observation of Varosa dam (in Portuguese)", Internal report, Lisbon.

LNEC 1976. "Basic date on earthquake hazard in Portugal (in Portuguese)", Internal report, Lisbon.

LNEC 1983. "Preliminary seismic survey for rock mass characterization of Bouçã dam (in Portuguese)", Internal report, Lisbon.

LNEC 1984a. "Varosa dam. Study of stability conditions by the finite element method (in Portuguese)", Internal report, Lisbon.

LNEC 1984b. "Study of joint sliding characteristics of Bouçã dam foundation (in Portuguese)", Internal report, Lisbon.

LNEC 1985. "Observation of Venda Nova dam. Analysis of the behaviour of the dam and foundation till December 1983 (in Portuguese)", Internal report, Lisbon.

LNEC 1986. "Geophysical characterization by seismic methods of the foundation rock mass of Varosa dam (in Portuguese)", Internal report, Lisbon.

LNEC 1987. "Study of behaviour up to failure of an arch dam by the finite element method (in Portuguese)", Internal report, Lisbon.

Neiva, J.M. and Sousa, A. 1981. "The geology of Venda Nova dam and uplift (in Portuguese)", University of Coimbra, Tech. Papers n. 91--92, Coimbra.

Neiva, J.M. 1982. "Geology of Bouçã dam site (in Portuguese)", EDP - Internal report, Porto.

Pedro, J.O. 1977. "Finite element stress analysis of arch dams", LNEC, Paper n. 479, Lisbon.

Pedro, J.O., et al. 1984. "Stress evaluation in concrete dams: the example of Varosa dam", International Conference on Safety of Dams, Coimbra.

Pedro, J.O. 1987. "Portuguese concrete dam engineering. The main structures and some studies (in Portuguese)", Iberian-American Conference on Hydraulic Schemes, Lisbon.

Pinto, J. 1983. "Deformability. Large flat jack method (in Portuguese)", LNEC, Lisbon.

PNCOLD - Portuguese Nat. Committee - ICOLD 1985. "Seepage and uplift measurements in the safety control of arch dams. The examples of Varosa and Bouçã dams", 15th Congress of ICOLD, Lausanne.

Rocha, M., et al. 1960. "Model tests and observation of Bouçã dam (in Portuguese)", LNEC, Tech. Paper n. 130, Lisbon.

Rocha, M. 1970. "New techniques in deformability testing of "in situ" rockmasses", LNEC, Tech. Paper n. 368, Lisbon.

RODIO 1946. "Report of the geologic survey programme for the Venda Nova dam (in Portuguese)", HICA, Internal report, Lisbon.

RODIO 1954a. "Bouçã dam. Report of the geologic survey of the site (in Portuguese)", HEZ, Internal report, Lisbon.

RODIO 1954b. "Bouçã dam. Grouting and drainage. Drawings (in Portuguese)", HEZ, Internal report, Lisbon.

RODIO 1965. "Varosa dam. Report of test hole programme (in Por-

tuguese)", CHENOP, Internal report, Lisbon.

RODIO 1986. "Venda Nova dam. Foundation Treatment. Final report (in Portuguese)", EDP, Internal report, Lisbon.

Silva, H. and Bravo, M. 1987. "Venda Nova dam. Some aspects of its behaviour and safety control (in Portuguese)", Iberian-American Conference on Hydraulic Schemes, Lisbon.

Silveira, A., et al. 1984. "Monitoring dams according to risk factors", International Conference on Safety of Dams, Coimbra.

STUCKY 1973. "Barrage du Varosa. Forages et injections du rocher de fondation et injection des joints du barrage. Spécifications techniques", CHENOP, Internal report, Lausanne.

STUCKY 1977. "Aménagement du Varosa. Rapport final", CHENOP, Internal report, Lausanne.

TECNASOL 1973. "Varosa dam. Drilling and grouting of foundation rock and grouting of structural joints. General comments on design and technical specifications. Basic general lines of an alternative proposal (in Portuguese)", CHENOP, Internal report, Lisbon.

TECNASOL 1983. "Report of geological survey (in Portuguese)", Internal report, Porto.

TECNASOL 1984. "Venda Nova dam. Report of foundation survey and improvement of drainage (in Portuguese)", EDP, Internal report, Lisbon.

TEIXEIRA DUARTE 1950. "Venda Nova dam. Watertightening and Strengthening of foundation (in Portuguese)", HICA, Internal technical paper, Lisbon.

USBR 1956. "Treatise on dams. United States Bureau of Reclamation", Denver.

Type	Name	River	Year of conclusion	General characteristics of the dam		General characteristics of the reservoir		
				Height (m)	Volume of concrete (10^3 m^3)	Volume of the reservoir (10^3 m^3)	Maximum capacity of spillways (m^3/sec)	Purpose
Multiple and massive gravity	Lindoso	Lima	1970	26	10	550	2 000	H
	Póvoa	Nisa	1938	32	32	2 000	110	H
	Poio	Nisa	1932	18	8	6 400	110	H
	Guilhofrei	Ave	1938	49	55	22 000	445	H
	Burgães	Caima	1940	30	4	400	74	I
	Andorinhas	Ave	1945	25	12	1 200	450	H
	Idanha	Ponsul	1949	56	64	77 800	800	IH
	Penide	Cávado	1951	15	9	500	2 228	H
	Freigil	Cabrum	1955	17		140	425	H
	Covão de Ferro	Alforfa	1956	35	111	1 100	52	H
	Vale do Rossim	Ferveça	1956	27	24	3 500	66	H
	Furadouro	Raia	1958	17	16	350	2 500	I
	Lagoa Comprida	Carriça	1958	29	100	13 800	92	H
	Gameiro	Raia	1960	30	11	1 250	2 800	IH
	Alto Cávado	Cávado	1964	29	29	3 300	410	H
	Alto Rabagão	Rabagão	1964	60	1 117	569 000	500	H
	Além da Fazenda	Além da Fazenda	1967	20	3	50	50	H
	Rio da Mula	Rio da Mula	1968	17		300		S
	Penha Garcia	Ponsul	1968	25	14	1 070	47	IS
	Raiva	Mondego	1968	36	85	21 000	2 000	H
	Cova de Viriato	Paiva	1968	28	19	1 500	4	S
	Monte Novo	Degebe	1968	30	31	15 280	600	IS
	Corgas	Lima	s.d.	25	13	660	140	S
	Torrão	Tâmega	1987	69	224	124 000	4 150	H
Spillweir	Belver	Tejo	1952	27	99	12 600	18 000	H
	Carrapatelo	Douro	1972	57	190	140 000	22 000	HN
	Fratel	Tejo	1973	43	124	93 000	16 500	H
	Régua	Douro	1973	42	198	91 000	21 500	HN
	Valeira	Douro	1974	48	220	97 000	18 000	HN
	Coimbra	Mondego	1981	40	61	1 600	2 000	IS
	Pocinho	Douro	1982	49	120	81 000	15 000	HN
	Crestuma	Douro	1985	60	290	106 000	26 000	HN
	Fagilde	Dão	1988	27	10	2 800	580	S
Arch-gravity	Santa Luzia	Ouhais	1942	76	80	53 700	230	H
	Alto Ceira	Ceira	1949	38	7	1 200	100	H
	Castelo do Bode	Zêzere	1951	115	446	1 100 000	4 000	H
	Venda Nova	Rabagão	1951	97	228	96 500	1 100	H
	Covão do Meio	Loriga	1953	25	9	1 400	40	H
	Bemposta	Douro	1964	87	316	128 000	11 000	H
Arch (double curvature)	Salamonde	Cávado	1953	75	93	63 000	1 700	H
	Cabril	Zêzere	1954	136	360	719 000	2 200	H
	Bouçã	Zêzere	1955	65	70	49 000	2 200	H
	Caniçada	Cávado	1955	76	90	152 700	1 700	H
	Bravura	Odeáxere	1958	41	19	35 000	21	IH
	Picote	Douro	1958	100	205	63 750	11 000	H
	Alto Rabagão	Rabagão	1964	94	1 117	569 000	500	H
	Vilar dos Paraus	Ramos	1972	94	294	118 000	280	H
	Varosa	Varosa	1976	76	81	14 440	1 200	H
	Fronhas	Alva	1985	62	153	89 000	560	HI
Buttresses	Pracana	Ocreza	1951	65	129	116 500	1 650	H
	Miranda	Douro	1961	80	260	28 900	11 000	H
	Caia	Caia	1967	52	242	203 000	430	IS
	Ponte	Ponte	1968	44	176	96 300	108	IS
Multi-arch	Odivelas	Odivelas	1947	55	47	96 000	650	I
	Aguieira	Mondego	1981	89	380	450 000	2 150	H

H - Power production
I - Irrigation
N - Navigation
S - Water supply

Fig. 1 - Main concrete dams of Portuguese hydraulic schemes

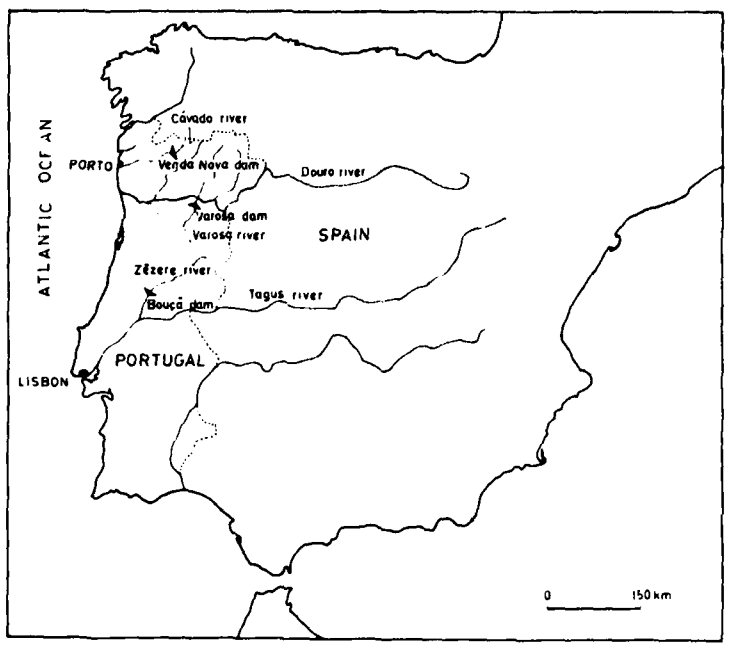
ATLANTIC OCEAN
PORTO
Cávado river
Venda Nova dam
Douro river
Varosa dam
Varosa river
SPAIN
Zêzere river
Bouça dam
Tagus river
PORTUGAL
LISBON
0
150 km

E-2

PLAN

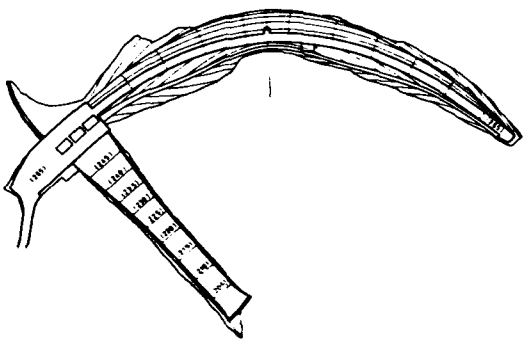

ELEVATION

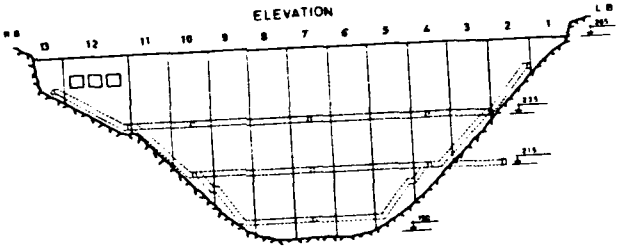

CROSS - SECTIONS

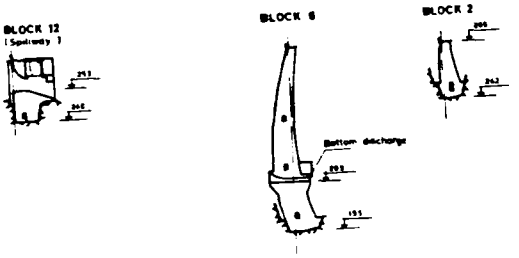

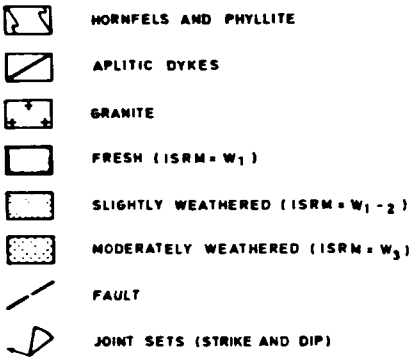
HORNFELS AND PHYLLITE
APLITIC DYKES
GRANITE
FRESH (ISRM = W_1)
SLIGHTLY WEATHERED (ISRM = W_{1-2})
MODERATELY WEATHERED (ISRM = W_3)
FAULT
JOINT SETS (STRIKE AND DIP)

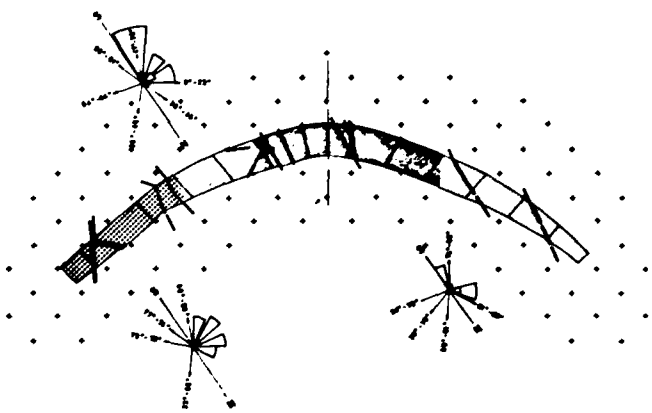

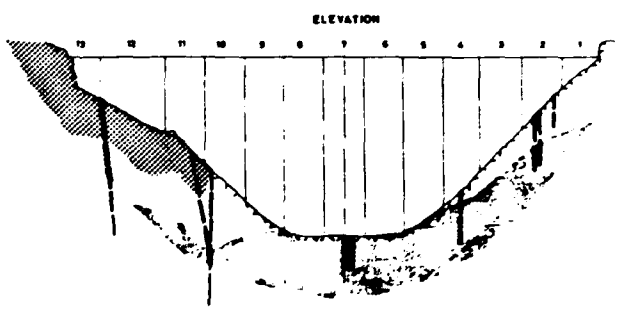
ELEVATION

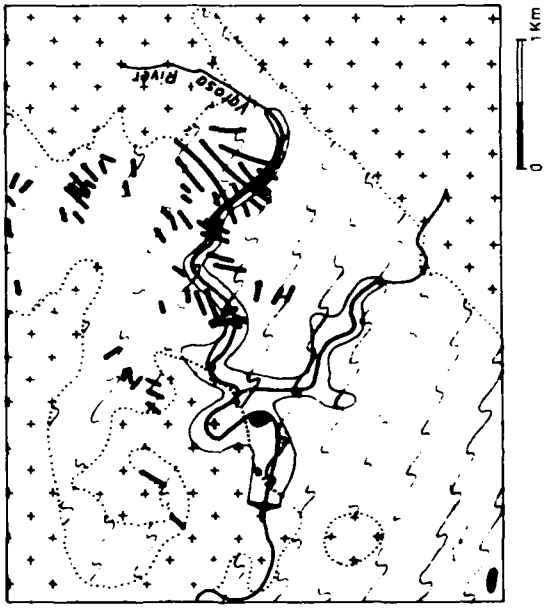
Yuroso River
1 Km
0

MECHANICAL TESTS DURING THE EXPLORATION PHASE

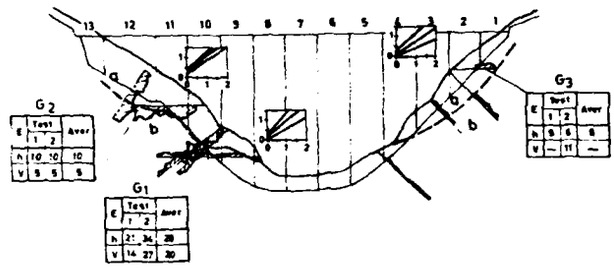

HYDRAULIC TESTS

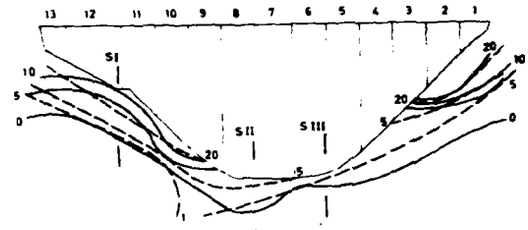

HYDRAULIC TESTS DURING CONSOLIDATION

SECTION I SECTION II SECTION III

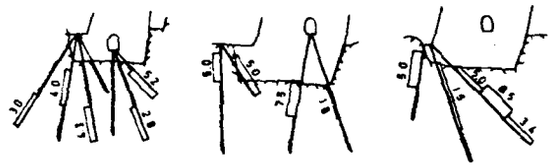

PERMEABILITY TESTS

K – Equivalent permeability of rock mass (10^{-7} m.s^{-1})

– Line of equal permeability

– Porosity index of rock specimens (%)

MECHANICAL TESTS

V_L – Longitudinal wave velocity (m.s^{-1})

– Wave velocity zoning

E – Deformability moduli of rock mass (10^3 MPa)

h - horizontal forces

v - vertical forces

– Sliding joint tests on rock specimens

σ – Normal forces (MPa)

τ – Tangential forces (MPa)

μ – Upper limit of Coulomb law

m – Medium limit of Coulomb law

l – Lower limit of Coulomb law

G1, 2, 3 – Gallerys for in situ tests

a – $V_L < 2500$ m/s

b – $V_L > 2500$ m/s

– – – – Before construction

———— – During grout injections


– Absorption in Lugeon units (LU)

– Less than 1LU

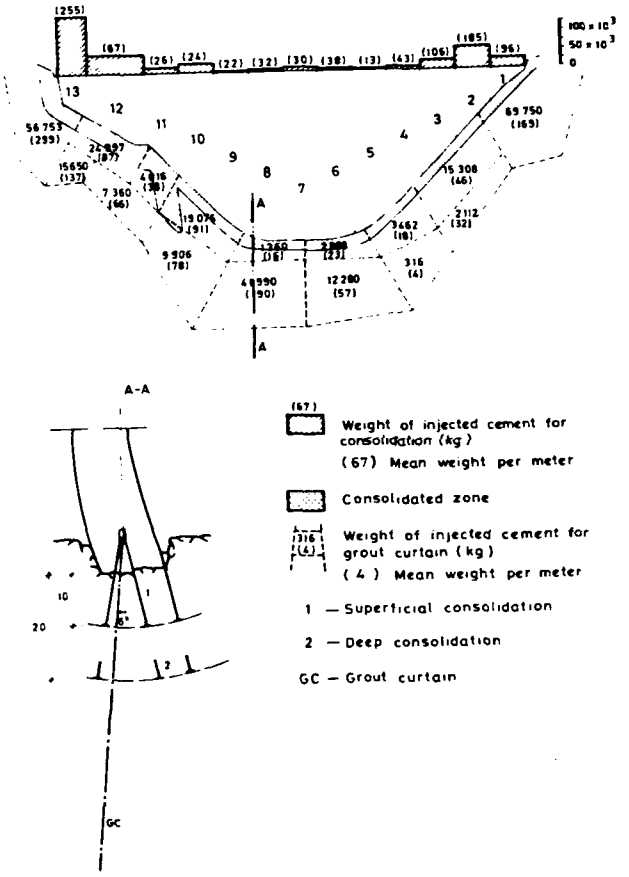
(255)
(67)
(26)
(24)
(22)
(32)
(30)
(38)
(13)
(43)
(106)
(185)
(96)
100 x 10³
50 x 10³
0
13
12
11
10
9
8
7
6
5
4
3
2
1
56 753
(299)
22 897
(87)
15650
(137)
7 360
(66)
4 316
(38)
15 076
(91)
9 906
(78)
360
(18)
2 988
(23)
40 990
(190)
12 280
(57)
3462
(18)
316
(4)
2112
(32)
15 308
(46)
89 750
(169)
A
A
A-A
10
20
1
2
GC
(67)
Weight of injected cement for consolidation (kg)
(67) Mean weight per meter
Consolidated zone
316
(4)
Weight of injected cement for grout curtain (kg)
(4) Mean weight per meter
1 — Superficial consolidation
2 — Deep consolidation
GC — Grout curtain

Plumb line and measuring points

▽ Joint meters

● Temperature measuring section

○ Strain measuring section

Rock meters

Piezometer

GEODETIC NETWORK

△ Pillar

▲ Fixed points

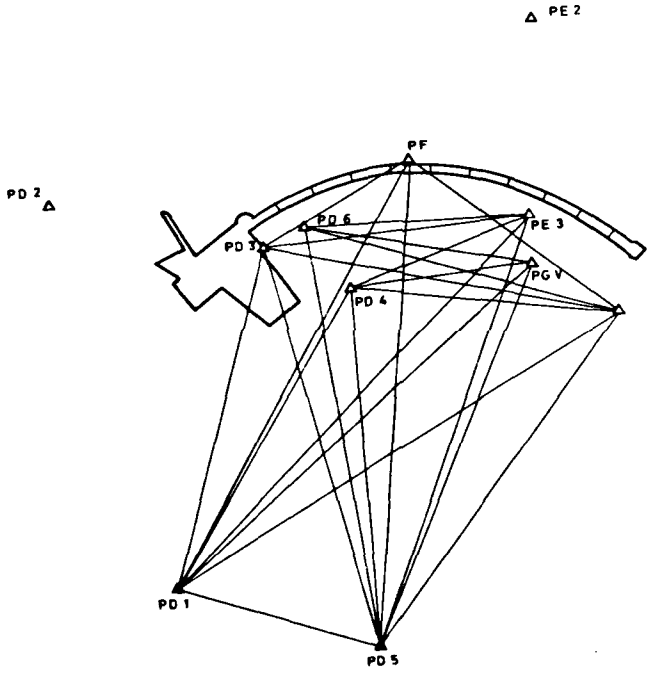

F-7

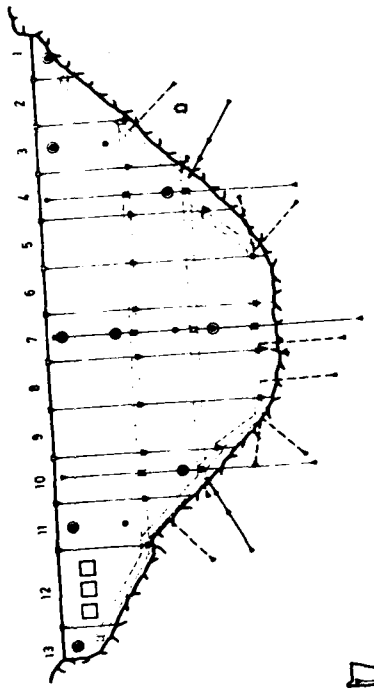
1
2
3
4
5
6
7
8
9
10
11
12
13

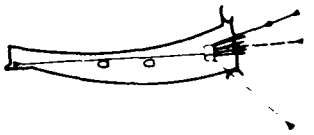

FEBRUARY, 77

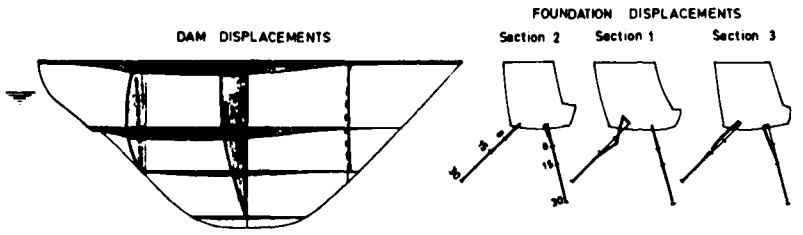

JANUARY, 78

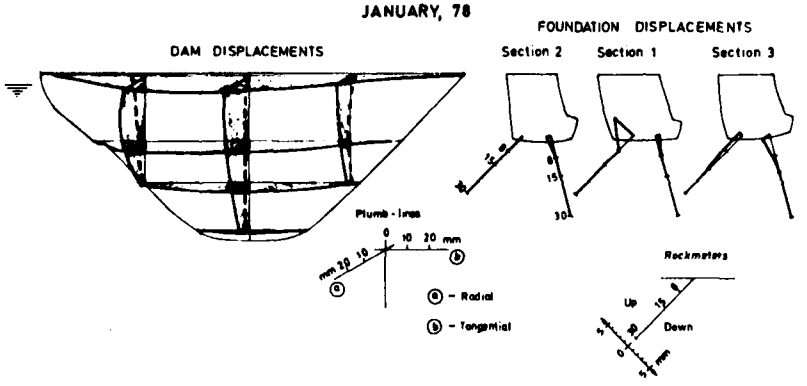

/ X

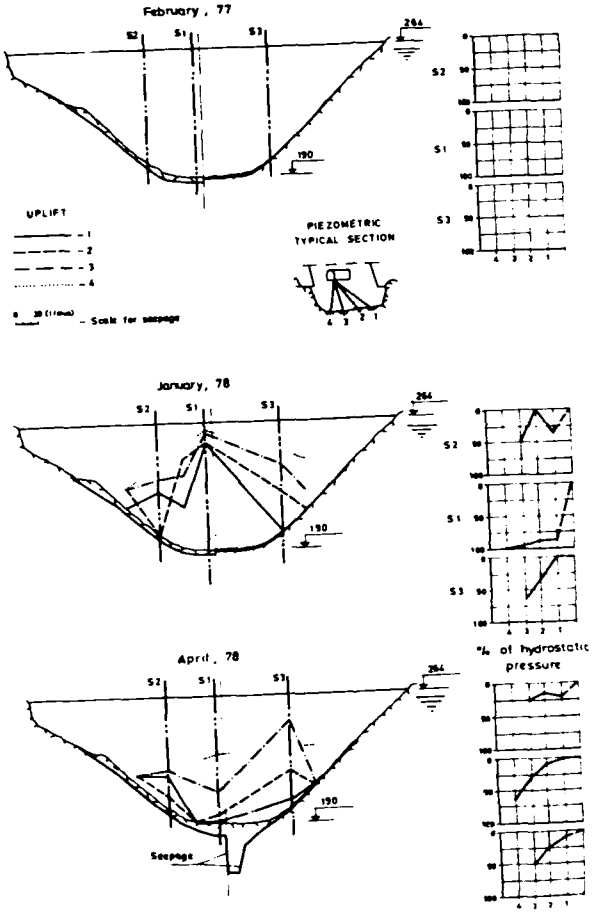
February , 77
S2
S1
S3
264
190
UPLIFT
1
2
3
4
PIEZOMETRIC
TYPICAL SECTION
January, 78
April , 78
Seepage
% of hydrostatic
pressure

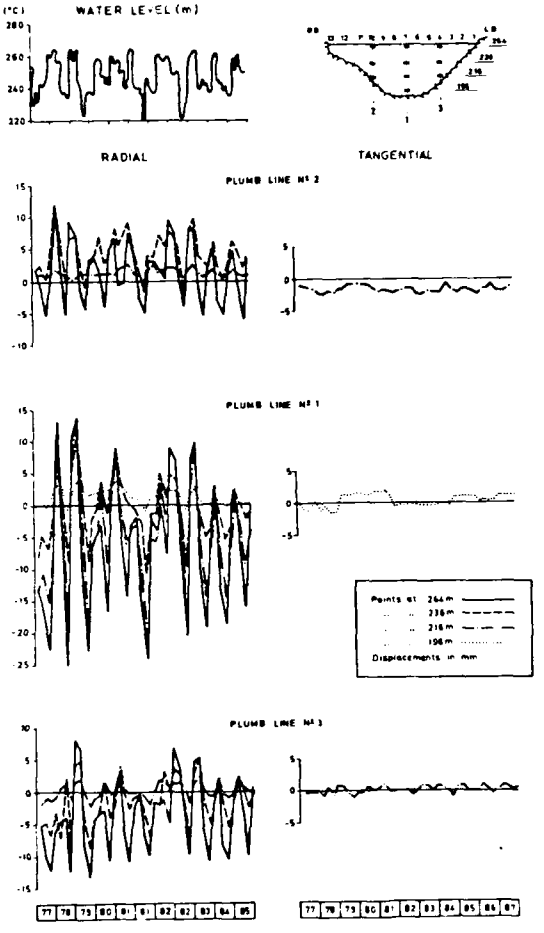
(°C)
WATER LEVEL (m)
280
260
240
220
RADIAL
TANGENTIAL
PLUMB LINE Nº 2
PLUMB LINE Nº 1
PLUMB LINE Nº 3
Points at 264 m
236 m
216 m
196 m
Displacements in mm
77 78 79 80 81 82 83 84 85
77 78 79 80 81 82 83 84 85 86 87

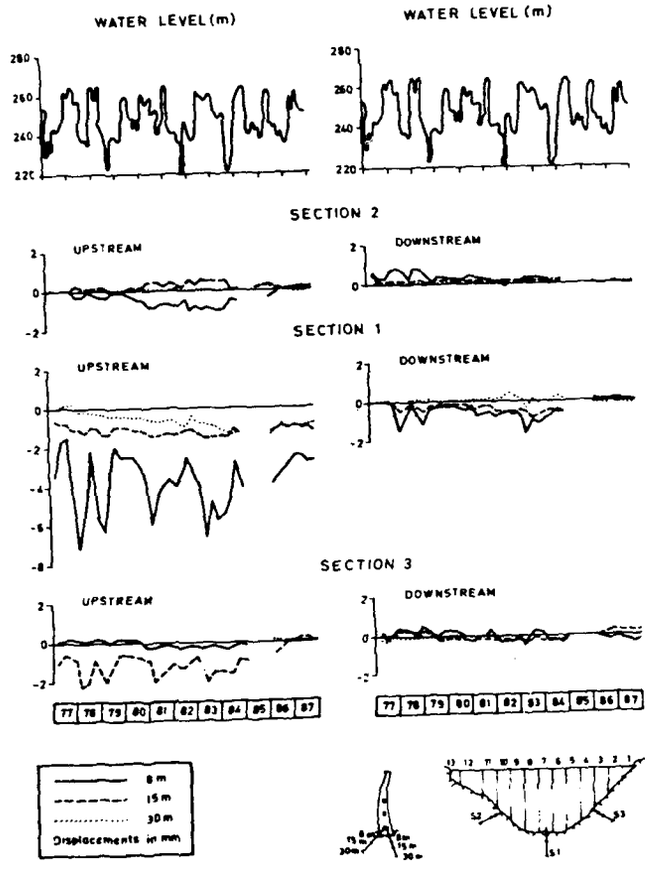
WATER LEVEL(m)
WATER LEVEL (m)
280
260
240
220
SECTION 2
UPSTREAM
DOWNSTREAM
SECTION 1
UPSTREAM
DOWNSTREAM
SECTION 3
UPSTREAM
DOWNSTREAM
77 78 79 80 81 82 83 84 85 86 87
8 m
15 m
30 m
Displacements in mm
S1
S2
S3

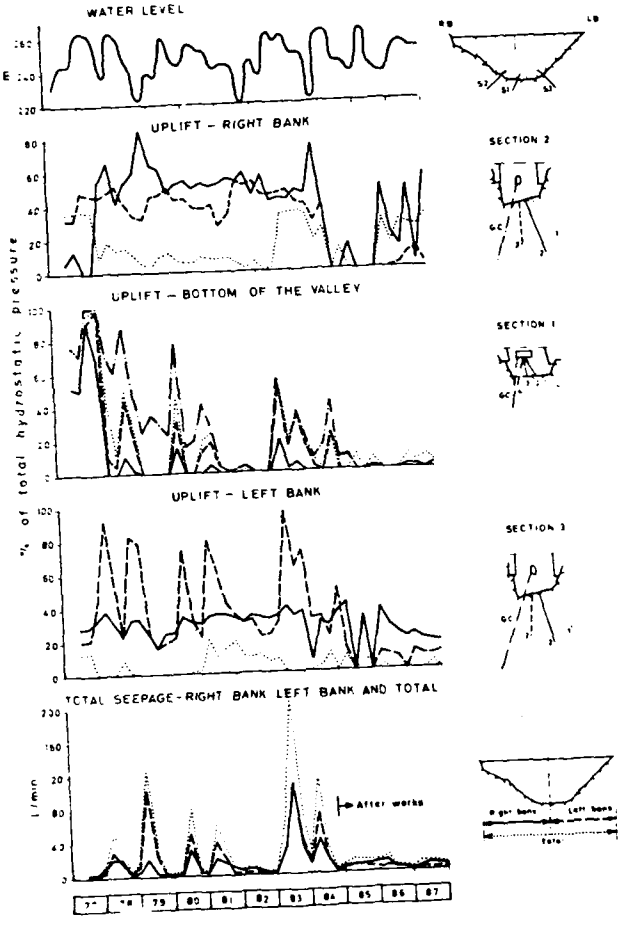
WATER LEVEL
UPLIFT – RIGHT BANK
UPLIFT – BOTTOM OF THE VALLEY
UPLIFT – LEFT BANK
% of total hydrostatic pressure
TOTAL SEEPAGE – RIGHT BANK LEFT BANK AND TOTAL
l/min
after works
SECTION 2
SECTION 1
SECTION 3
RB
LB
79
80
81
82
83
84
85
86
87

FEBRUARY

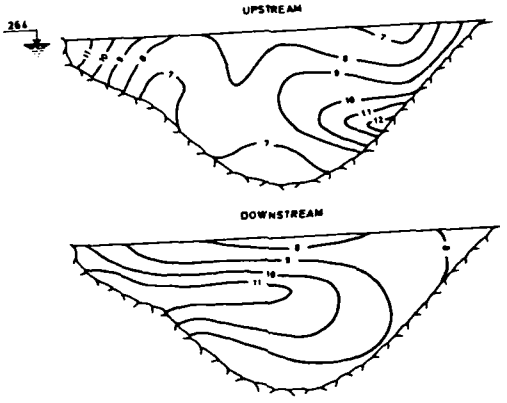

MAY

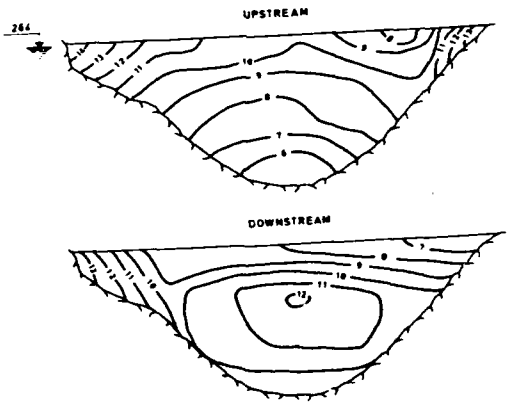

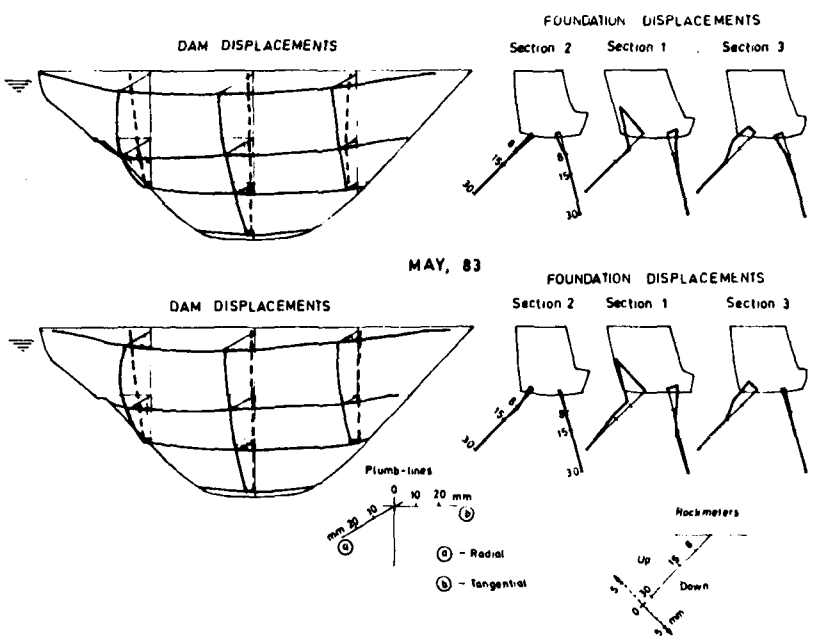
MARS, 78
DAM DISPLACEMENTS
FOUNDATION DISPLACEMENTS
Section 2
Section 1
Section 3
MAY, 83
DAM DISPLACEMENTS
FOUNDATION DISPLACEMENTS
Section 2
Section 1
Section 3
Plumb-lines
Radial
Tangential
Rockmeters
Up
Down

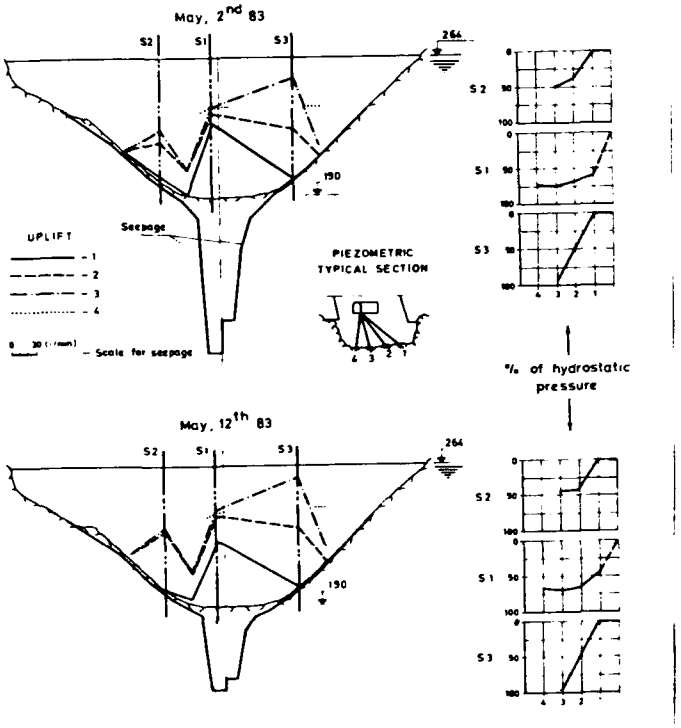
May, 2nd 83
S2
S1
S3
264
190
Seepage
UPLIFT
1
2
3
4
Scale for seepage
PIEZOMETRIC
TYPICAL SECTION
S2
S1
S3
% of hydrostatic
pressure
May, 12th 83
S2
S1
S3
264
190
S2
S1
S3

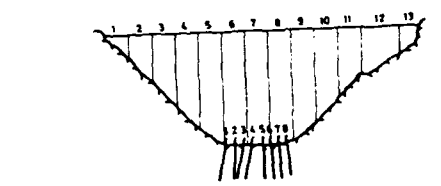

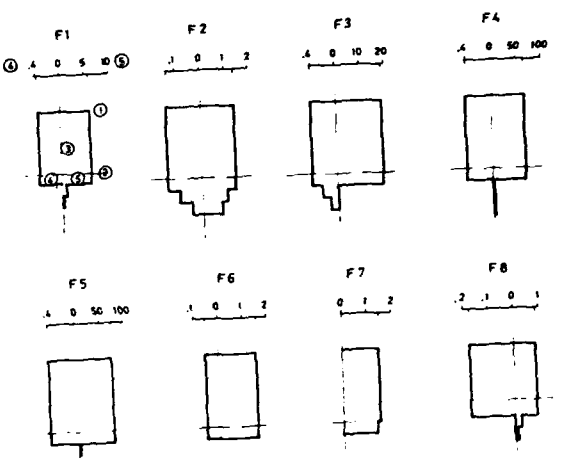

① Floor of drainage gallery
② Base of dam
③ Drain
④ Uplift when drains plugged (MPa)
⑤ Seepage when drains opened (l/min)

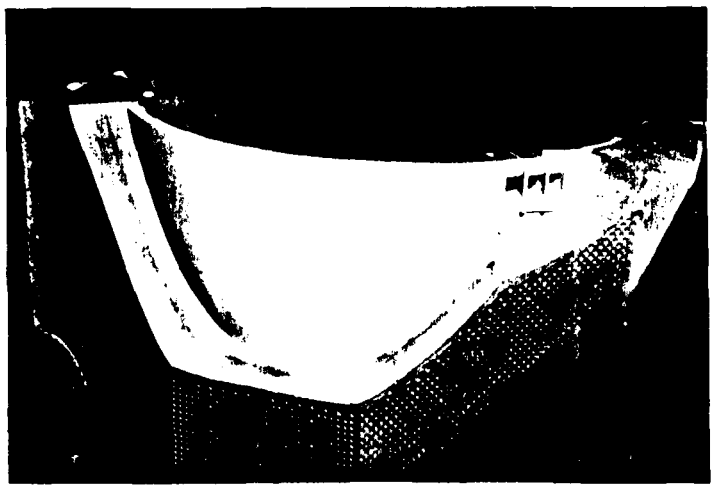

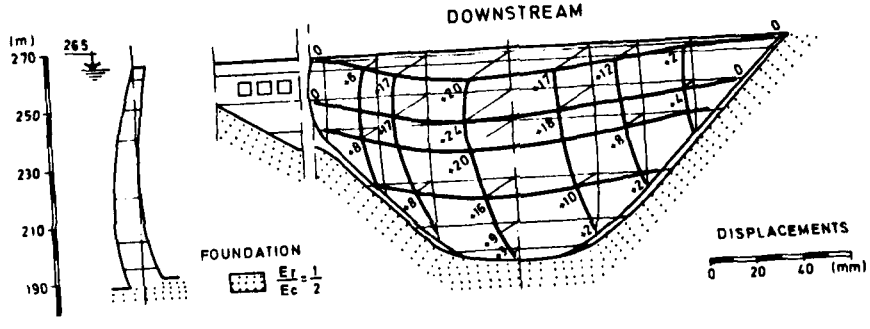
DOWNSTREAM
(m)
270
250
230
210
190
265
FOUNDATION
Er/Ec = 1/2
DISPLACEMENTS
0 20 40 (mm)

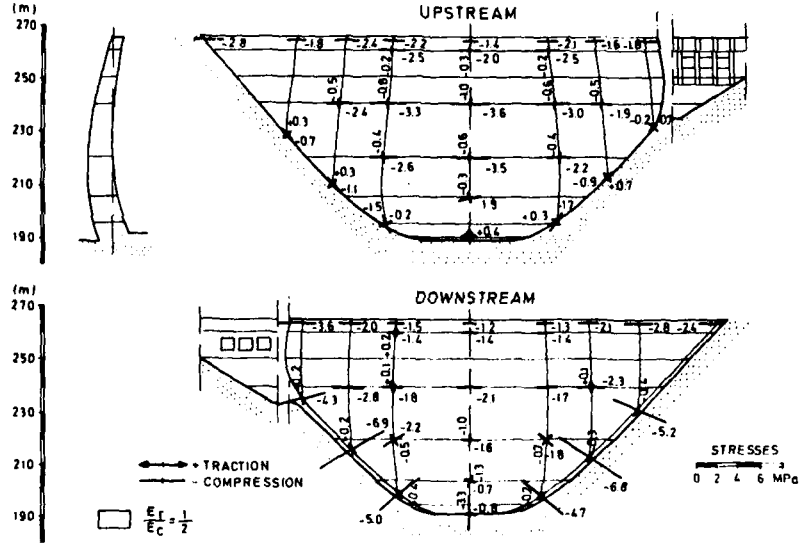
(m)
270
250
230
210
190
UPSTREAM
DOWNSTREAM
+ TRACTION
- COMPRESSION
$\frac{E_I}{E_C} = \frac{1}{2}$
STRESSES
0 2 4 6 MPa

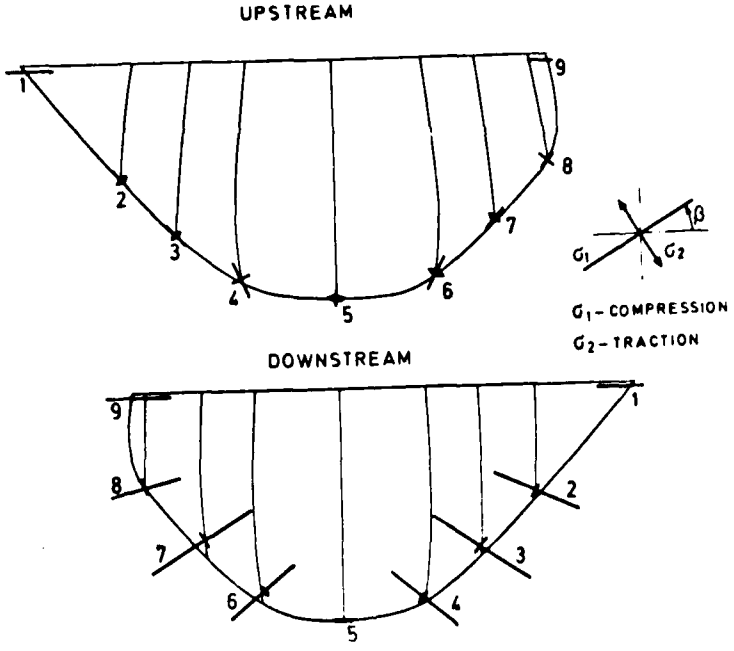
UPSTREAM
1
2
3
4
5
6
7
8
9
β
σ1
σ2
σ1 - COMPRESSION
σ2 - TRACTION
DOWNSTREAM
9
8
7
6
5
4
3
2
1

Point	Elevation	Upstream			Downstream		
	(m)	σ_1	σ_2	$\beta°$	σ_1	σ_2	$\beta°$
1	264.0	-2.8	0.0	0	-2.4	0.0	0
2	233.5	-0.7	+0.3	-48	-5.2	-0.4	-24
3	214.5	-1.1	-0.3	-44	-6.8	-0.3	-32
4	200.0	-1.5	-0.2	-63	-4.7	+0.2	-38
5	190.0	+0.4	+0.8	90	-3.3	-0.8	90
6	200.0	-1.7	+0.3	62	-5.0	+0.4	39
7	214..	-0.9	+0.7	50	-6.9	-0.2	30
8	233.5	-0.7	-0.2	54	-4.3	-0.2	15
9	264.0	-1.8	0.0	0	-3.6	0.0	0

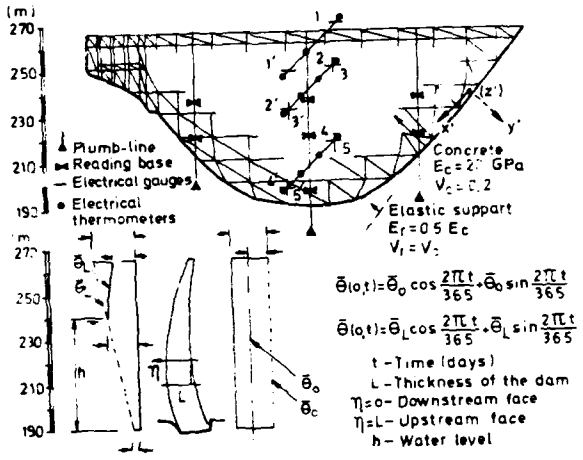
(m)
270
250
230
210
190
Plumb-line
Reading base
Electrical gauges
Electrical thermometers
Concrete
Elastic suppart
$E_f = 0.5\ E_c$
$V_f = V_c$
$\bar{\theta}(o,t)=\bar{\theta}_o \cos\frac{2\pi t}{365}+\bar{\theta}_o \sin\frac{2\pi t}{365}$
$\bar{\theta}(o,t)=\bar{\theta}_L \cos\frac{2\pi t}{365}+\bar{\theta}_L \sin\frac{2\pi t}{365}$
t – Time (days)
L – Thickness of the dam
η=o – Downstream face
η=L – Upstream face
h – Water level

F-21

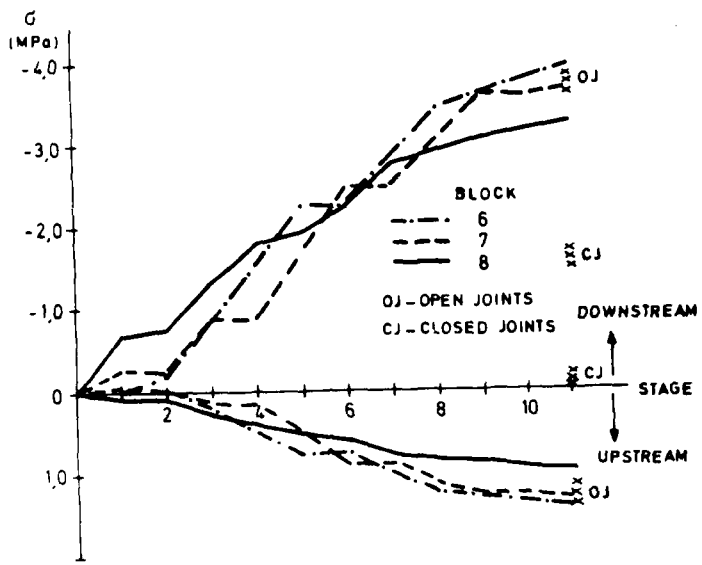
σ
(MPa)
-4,0
-3,0
-2,0
-1,0
0
1,0
2
4
6
8
10
OJ
CJ
BLOCK
6
7
8
OJ - OPEN JOINTS
CJ - CLOSED JOINTS
DOWNSTREAM
STAGE
UPSTREAM

1 11

Act.	crown of the crest			base cent. cantilever		
	TD	RD	VD	TD	RD	VD
HP	-0.69	+26.04	-4.10	-0.00	+2.92	-0.92
UP	-0.05	-0.07	-0.80	-0.00	-0.16	-0.84
DT	-0.01	+17.79	+4.65	-0.00	+0.37	-0.71
UT	+0.18	-15.60	-4.99	+0.00	-0.92	+1.31

displ.
(mm)
TD-tang.
RD-radial
VD-vert.

Acti.	σ_U	σ_D	τ
W	-3.76	+1.25	0
HP	+3.71	-3.05	+0.75
UP	+0.44	+0.21	-0.05
DT	+0.70	-0.17	+0.09
UT	-1.88	+0.90	-0.22

σ_U -upstream normal stress

σ_D -downstream normal stress

τ - shear stress

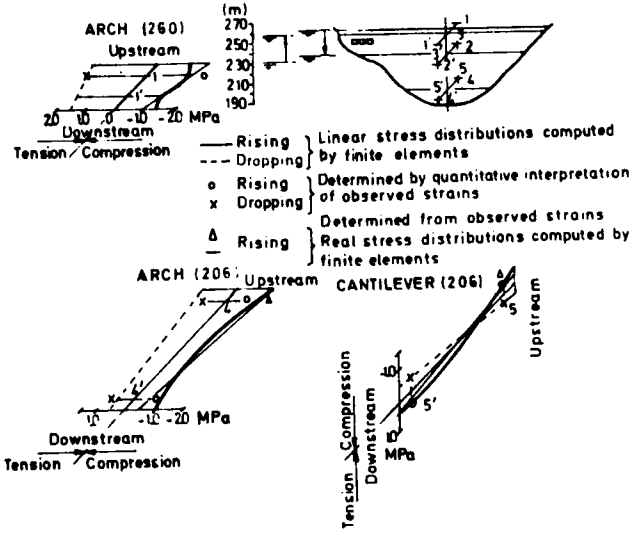
ARCH (260)
Upstream
Downstream
Tension / Compression
20 10 0 -10 -20 MPa
(m)
270
250
230
210
190
Rising
Dropping
Linear stress distributions computed by finite elements
o Rising
x Dropping
Determined by quantitative interpretation of observed strains
Δ Rising
Determined from observed strains
Real stress distributions computed by finite elements
ARCH (206)
Upstream
Downstream
Tension / Compression
10 -10 -20 MPa
CANTILEVER (206)
Upstream
Tension / Compression
Downstream
10
MPa

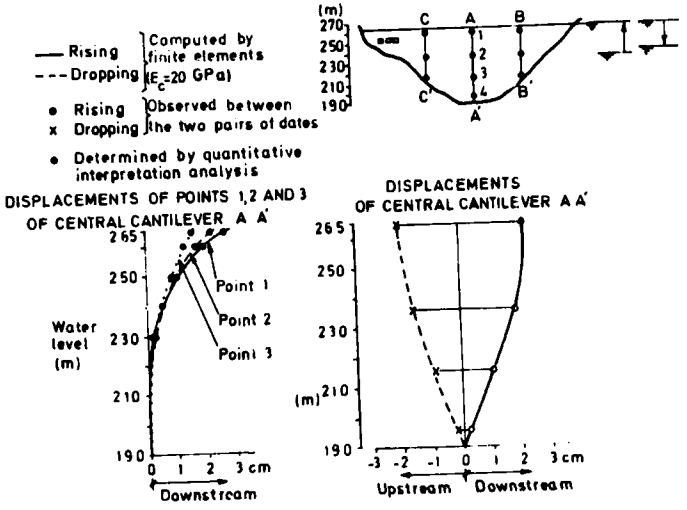
Rising
Dropping
Computed by finite elements (E_c=20 GPa)
Rising
Dropping
Observed between the two pairs of dates
Determined by quantitative interpretation analysis
DISPLACEMENTS OF POINTS 1,2 AND 3 OF CENTRAL CANTILEVER A A'
Water level (m)
265
250
230
210
190
Point 1
Point 2
Point 3
0 1 2 3 cm
Downstream
(m)
270
250
230
210
190
C
A
B
C'
A'
B'
1
2
3
4
DISPLACEMENTS OF CENTRAL CANTILEVER A A'
265
250
230
(m) 210
190
-3 -2 -1 0 1 2 3 cm
Upstream
Downstream

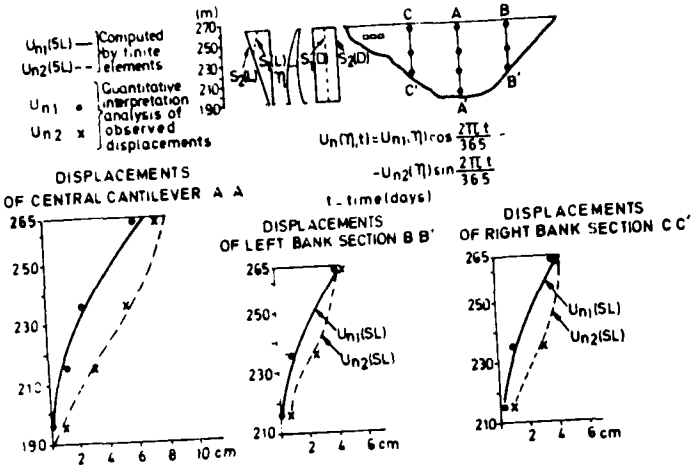
Un1(SL) — Computed by finite
Un2(SL) -- elements
Un1 • Quantitative interpretation
Un2 x analysis of observed displacements
(m)
270
250
230
210
190
S1(L)
S2(L)
S1(D)
S2(D)
C
A
B
C'
A'
B'
Un(η,t)=Un1(η)cos 2πt/365 -
-Un2(η)sin 2πt/365
t - time(days)
DISPLACEMENTS
OF CENTRAL CANTILEVER A A'
265
250
230
210
190
2 4 6 8 10 cm
DISPLACEMENTS
OF LEFT BANK SECTION B B'
Un1(SL)
Un2(SL)
2 4 6cm
DISPLACEMENTS
OF RIGHT BANK SECTION C C'
Un1(SL)
Un2(SL)
2 4 6cm

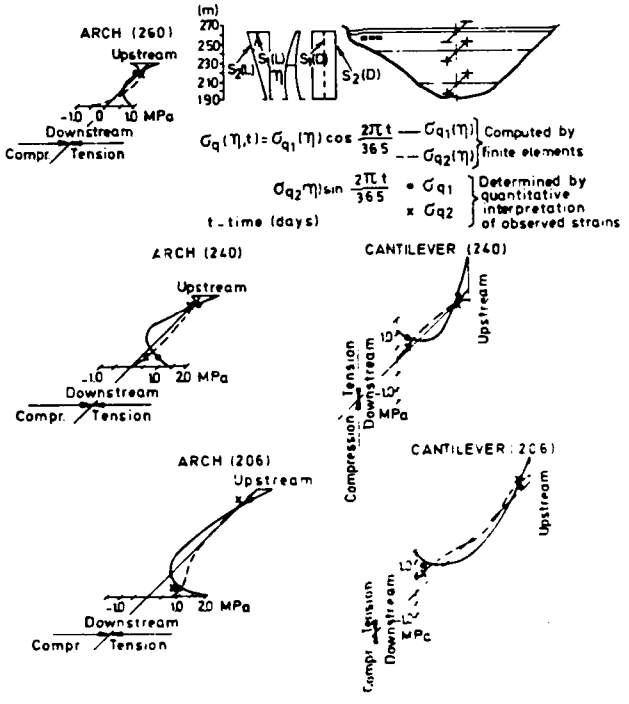
ARCH (260)
Upstream
-1.0 0 1.0 MPa
Downstream
Compr. Tension
(m)
270
250
230
210
190
S1(U)
S1(D)
S2(U)
S2(D)
$\sigma_q(\eta,t) = \sigma_{q_1}(\eta)\cos\frac{2\pi t}{365} - \sigma_{q_1}(\eta)$ Computed by
$- - \sigma_{q_2}(\eta)$ finite elements
$\sigma_{q_2}(\eta)\sin\frac{2\pi t}{365}$ • σ_{q_1}
× σ_{q_2} Determined by quantitative interpretation of observed strains
t - time (days)
ARCH (240)
Upstream
-1.0 1.0 2.0 MPa
Downstream
Compr. Tension
CANTILEVER (240)
Upstream
1.0
-1.0
MPa
Compression Tension
Downstream
ARCH (206)
Upstream
-1.0 1.0 2.0 MPa
Downstream
Compr Tension
CANTILEVER (206)
Upstream
1.0
-1.0
MPa
Compr Tension
Downstream

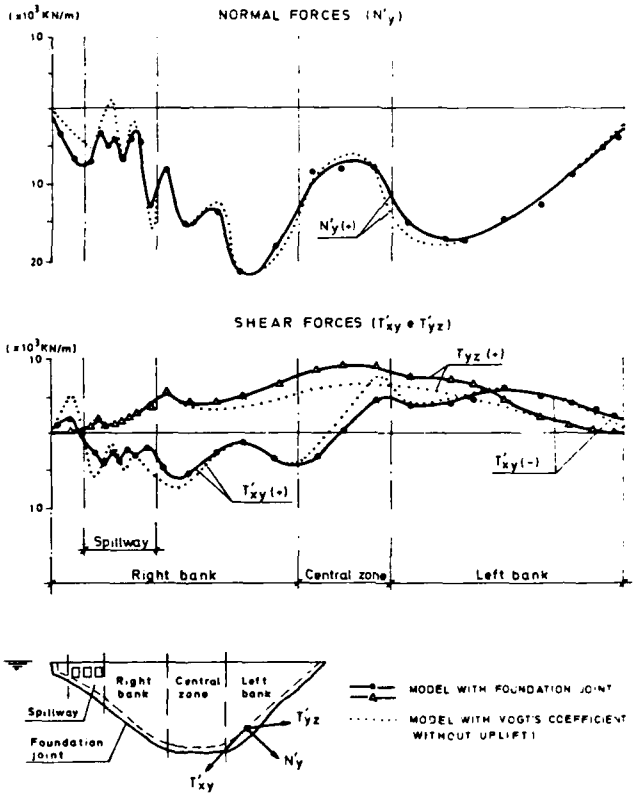
(x10³KN/m)
NORMAL FORCES (N'y)
10
10
20
N'y(+)
SHEAR FORCES (T'xy e T'yz)
(x10³KN/m)
10
10
Tyz (+)
T'xy(-)
T'xy(+)
Spillway
Right bank
Central zone
Left bank
Right bank
Central zone
Left bank
Spillway
Foundation joint
T'yz
N'y
T'xy
MODEL WITH FOUNDATION JOINT
MODEL WITH VOGT'S COEFFICIENT WITHOUT UPLIFT)

Zone	Rt (MPa)	C (MPa)		ϕ (°)	
		med.	min.	med.	min.
1	0	0.07	0	35	24
2	0	0.13	0	41	30
3	0	0.27	0.11	40	36

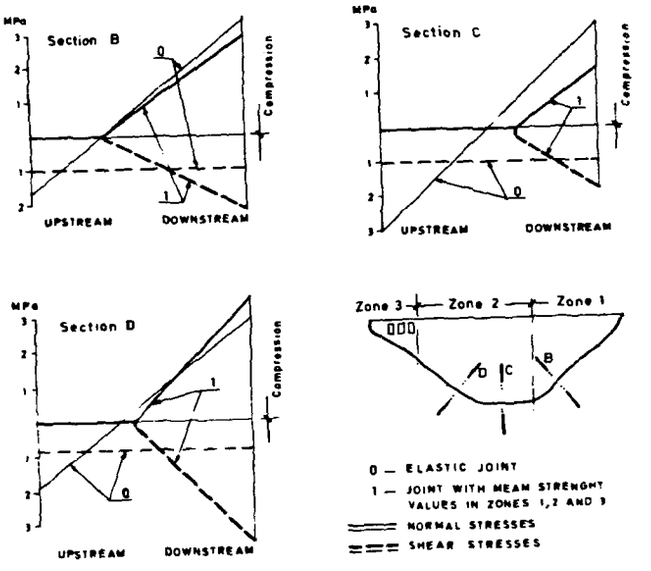
MPa
Section B
Compression
UPSTREAM
DOWNSTREAM
Section C
Section D
Zone 3
Zone 2
Zone 1
0 — ELASTIC JOINT
1 — JOINT WITH MEAN STRENGHT VALUES IN ZONES 1,2 AND 3
NORMAL STRESSES
SHEAR STRESSES

LEFT BANK TREATMENT

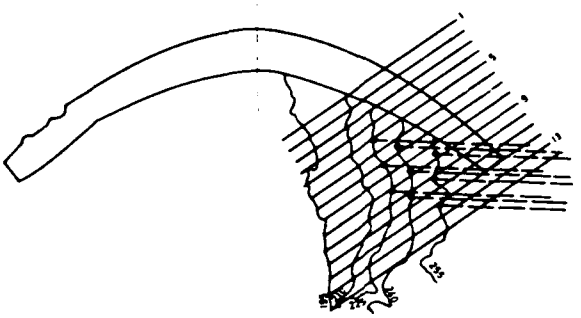

SECTION 1

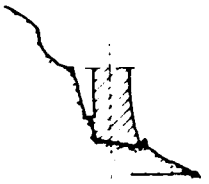

SECTION 5

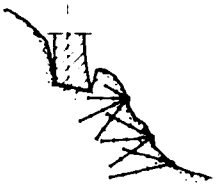

SECTION 9

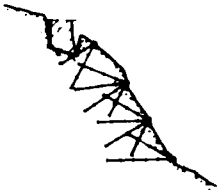

Consolidation profil

Anchorage

Heading level of fans

Injection borehole

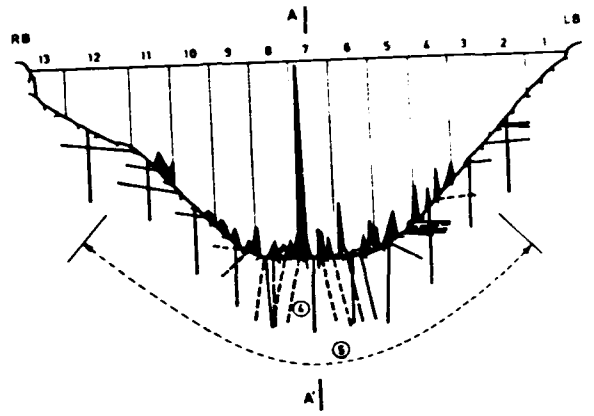

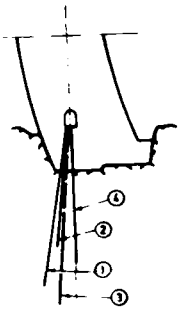

① - Upstream cut-off curtain
② - Resine grout curtain
③ - Downstream cut-off curtain
④ - Drains (—— ancient, —— new)
⑤ - Grouting zone
⑥ - Resine absorption (1mm = 100 liters)

0 10 (m)

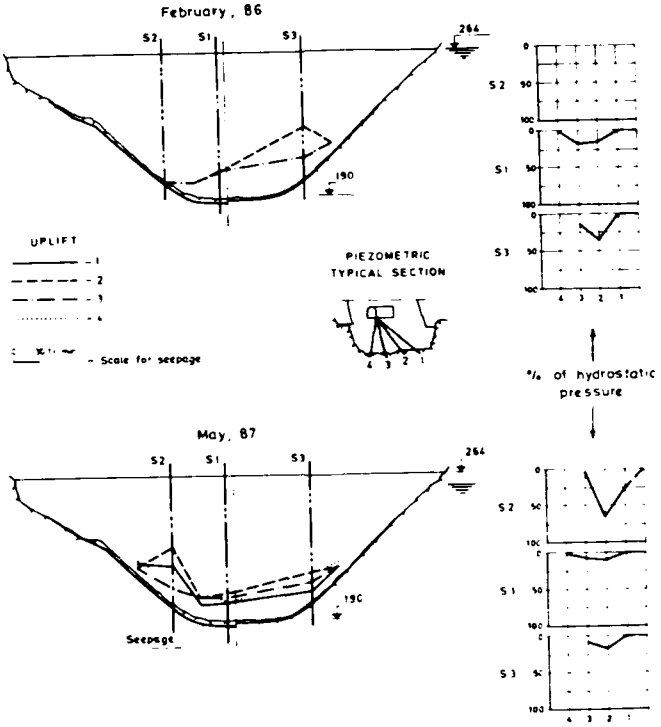
February, 86
S2
S1
S3
264
190
UPLIFT
1
2
3
4
Scale for seepage
PIEZOMETRIC
TYPICAL SECTION
4 3 2 1
S2
S1
S3
0
50
100
% of hydrostatic
pressure
May, 87
Seepage

FEBRUARY, 86

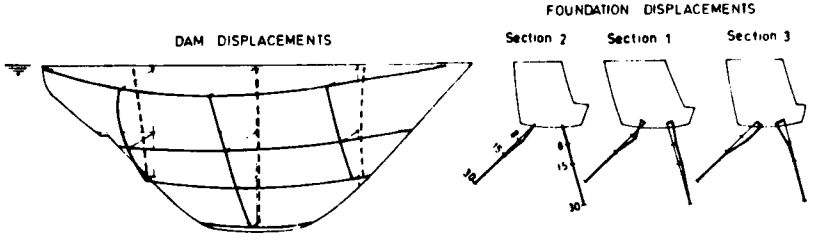

MAY, 87

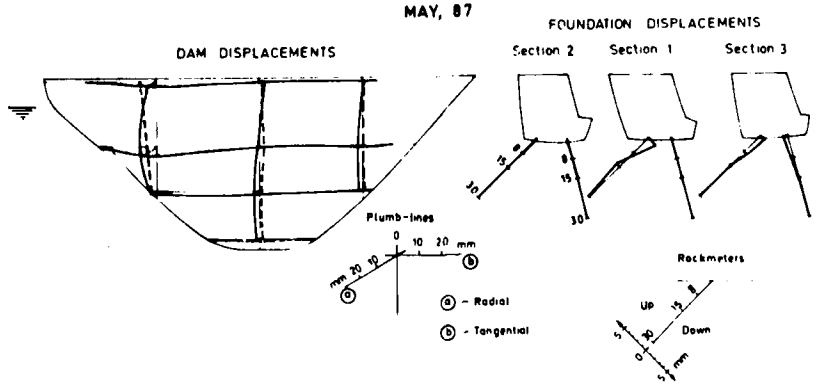

CROSSHOLE AND UPHOLE
SEISMIC TESTS

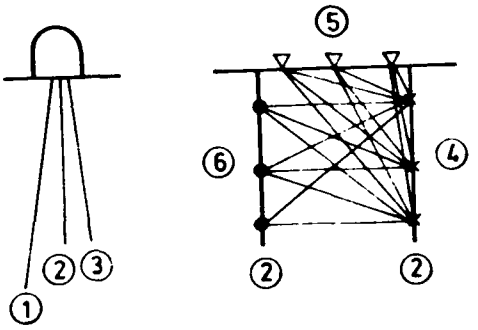

① Grout curtain
② Borehole
③ Drain
④ Seismic shoot
⑤ Geophone
⑥ Hydrophone

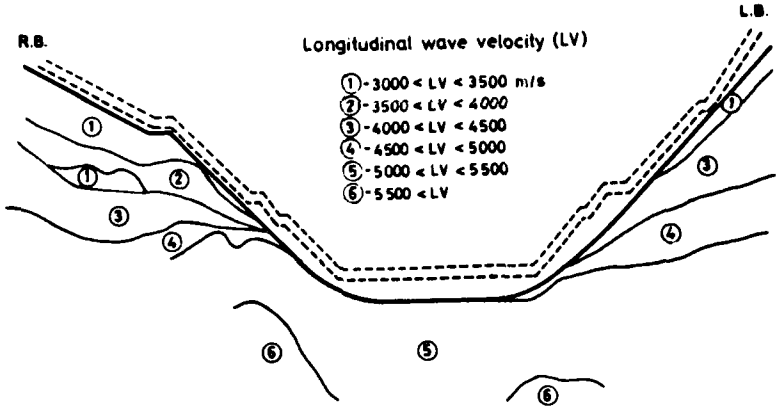
R.B.
L.B.
Longitudinal wave velocity (LV)
① - 3000 < LV < 3500 m/s
② - 3500 < LV < 4000
③ - 4000 < LV < 4500
④ - 4500 < LV < 5000
⑤ - 5000 < LV < 5500
⑥ - 5500 < LV

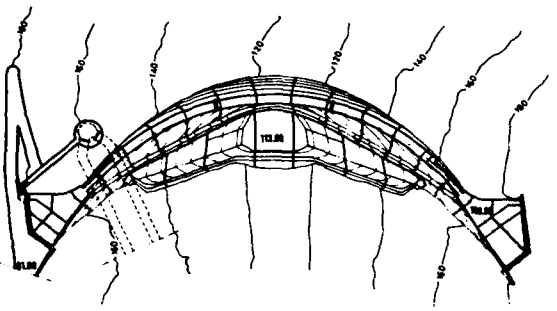

ELEVATION

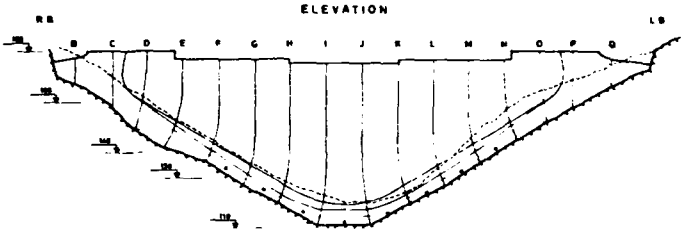

CROSS - SECTIONS

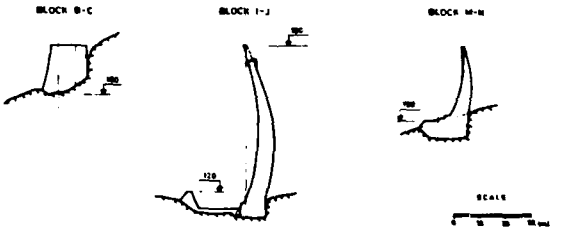

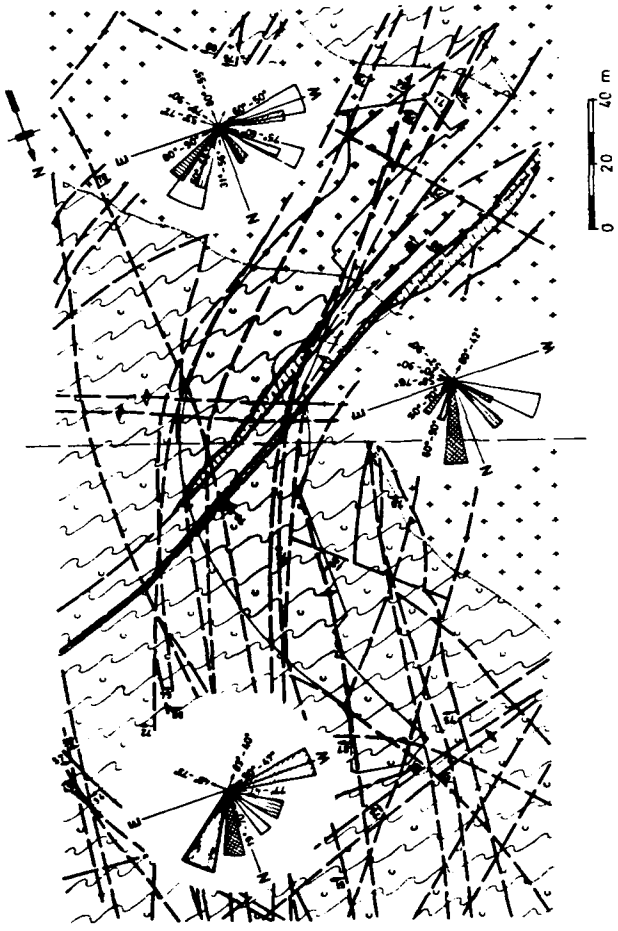
N
0
20
40 m

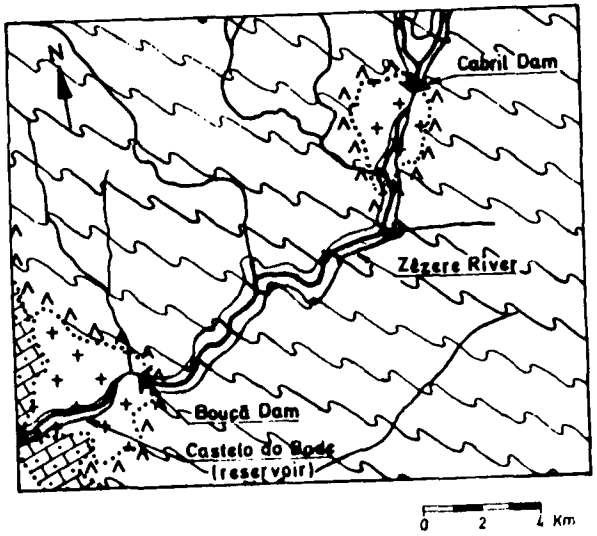
N
Cabril Dam
Zêzere River
Bouçã Dam
Castelo do Bode
(reservoir)
0
2
4 Km

F. 38

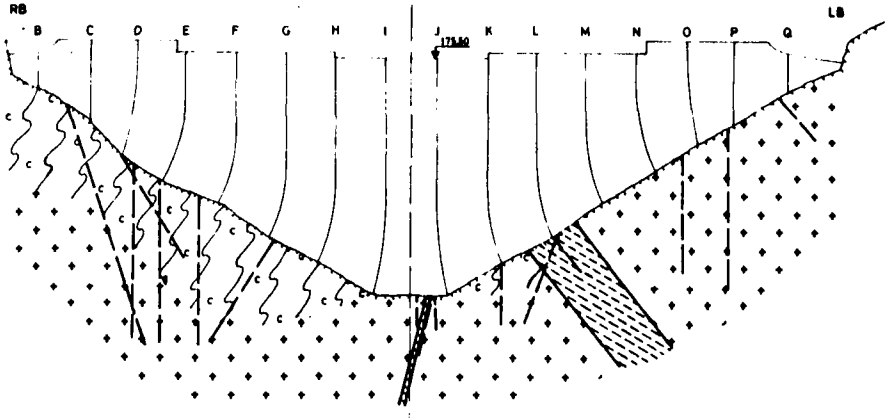
RB
B
C
D
E
F
G
H
I
J
K
L
M
N
O
P
Q
LB

HORNFELS AND PHYLLITE

GRANITE

QUARTZITE

HORNFELS

THERMAL METAMORPHISM

DAM AND RESERVOIR EMPLACEMENT

QUARTZ VEINS

FAULT

JOINT SETS (STRIKE AND DIP)

GEOLOGIC BOUNDARY

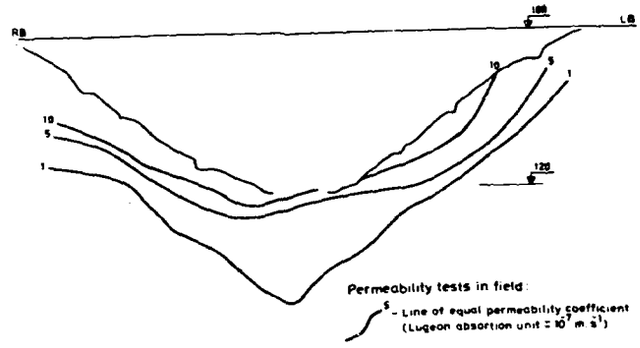

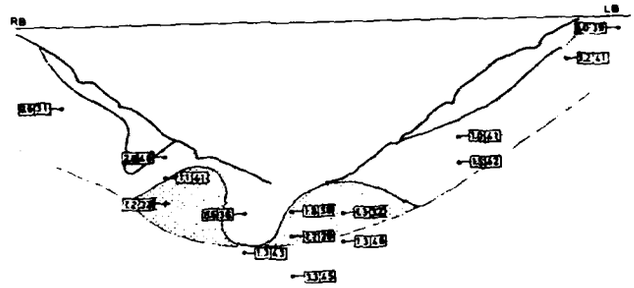

Mechanical tests in laboratory :

E - Elasticity moduli of rock (X 10^3 MPa)

- E ≤ 25
- 25 < E ≤ 50
- 50 < E ≤ 100
- 1.3 | 46 - Sliding joint tests
  - 1.3 - Cohesion (X 10^{-1} MPa)
  - 46 - Friction angle (degree)

CROSSHOLE AND UPHOLE
SEISMIC TESTS

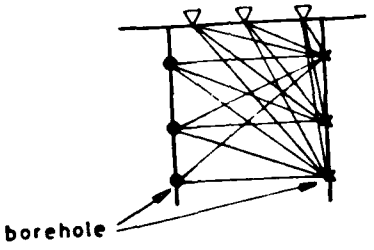

▽ – Geophone
● – Hydrophone
× – Seismic shoot

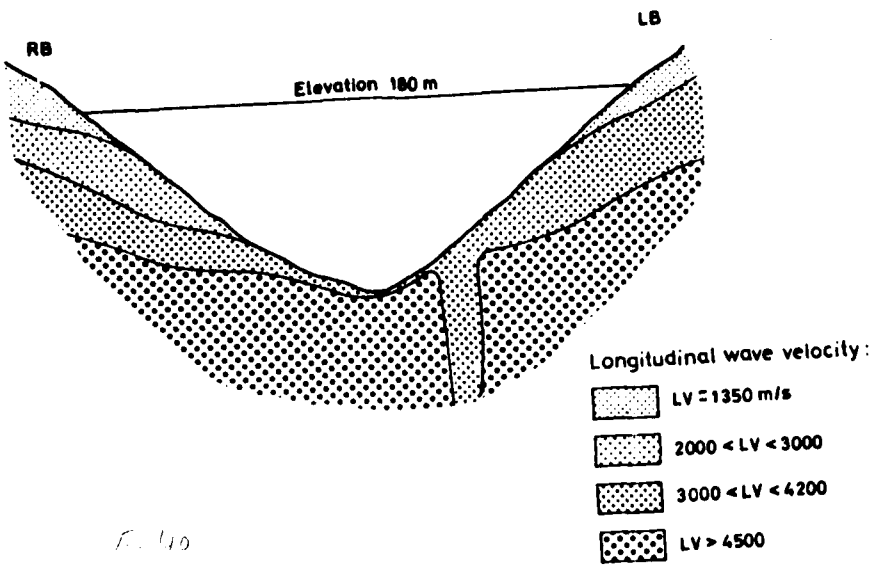
RB
LB
Elevation 180 m
Longitudinal wave velocity :
LV = 1350 m/s
2000 < LV < 3000
3000 < LV < 4200
LV > 4500

FOUNDATION TREATMENT SCHEME

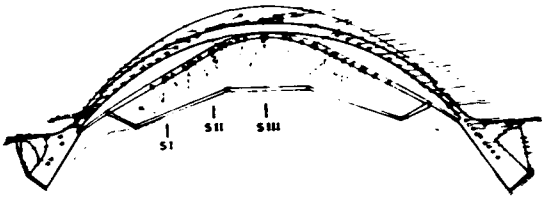

CEMENT ABSORTION IN GROUT CURTAIN

(Kg per meter)

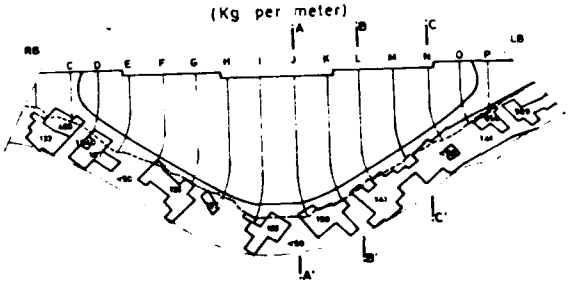

GROUT CURTAIN AND BASE DAM CONSOLIDATION

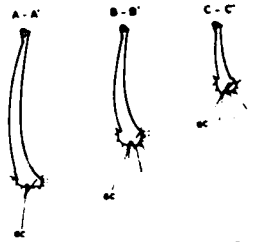

CONSOLIDATION OF RECEPTION BASIN

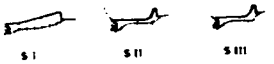

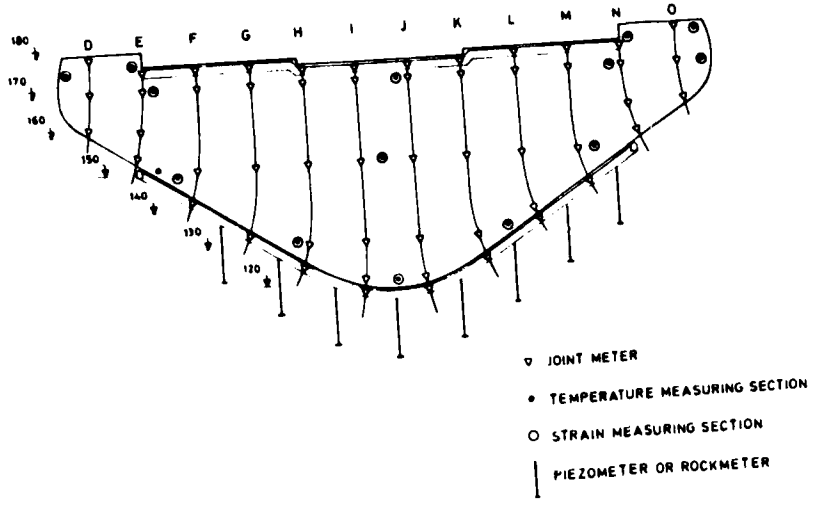
D
E
F
G
H
I
J
K
L
M
N
O
180
170
160
150
140
130
120
▽ JOINT METER
• TEMPERATURE MEASURING SECTION
○ STRAIN MEASURING SECTION
PIEZOMETER OR ROCKMETER

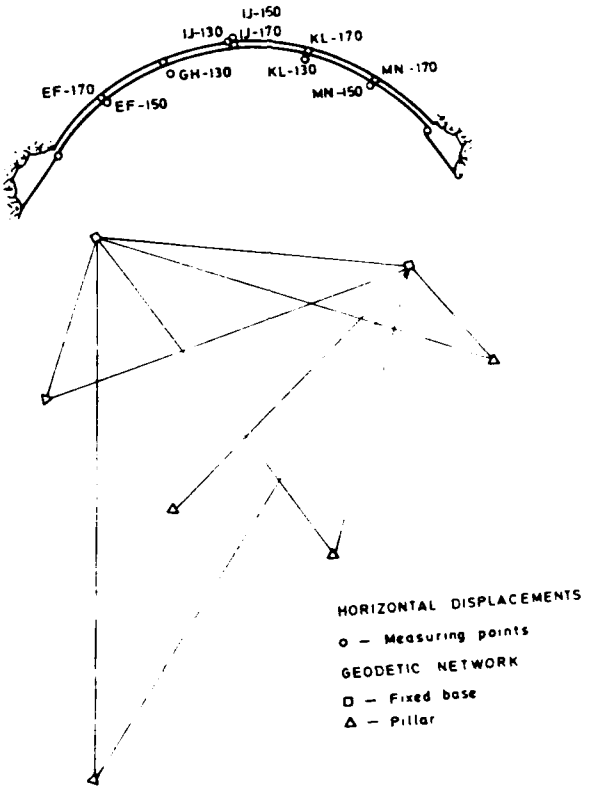
IJ-150
IJ-130
IJ-170
KL-170
EF-170
GH-130
KL-130
MN-170
EF-150
MN-150
HORIZONTAL DISPLACEMENTS
o — Measuring points
GEODETIC NETWORK
□ — Fixed base
△ — Pillar

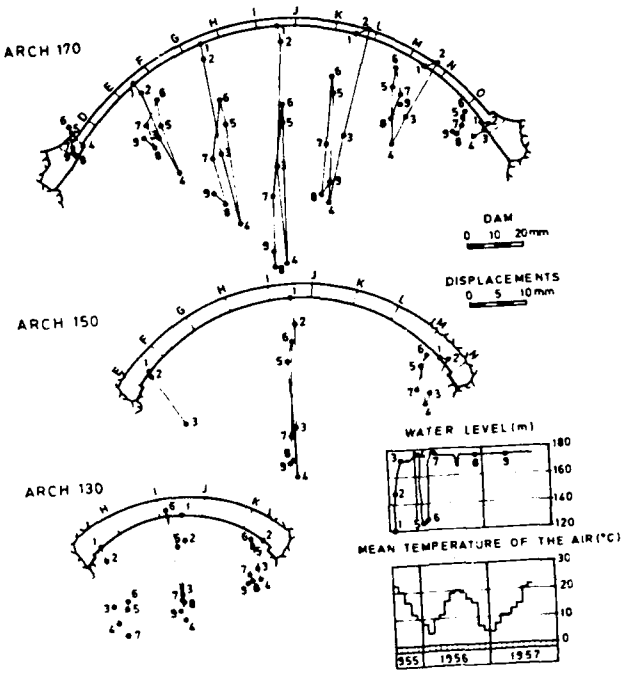
ARCH 170
DAM
0 10 20mm
DISPLACEMENTS
0 5 10mm
ARCH 150
WATER LEVEL(m)
180
160
140
120
ARCH 130
MEAN TEMPERATURE OF THE AIR(°C)
30
20
10
0
1955
1956
1957

SITUATION 1 — 1955/09/02

DOWNSTREAM FACE

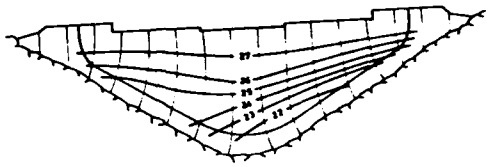

UPSTREAM FACE

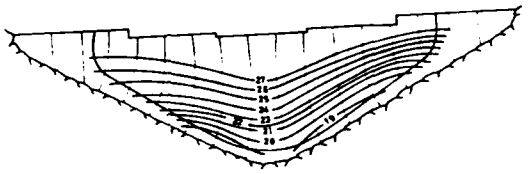

SITUATION 2 — 1955/09/12

DOWNSTREAM FACE

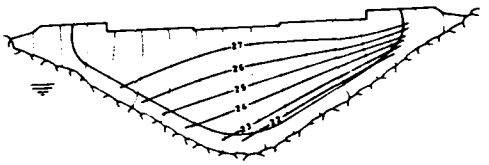

UPSTREAM FACE

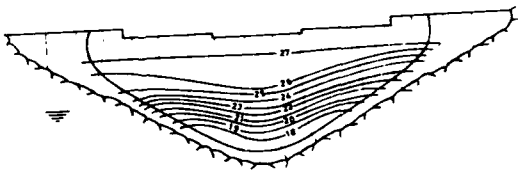

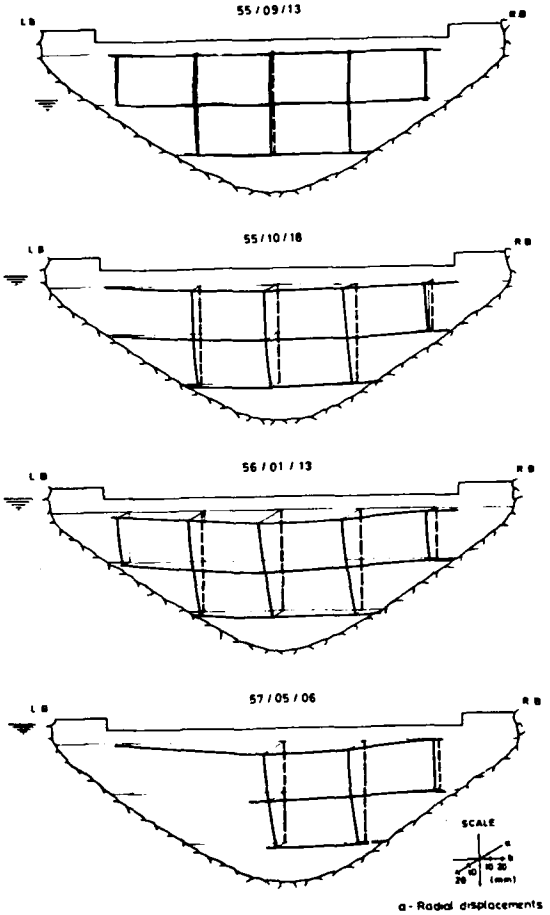

a - Radial displacements
b - Tangential displacements

STRESS VARIATIONS

DOWNSTREAM FACE

UPSTREAM FACE

TEMPERATURE VARIATIONS

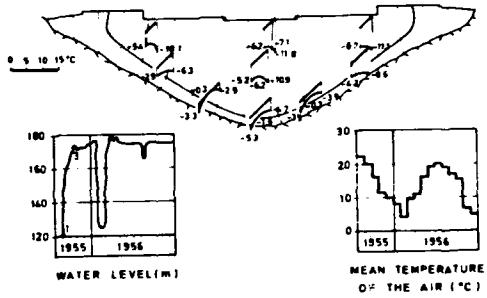

SUMMER 1959

DOWNSTREAM FACE

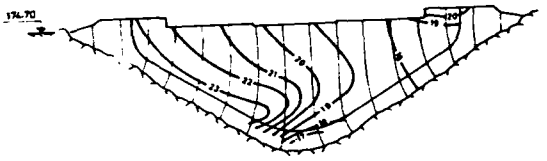

UPSTREAM FACE

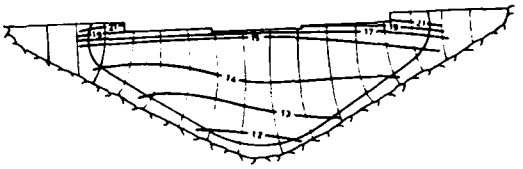

WINTER 1958

DOWNSTREAM FACE

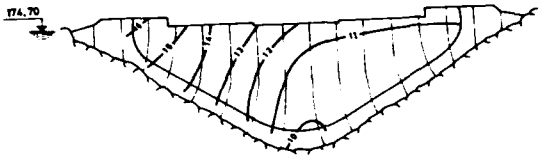

UPSTREAM FACE

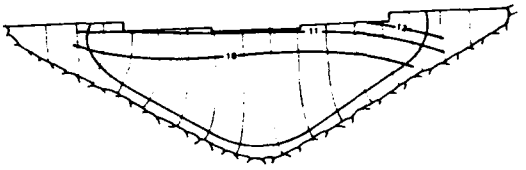

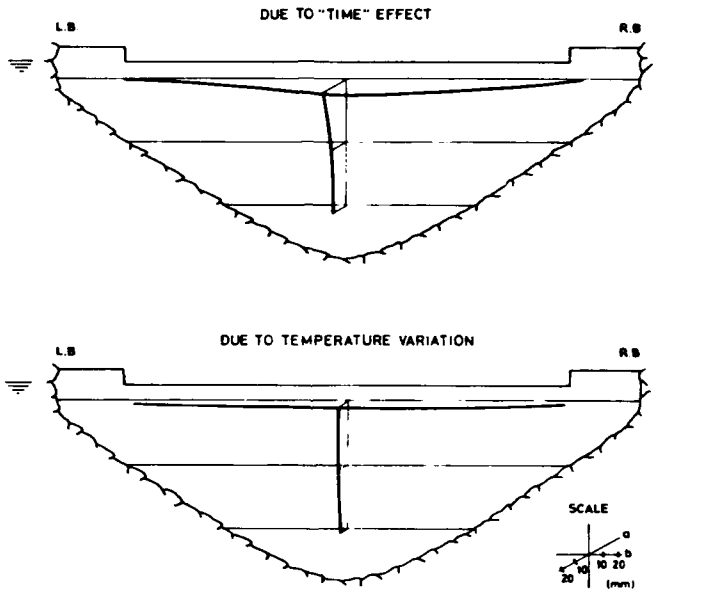

a - Radial displacements
b - Tangencial displacements

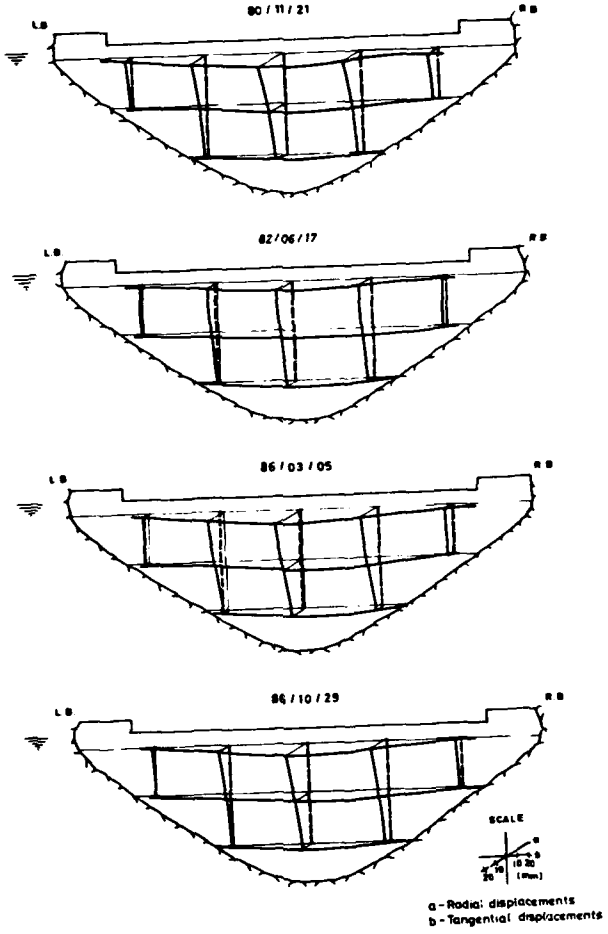

a - Radial displacements
b - Tangential displacements

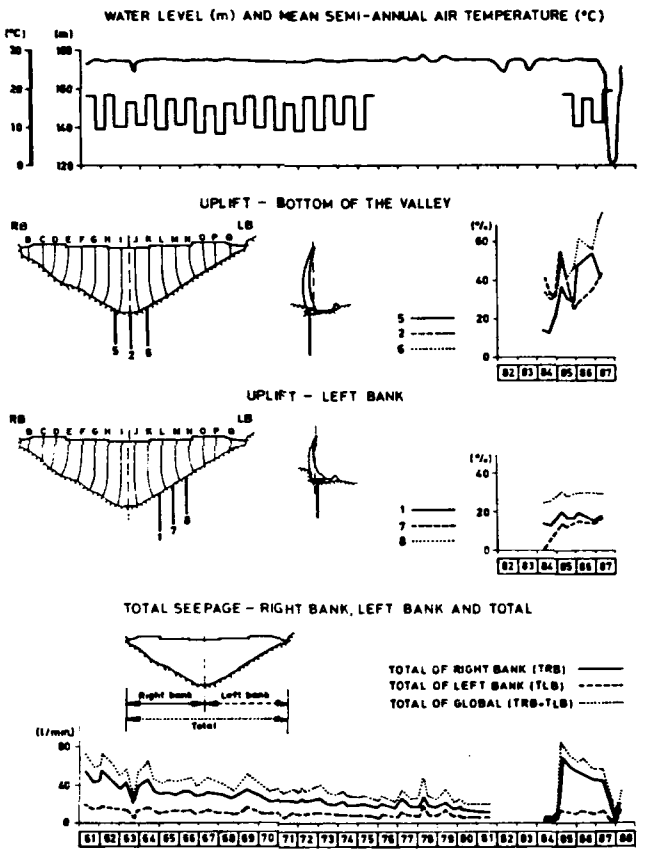
WATER LEVEL (m) AND MEAN SEMI-ANNUAL AIR TEMPERATURE (°C)
UPLIFT - BOTTOM OF THE VALLEY
RB
LB
UPLIFT - LEFT BANK
TOTAL SEEPAGE - RIGHT BANK, LEFT BANK AND TOTAL
Right bank
Left bank
Total
TOTAL OF RIGHT BANK (TRB)
TOTAL OF LEFT BANK (TLB)
TOTAL OF GLOBAL (TRB+TLB)

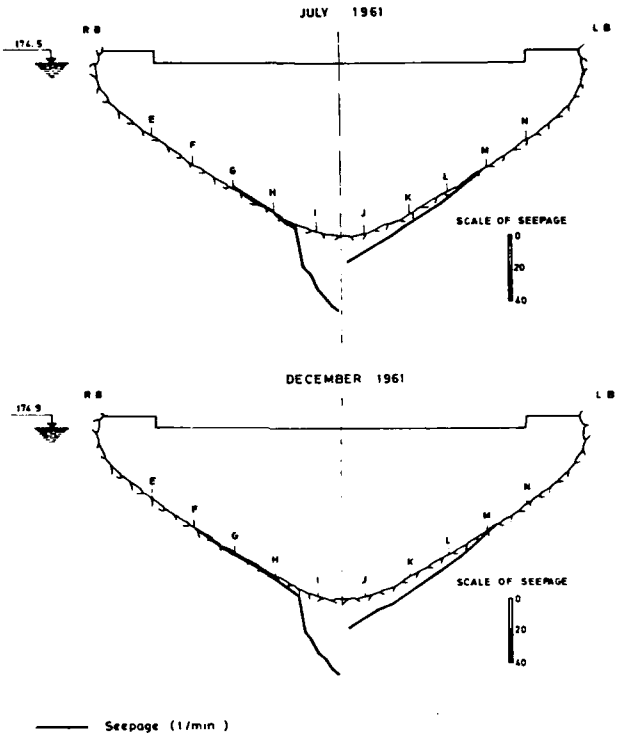
JULY 1961
R B
L B
176.5
E
F
G
H
I
J
K
L
M
N
SCALE OF SEEPAGE
0
20
40
DECEMBER 1961
R B
L B
176.9
E
F
G
H
I
J
K
L
M
N
SCALE OF SEEPAGE
0
20
40
Seepage (l/min)

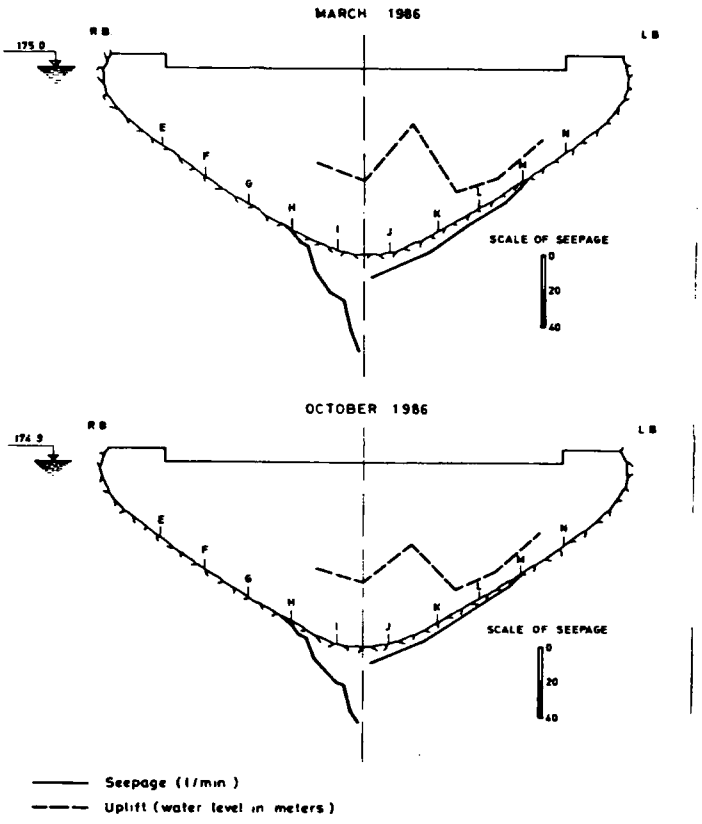
MARCH 1986
R B
L B
175.0
E
F
G
H
I
J
K
L
M
N
SCALE OF SEEPAGE
0
20
40
OCTOBER 1986
R B
L B
174.9
E
F
G
H
I
J
K
L
M
N
SCALE OF SEEPAGE
0
20
40
Seepage (l/min)
Uplift (water level in meters)

E-5'

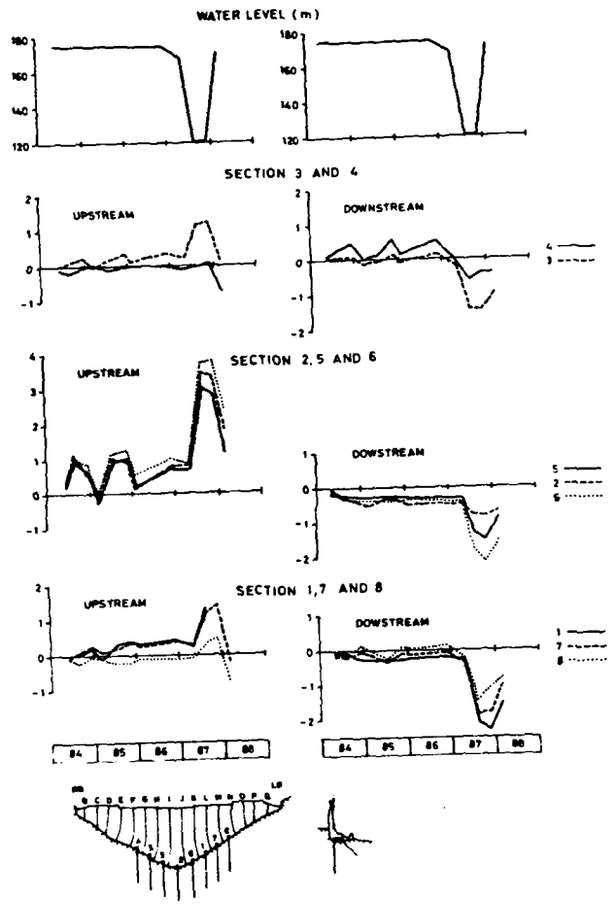
WATER LEVEL (m)
SECTION 3 AND 4
UPSTREAM
DOWNSTREAM
SECTION 2,5 AND 6
UPSTREAM
DOWSTREAM
SECTION 1,7 AND 8
UPSTREAM
DOWSTREAM
84
85
86
87
88

Level of the base (m)	Stresses (MPa)	
	σ_U	σ_D
115	-2.6	0.9
130	-1.5	0.4
145	-1.1	0.3
160	-0.6	0.2

Arch level (m)	Action	Crown		Springing		
		σ_U	σ_D	σ_U	σ_D	τ
173	HP	-3.3	-3.5	-3.0	-2.4	0.0
	VT	-0.1	0.1	0.2	-0.2	0.0
160	HP	-5.9	-4.3	-4.3	-3.5	0.1
	VT	-0.2	0.3	0.4	-0.4	0.0
145	HP	-6.4	-3.7	-2.8	-5.1	0.2
	VT	-0.5	0.6	0.8	-0.7	0.0
130	HP	-6.4	-1.2	-0.1	-5.8	-0.5
	VT	-0.7	1.2	1.4	-1.1	0.1

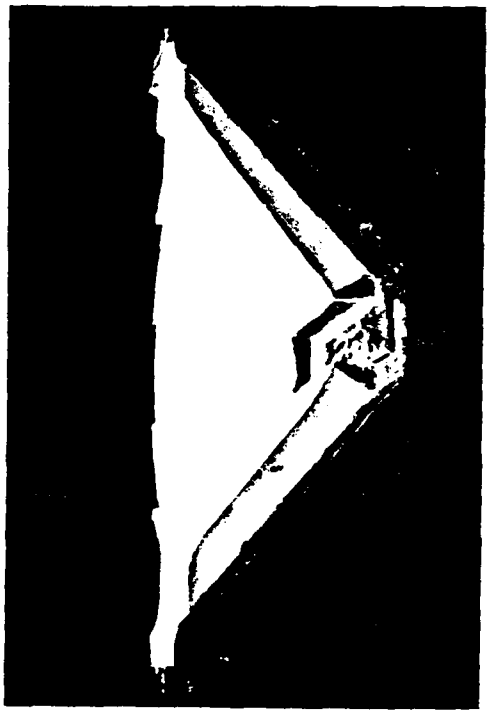

A) DIRECTIONS OF THE PRINCIPAL STRESSES

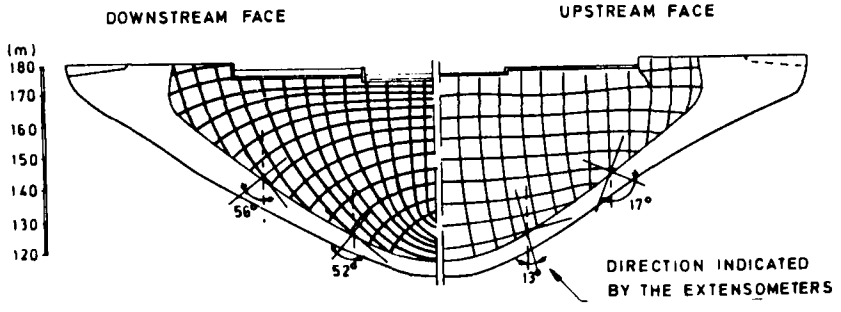

B) PRINCIPAL STRESSES

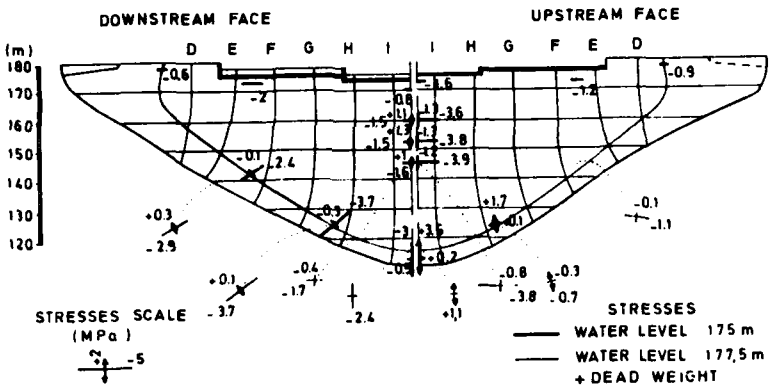

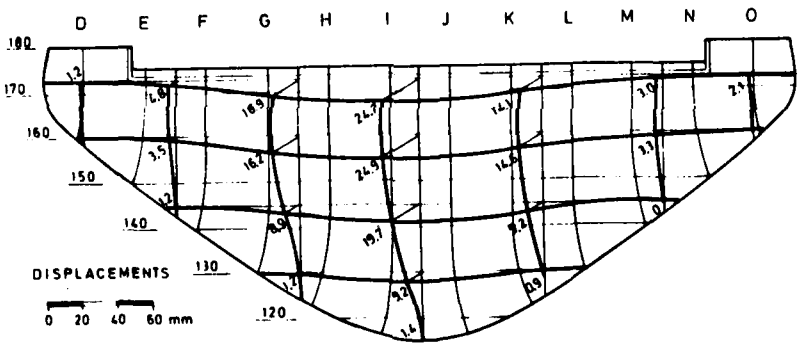
D
E
F
G
H
I
J
K
L
M
N
O
180
170
160
150
140
130
120
1.2
4.8
18.5
24.7
14.1
3.0
2.9
3.5
16.2
24.5
14.6
3.3
1.2
8.9
19.7
8.2
0
1.1
3.2
2.9
1.4
DISPLACEMENTS
0 20 40 60 mm

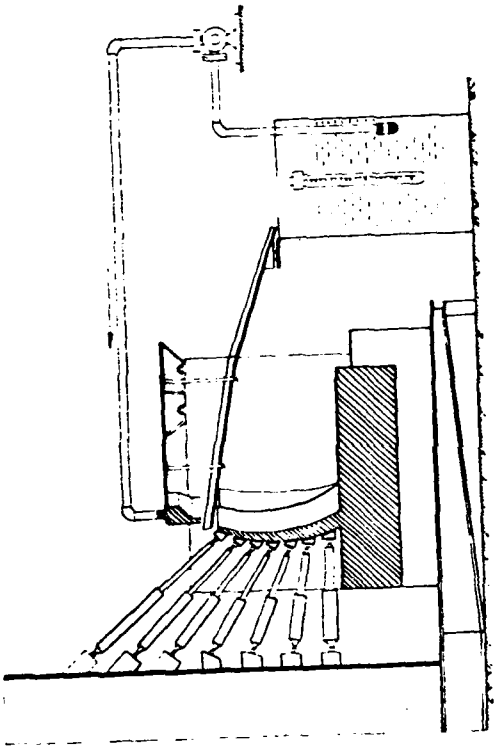

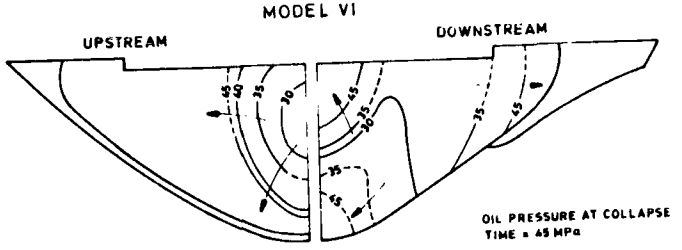
MODEL VI
UPSTREAM
DOWNSTREAM
45
40
35
30
45
35
30
35
45
35
45
OIL PRESSURE AT COLLAPSE
TIME = 45 MPa

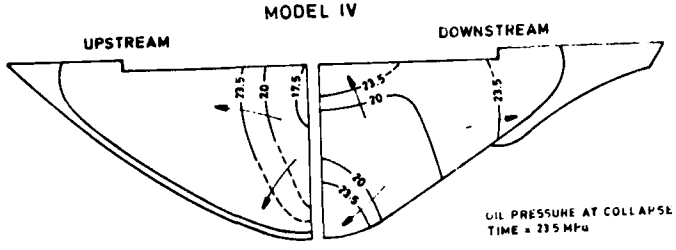
MODEL IV
UPSTREAM
DOWNSTREAM
23.5
20
17.5
23.5
20
23.5
20
23.5
OIL PRESSURE AT COLLAPSE
TIME = 23.5 MPa

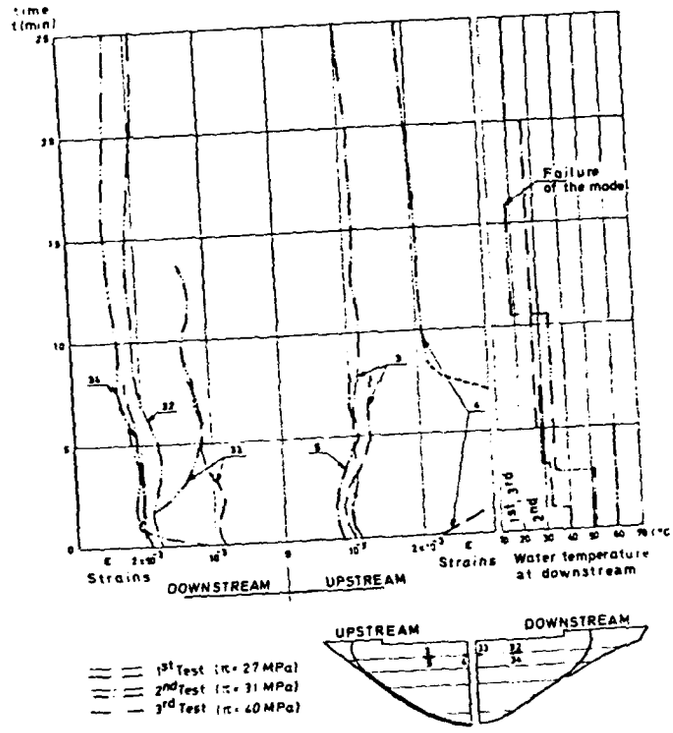
time
t(min)
Failure
of the model
Strains
DOWNSTREAM
UPSTREAM
Strains
Water temperature
at downstream
1st
2nd
UPSTREAM
DOWNSTREAM
1st Test (π= 27 MPa)
2nd Test (π= 31 MPa)
3rd Test (π= 40 MPa)

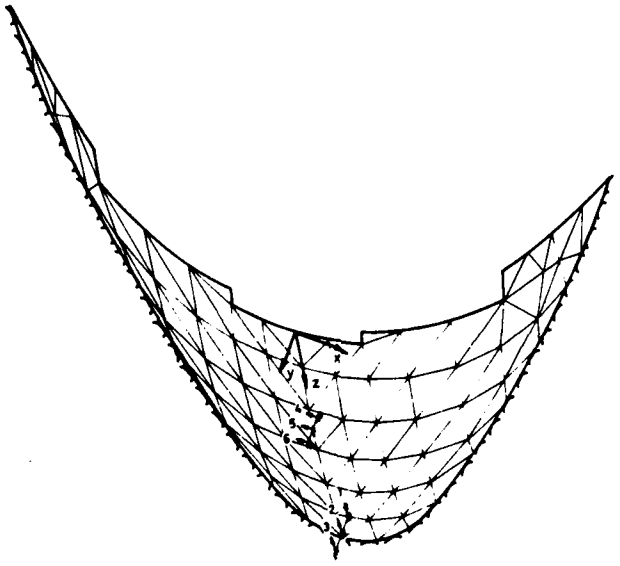

⊢ Stress measuring sections

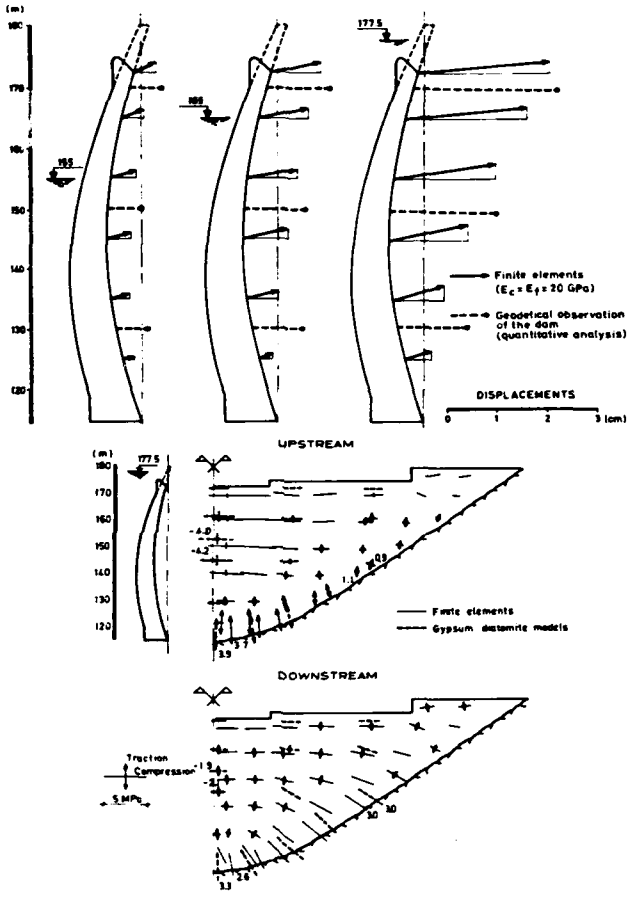
(m)
180
170
160
150
140
130
120
155
165
177.5
Finite elements
($E_c = E_f = 20$ GPa)
Geodetical observation
of the dam
(quantitative analysis)
DISPLACEMENTS
0 1 2 3 (cm)
UPSTREAM
Finite elements
Gypsum dolomite models
DOWNSTREAM
Traction
Compression
5 MPa

F-62

STRESSES AT THE CENTRAL CANTILEVER

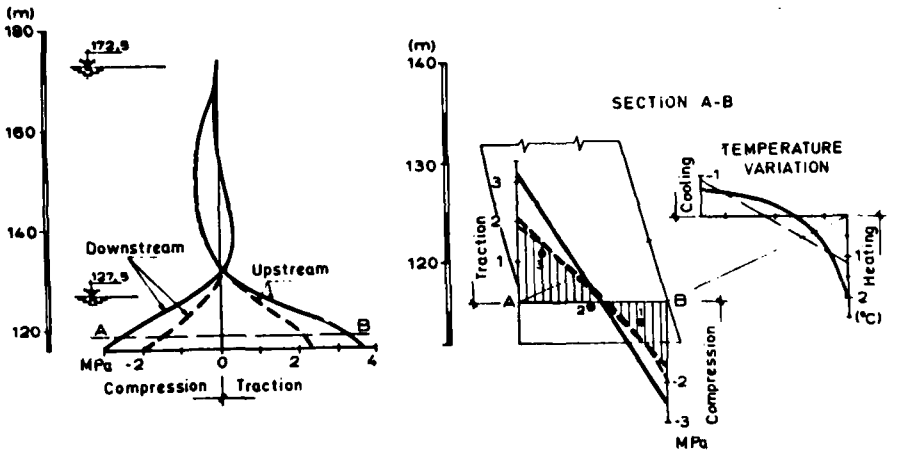

——— Finite elements
Hydrostatic pressure on the dam
(half-space)

— — — Finite elements
Hydrostatic pressure on the dam
and on the foundation
(quarter-space)

● Observation (stress meters)

F-63

- Observation (stress meters)

STRESSES AT THE CENTRAL CANTILEVER

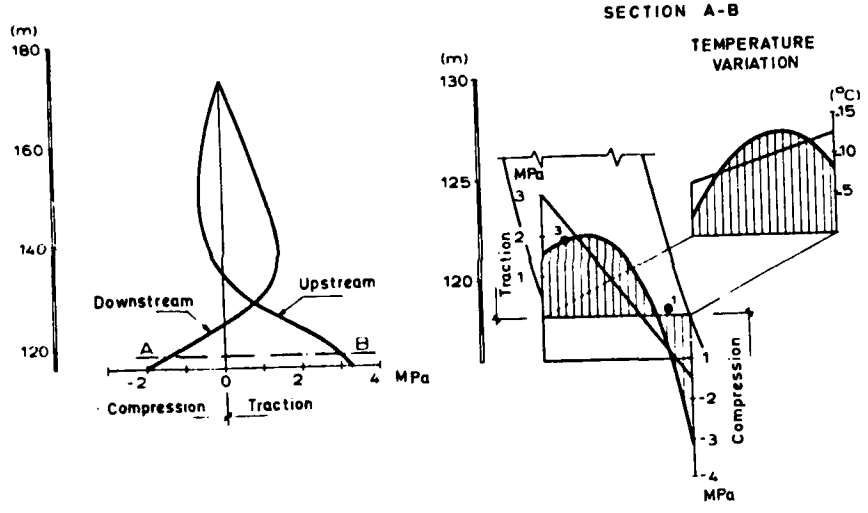

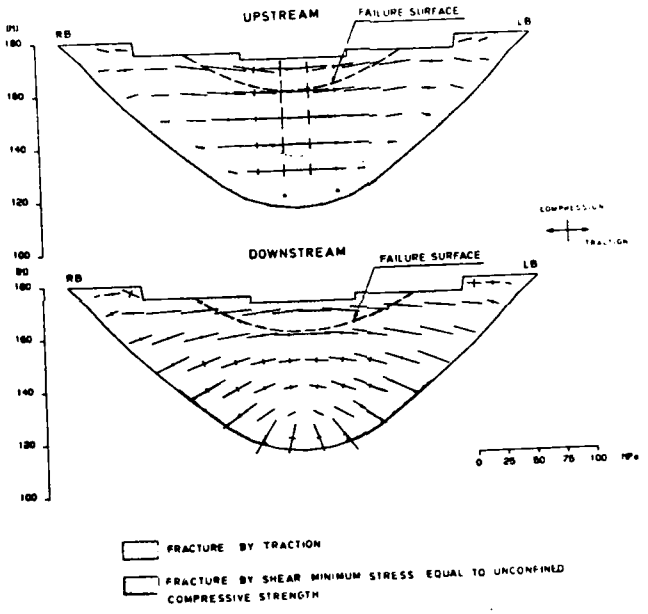
UPSTREAM
FAILURE SURFACE
RB
LB
DOWNSTREAM
FAILURE SURFACE
RB
LB
0 25 50 75 100
FRACTURE BY TRACTION
FRACTURE BY SHEAR MINIMUM STRESS EQUAL TO UNCONFINED COMPRESSIVE STRENGTH

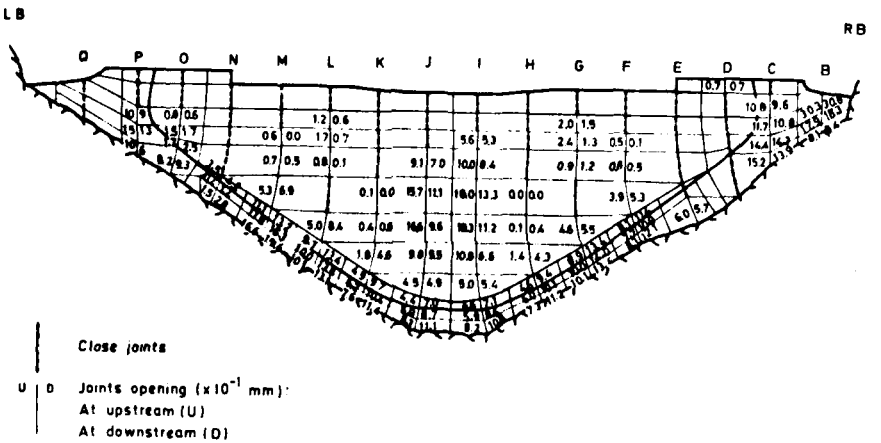
LB
RB
O
P
O
N
M
L
K
J
I
H
G
F
E
D
C
B
Close joints
U | D Joints opening (x10⁻¹ mm):
At upstream (U)
At downstream (D)

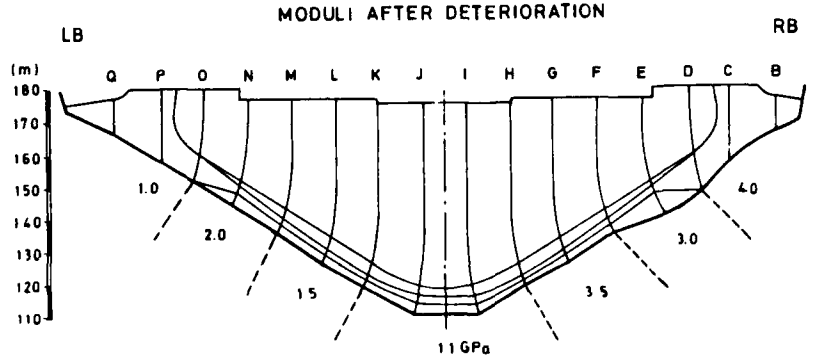
MODULI AFTER DETERIORATION
LB
RB
(m)
180
170
160
150
140
130
120
110
Q P O N M L K J I H G F E D C B
1.0
2.0
1.5
1.1 GPa
3.5
3.0
4.0

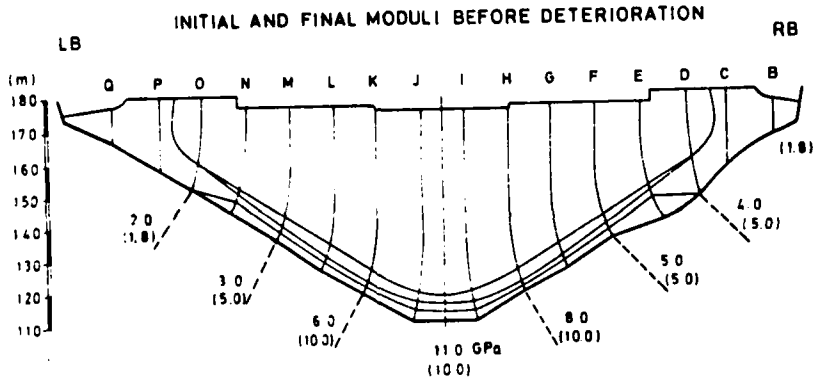
INITIAL AND FINAL MODULI BEFORE DETERIORATION
LB
RB
(m)
180
170
160
150
140
130
120
110
Q P O N M L K J I H G F E D C B
2.0
(1.8)
3.0
(5.0)
6.0
(10.0)
11.0 GPa
(10.0)
8.0
(10.0)
5.0
(5.0)
4.0
(5.0)
(1.8)

Case	Calc.	W	HP				UP				VT		S
			U		D		U		D		DT	UT	
			0	5.4	44	58	0	5.5	44	58			
N	15-32	1	0	1	0	1	0	1	0	1	0	0	0
	18-36	1	0	1	0	1	0	1	0	1	1	0	0
	19-41	1	0	1	0	1	0	1	0	1	0	1	0
E	20-37	1	0	1	0	0	0	1	0	0	1	0	1
	25-39	1	1	0	1	0	1	0	1	0	1	0	0
	21-42	1	0	1	0	0	0	1	0	0	0	1	1
	26-33	1	0	0	0	1	0	0	0	1	0	1	0
	29-34	1	0	0	0	0	0	0	0	0	0	1	0
T	12-30	1	0	0	0	0	0	0	0	0	0	0	0
	13-31	1	0	1	0	0	0	0	0	0	0	0	0
	14-35	1	0	1	0	0	0	1	0	0	0	0	0
	16-40	1	0	1	0	0	0	1	0	0	1	0	0
	17-43	1	0	1	0	0	0	1	0	0	0	1	0
	22-44	1	1	0	0	0	0	0	0	0	0		0
	23-39	1	1	0	0	0	1	0	0	0	0	0	0
	24	1	1	0	0	0	1	0	0	0	1	0	0

N - normal E - extraordinary T - work

1 - afirmative case ; 0 - negative case

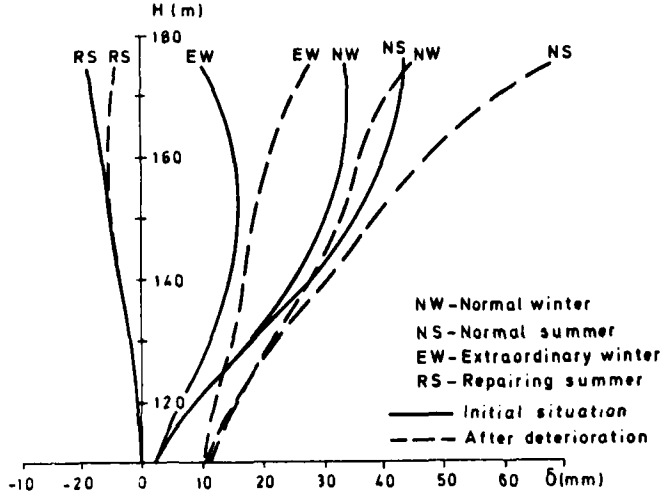
H (m)
180
160
140
120
RS RS
EW
EW NW
NS NW
NS
-10 -20 0 10 20 30 40 50 60 δ(mm)
NW-Normal winter
NS-Normal summer
EW-Extraordinary winter
RS-Repairing summer
Initial situation
After deterioration

F. 69

Joint	Case	NW			EW			NS			SR		
		X	Y	Z	X	Y	Z	X	Y	Z	X	Y	Z
N	1	2.1	3.4	2.9	2.6	4.1	3.6	1.3	2.0	1.8	-.3	-.5	-.4
	2	3.8	5.1	5.3	4.6	6.3	6.4	2.6	3.3	3.7	-.5	-.6	-.7
L	1	1.1	3.2	1.4	1.4	3.3	1.8	.9	2.6	1.1	-.1	-.2	-.1
	2	3.7	7.7	4.6	4.1	7.7	5.3	3.0	6.3	3.7	-.3	-.4	-.3
J	1	-.4	1.5	-1.6	-.4	1.4	-1.6	-.2	1.3	-.7	.1	.0	.3
	2	-.2	12.2	-.9	-.2	11.1	-.9	.0	10.1	-.2	.1	-.4	.2
H	1	-.2	2.6	.0	-.2	2.5	.1	-.2	2.1	.2	.0	-.1	.0
	2	-1.0	7.8	1.3	-1.1	7.2	1.4	-.9	6.4	1.1	.0	-.3	.0
E	1	-.7	2.4	1.3	-.9	2.8	1.7	-.5	1.7	1.0	.1	-.3	.1
	2	-.9	2.5	1.6	-1.1	3.1	2.0	-.6	1.9	1.2	.1	-.2	-.2

Calc.	Block JK				Block IJ				Block HI			
	σ_u	σ_b	τ	tg θ	σ_u	σ_b	τ	tg θ	σ_u	σ_b	τ	tg θ
NW												
Case 1	2.0	-2.7	.6	1.83	2.7	-2.3	.6	-3.42	1.9	-2.5	.6	1.82
Case 2	.2	-1.9	.0	.03	.6	-0.9	.0	.09	.4	-1.9	.3	.04
EW												
Case 1	2.2	-3.0	.6	1.51	2.9	-2.5	.5	-2.86	2.1	-2.8	.5	1.52
Case 2	.6	-2.3	.3	.03	1.0	1.3	.0	.09	.7	-2.3	.0	.04
NS												
Case 1	1.0	-2.2	.5	.93	1.5	-2.2	.5	1.35	.9	-2.0	.5	.90
Case 2	-.4	-1.5	.0	.03	-.1	-1.0	.0	.02	-.2	-1.5	.3	.03
SR												
Case 1	-2.4	1.0	.0	.01	-2.6	.8	.0	.00	-2.3	.9	.0	.02
Case 2	-2.3	.9	.0	.04	-2.6	.8	.0	.01	-2.3	.9	.0	.04

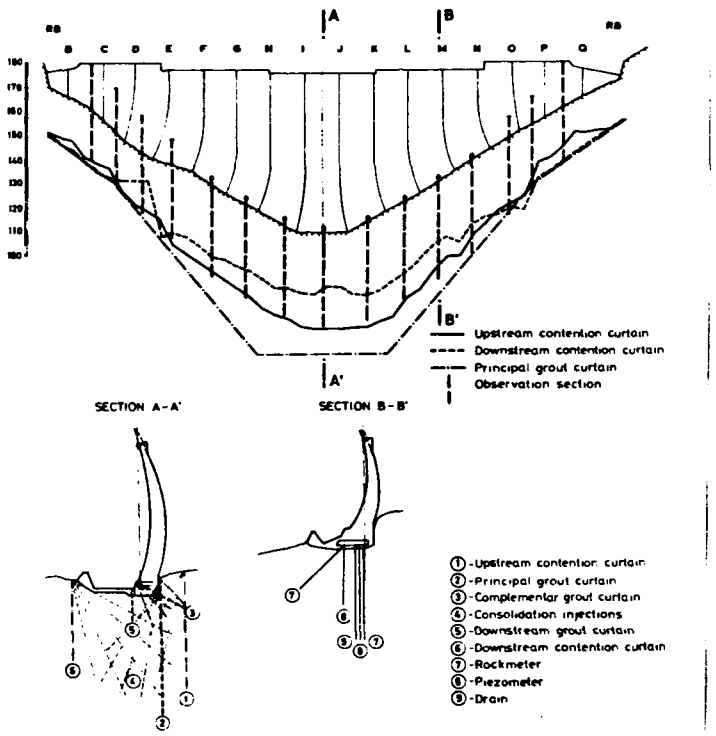
A
B
RB
RB
B C D E F G H I J K L M N O P Q
B'
A'
Upstream contention curtain
Downstream contention curtain
Principal grout curtain
Observation section
SECTION A-A'
SECTION B-B'
①-Upstream contention curtain
②-Principal grout curtain
③-Complementar grout curtain
④-Consolidation injections
⑤-Downstream grout curtain
⑥-Downstream contention curtain
⑦-Rockmeter
⑧-Piezometer
⑨-Drain

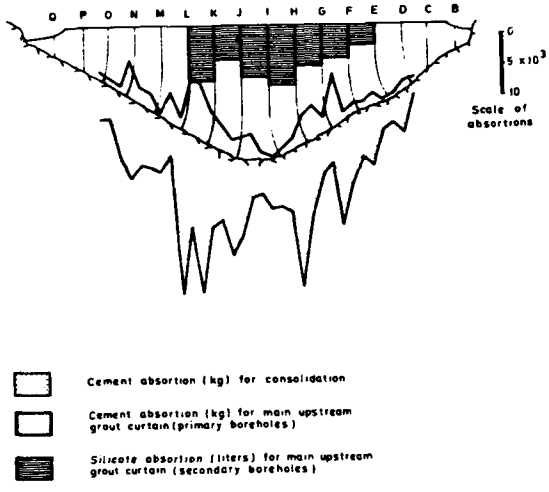

Cement absortion (kg) for consolidation

Cement absortion (kg) for main upstream grout curtain (primary boreholes)

Silicate absortion (liters) for main upstream grout curtain (secondary boreholes)

C.23

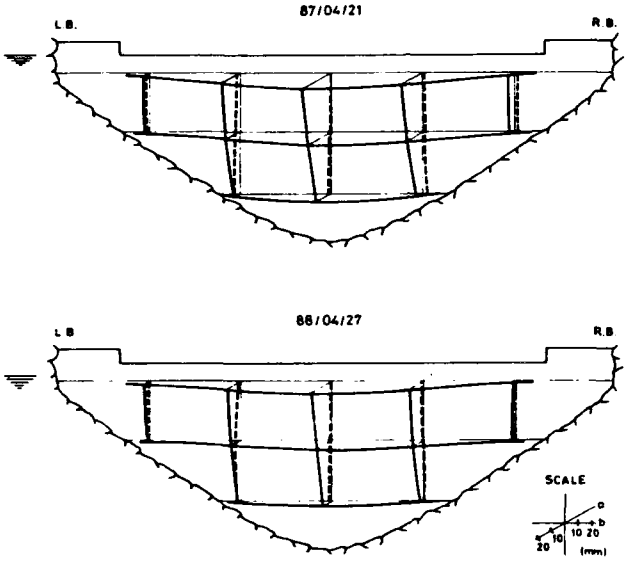

a - Radial displacements
b - Tangential displacements

F 74

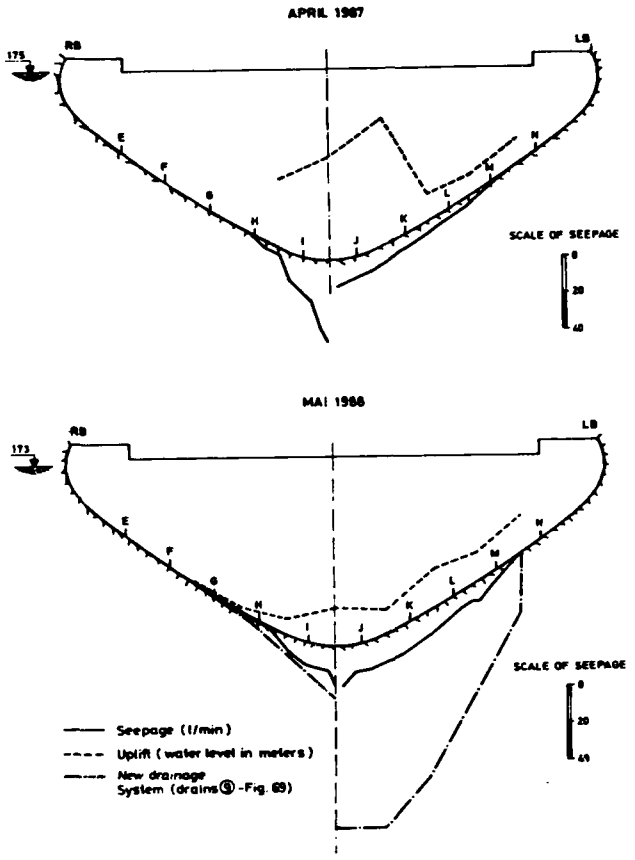
APRIL 1987
175
RB
LB
E
F
G
H
I
J
K
L
M
N
SCALE OF SEEPAGE
0
20
40
MAI 1988
173
RB
LB
E
F
G
H
I
J
K
L
M
N
SCALE OF SEEPAGE
0
20
44
Seepage (l/min)
Uplift (water level in meters)
New drainage System (drains ⑤ -Fig. 69)

E. 25

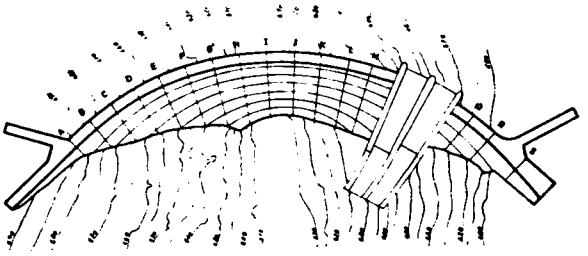

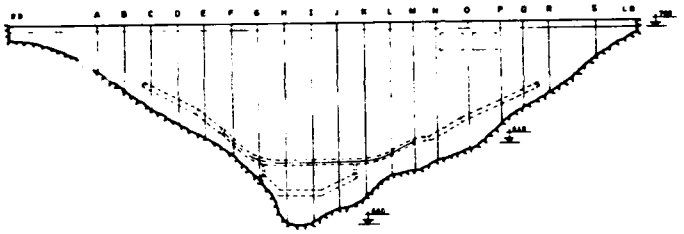

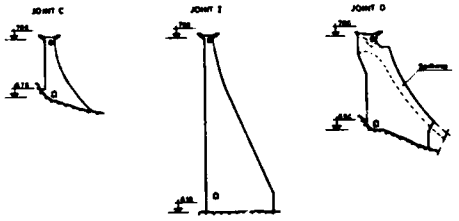

E-26

HORNFELS

FAULT

GEOLOGIC BOUNDARY

JOINT SETS (STRIKE AND DIP)

GRANITE PORPHYRY

MEDIUM-GRAINED GRANITE WITH GARNET

PHYLLITE AND PELITIC SCHISTS

QUARTZITIC SCHISTS

F. 47

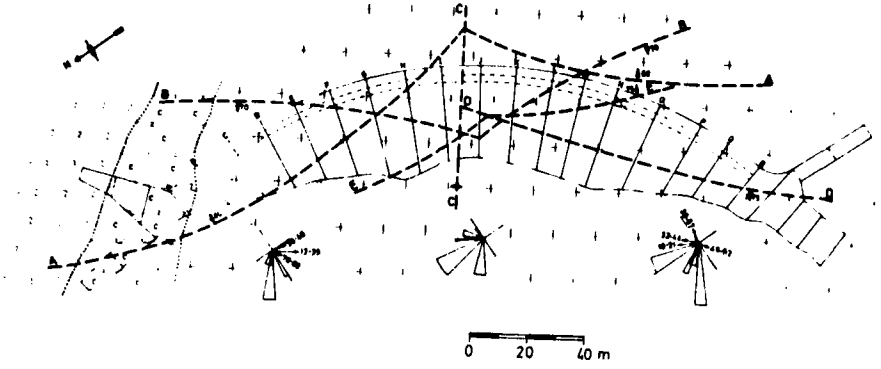
0
20
40 m

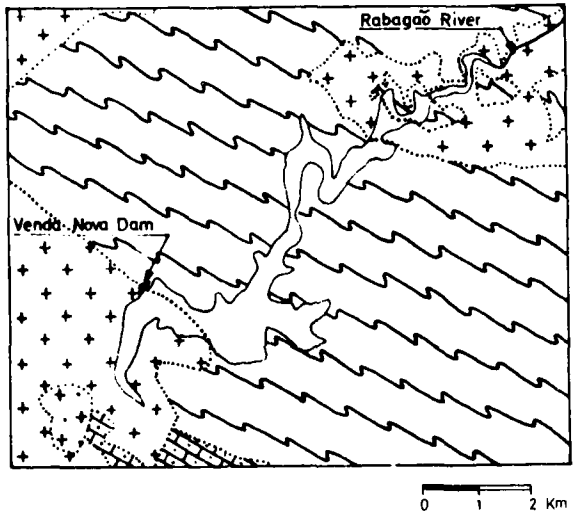
Rabagão River
Venda Nova Dam
0
1
2 Km

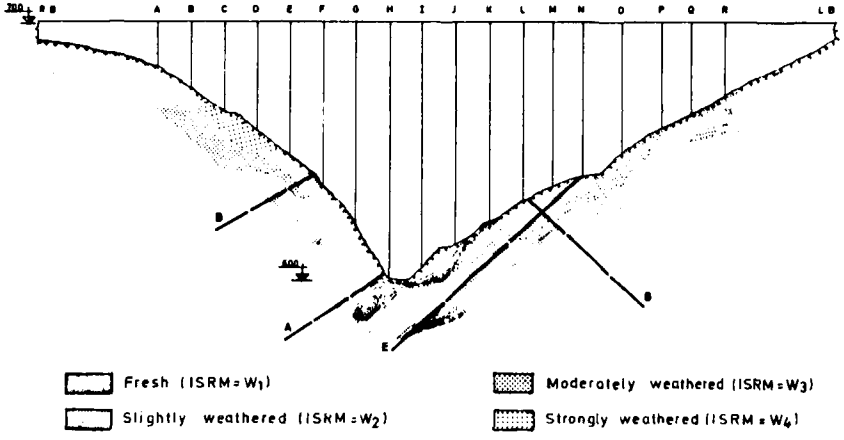
RB
A
B
C
D
E
F
G
H
I
J
K
L
M
N
O
P
Q
R
LB
D
A
E
B
Fresh (ISRM=W1)
Slightly weathered (ISRM=W2)
Moderately weathered (ISRM=W3)
Strongly weathered (ISRM=W4)

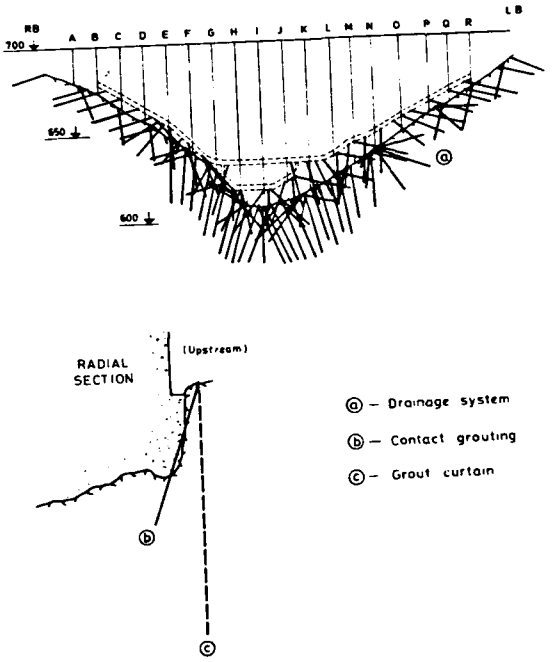
RB
LB
A B C D E F G H I J K L M N O P Q R
700
650
600
RADIAL SECTION
(Upstream)
ⓐ – Drainage system
ⓑ – Contact grouting
ⓒ – Grout curtain

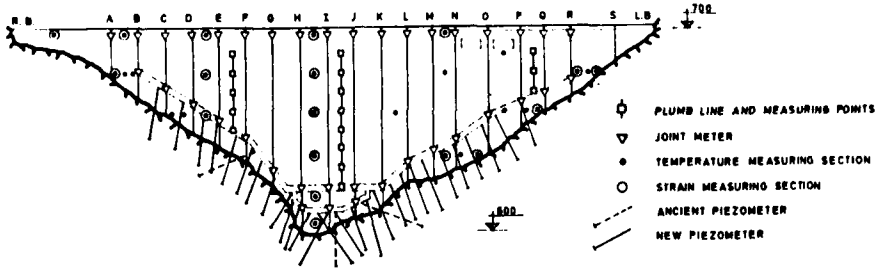

MEASURING POINTS
- ○ HORIZONTAL DISPLACEMENTS
- ● VERTICAL DISPLACEMENTS

GEODETIC NETWORK
- △ PILLAR
- □ FIXED POINTS

F-79

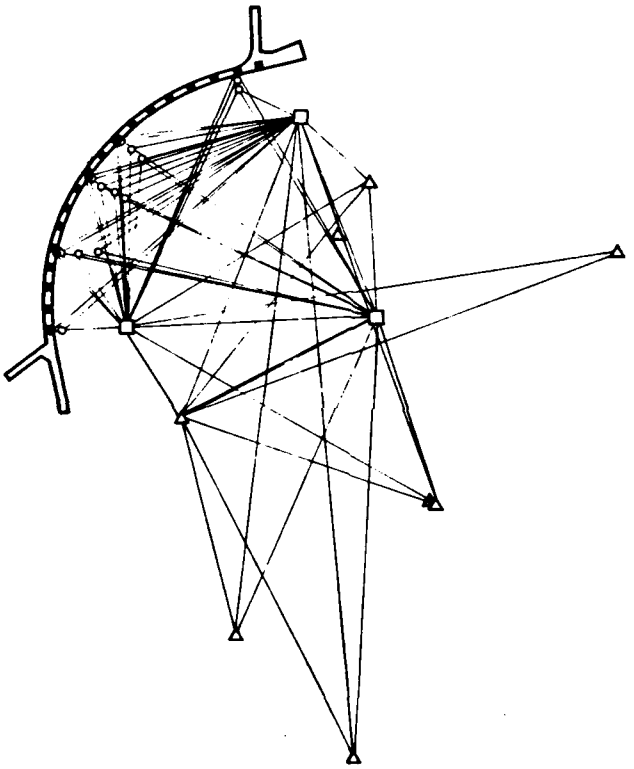

HORIZONTAL DISPLACEMENTS

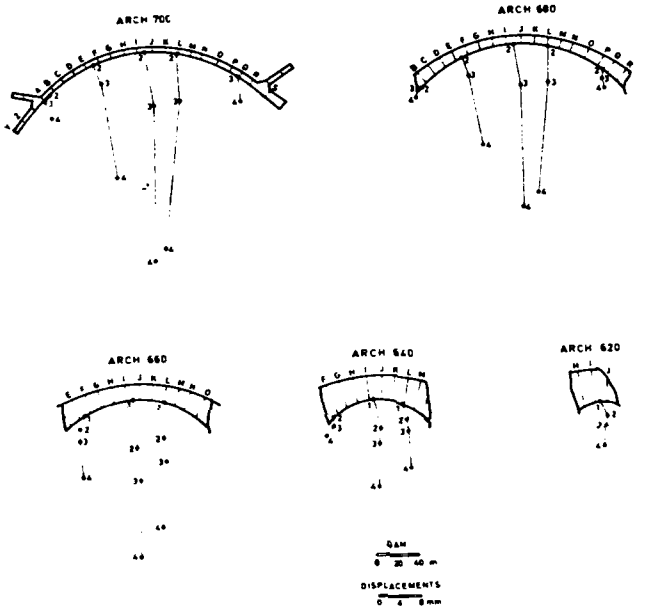

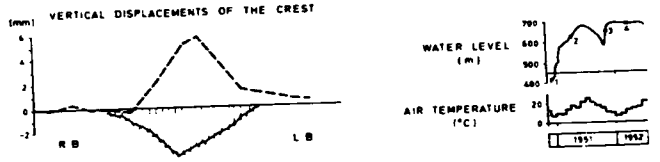

F - 80

SUMMER

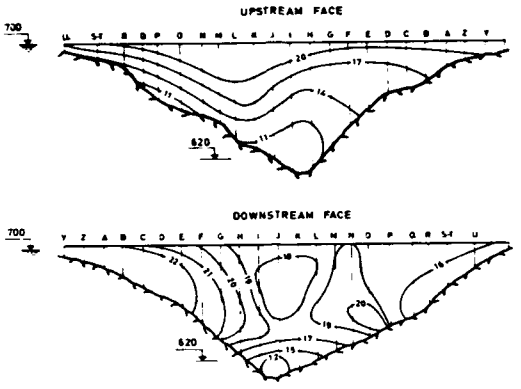

WINTER

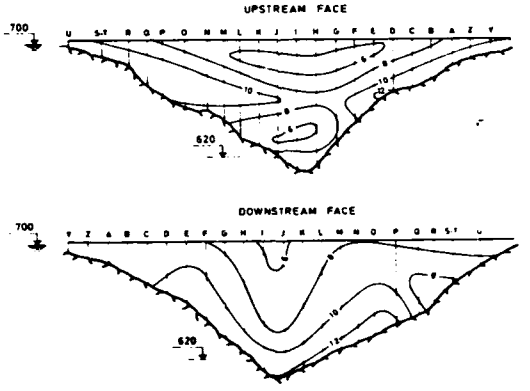

X1

WATER LEVEL AND AIR TEMPERATURE

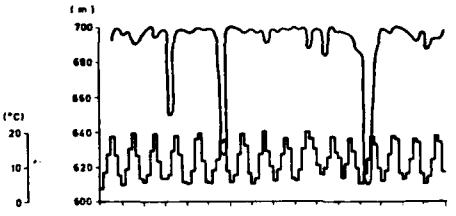

TOTAL SEEPAGE

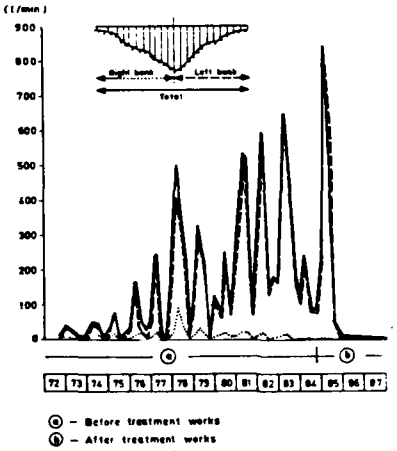

ⓐ – Before treatment works
ⓑ – After treatment works

F-12

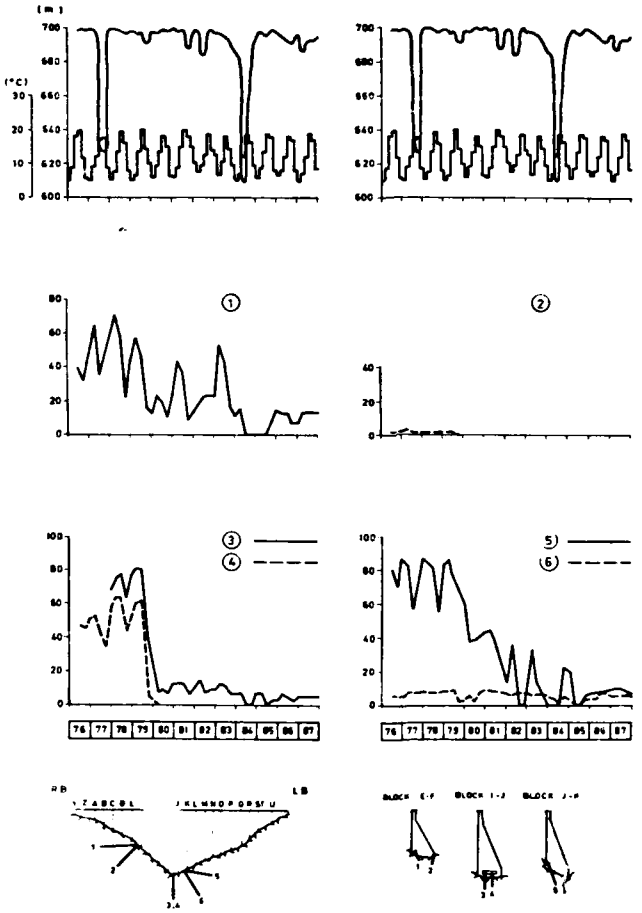
(m)
700
680
660
640
620
600
(°C)
30
20
10
0
①
②
③
④
⑤
⑥
76 77 78 79 80 81 82 83 84 85 86 87

F-X3

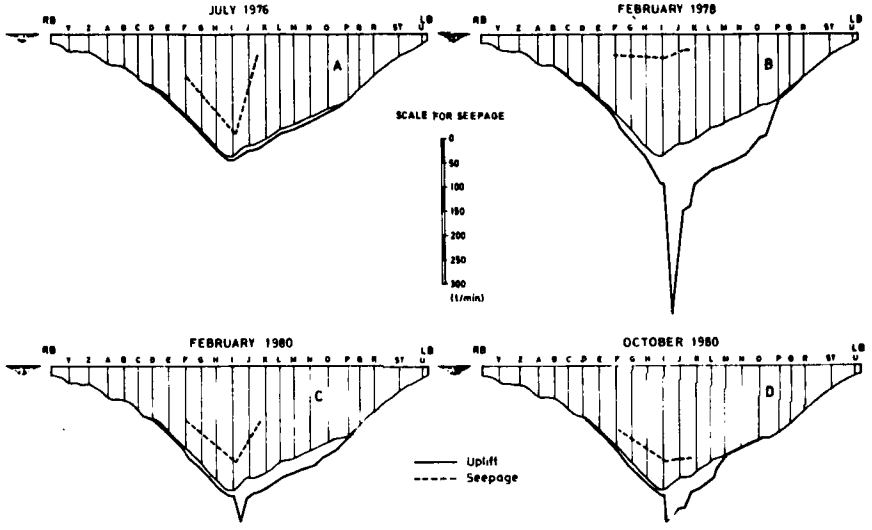
JULY 1976
FEBRUARY 1978
FEBRUARY 1980
OCTOBER 1980
RB
LB
A
B
C
D
SCALE FOR SEEPAGE
0
50
100
150
200
250
300
(l/min)
Uplift
Seepage

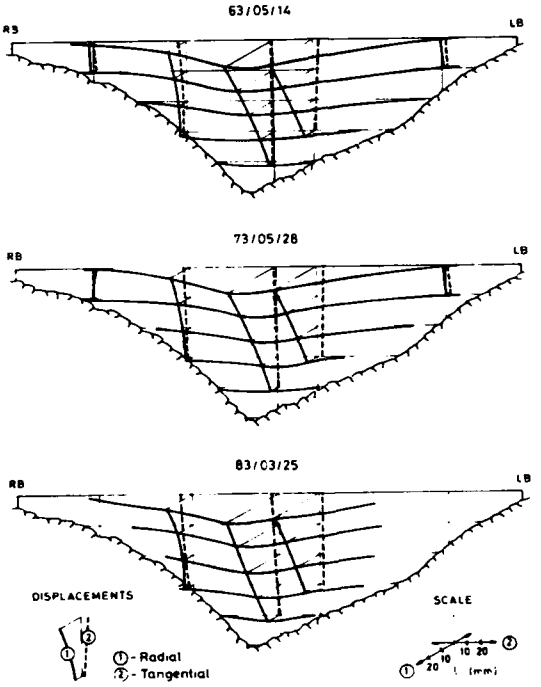
63/05/14
RB
LB
73/05/28
RB
LB
83/03/25
RB
LB
DISPLACEMENTS
① - Radial
② - Tangential
SCALE
20 10 0 10 20 (mm)

F. 8 C

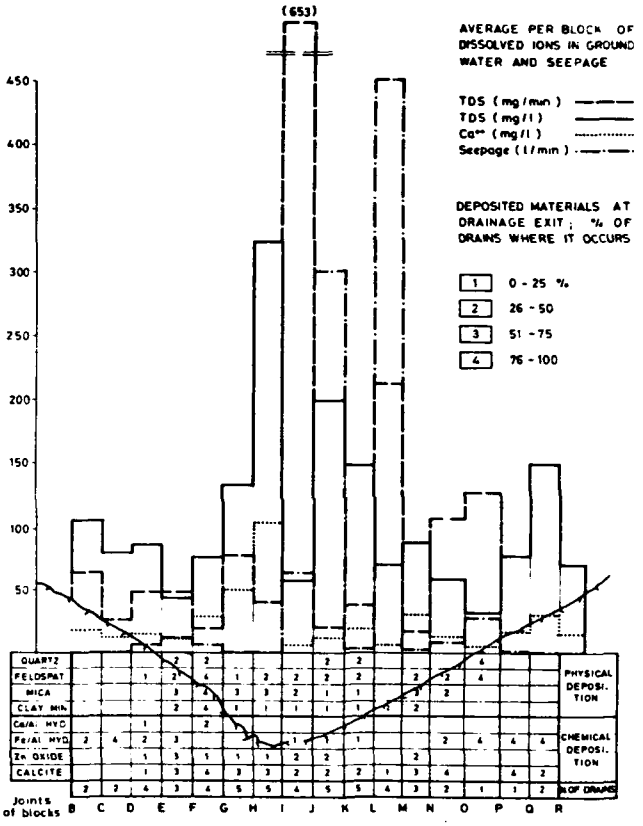
(653)
AVERAGE PER BLOCK OF DISSOLVED IONS IN GROUND WATER AND SEEPAGE
TDS (mg/mm)
TDS (mg/l)
Ca++ (mg/l)
Seepage (l/mm)
DEPOSITED MATERIALS AT DRAINAGE EXIT; % OF DRAINS WHERE IT OCCURS
1 0 - 25 %
2 26 - 50
3 51 - 75
4 76 - 100
450
400
350
300
250
200
150
100
50
QUARTZ
FELDSPAT
MICA
CLAY MIN.
Ca/Al HYD.
Fe/Al HYD.
Zn OXIDE
CALCITE
PHYSICAL DEPOSITION
CHEMICAL DEPOSITION
% OF DRAINS
Joints of blocks
B C D E F G H I J K L M N O P Q R

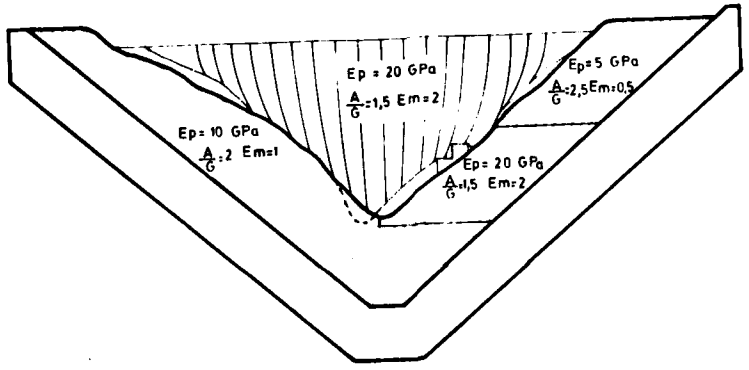
Ep = 20 GPa
A/G=1,5 Em=2
Ep=5 GPa
A/G=2,5 Em=0,5
Ep= 10 GPa
A/G=2 Em=1
Ep= 20 GPa
A/G=1,5 Em=2

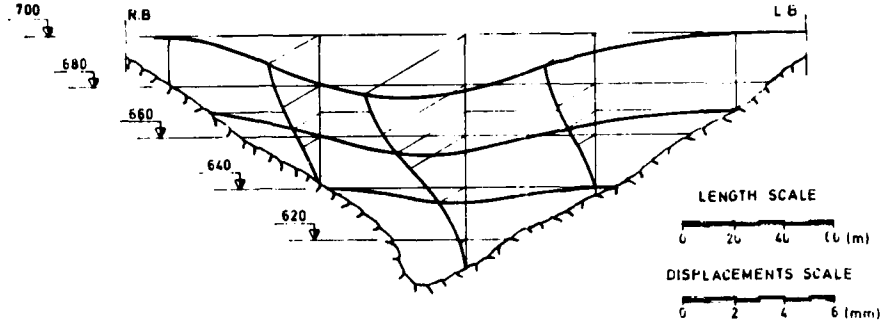
700
680
660
640
620
R.B
L.B
LENGTH SCALE
0 20 40 60 (m)
DISPLACEMENTS SCALE
0 2 4 6 (mm)

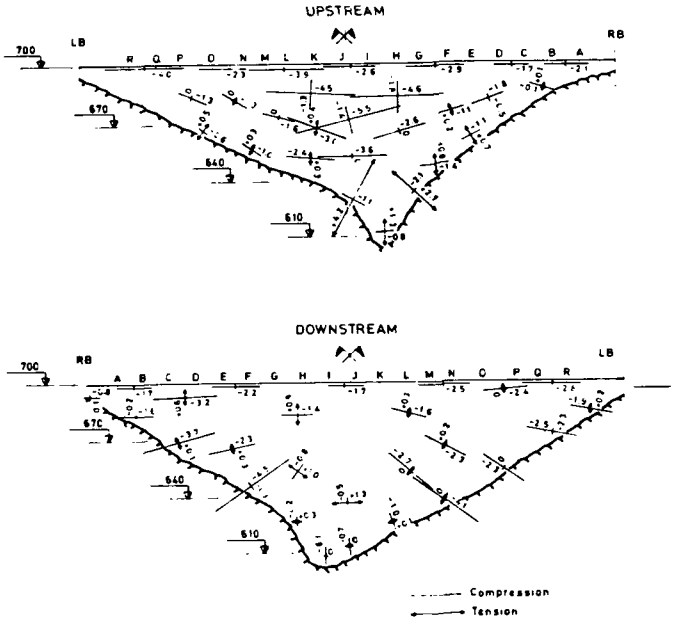
UPSTREAM
LB
RB
700
670
640
610
R Q P O N M L K J I H G F E D C B A
DOWNSTREAM
RB
LB
700
670
640
610
A B C D E F G H I J K L M N O P Q R
Compression
Tension

Water level (m)	Results	Springings				Hoop	
		I. B		R B			
		U	D	U	D	U	D
700	calc. model	-1.5 -4.1	-1.3 -3.0	-1.5 -2.2	-1.3 -1.7	-2.1 -2.8	-0.7 -2.3
680	calc. model	-1.2 -1.2	-0.9 -2.0	-1.2 -1.4	-0.9 -1.7	-1.9 -4.8	+0.7 -0.6
660	calc. model	+0.3 -0.4	-1.8 -1.9	+0.3 -1.0	-1.8 -3.5	-2.5 -4.2	+0.4 +0.3
640	calc. model	+0.7 -0.7	-1.5 -2.5	+0.7 -0.2	-1.5 -3.0	-1.7 -1.5	+0.5 +1.3

U - upstream
D - downstream

LB - left bank
RB - right bank

\+ traction
\- compression
(MPa)

Water level (m)	Results	Lateral zones				Central zone	
		L B		R B			
		U	D	U	D	U	D
680	calc. model	+0.2 -0.3	-0.2 -0.3	+0.2 +0.1	-0.2 +0.5	+0.1 -1.3	-0.1 +0.5
660	calc. model	+0.9 +0.0	-0.9 -0.8	+0.9 +0.7	-0.9 -0.4	+1.0 -0.7	-1.0 -0.1
640	calc. model	+1.2 -	-1.3 -1.5	+1.2 -	-1.3 -1.1	+1.6 +1.8	-1.7 -0.5
620	calc. model	- -	- -	- -	- -	+2.3 +2.9	-2.5 -0.7

U - upstream
D - downstream

LB - left bank
RB - right bank

\+ traction
\- compression

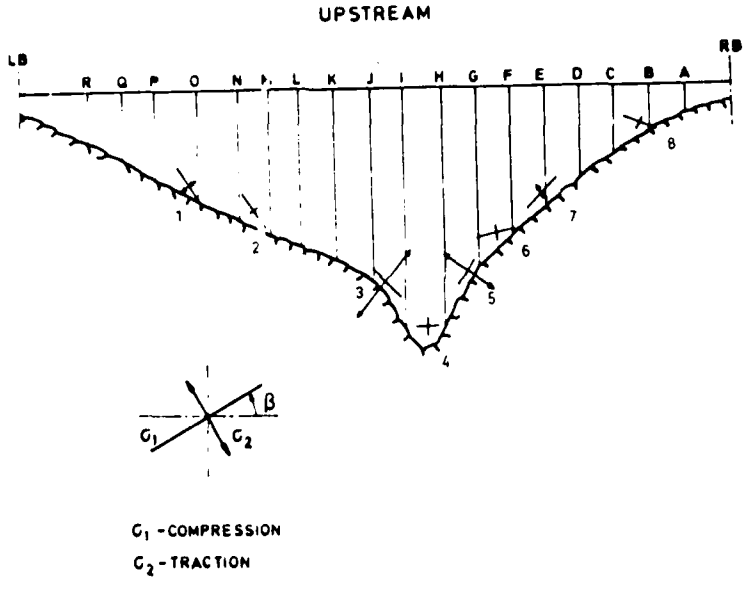

σ_1 - COMPRESSION

σ_2 - TRACTION

Point	Principal stresses (MPa)		
	σ_1	σ_2	β°
1	-1.06	+0.15	-67
2	-1.46	-0.24	-63
3	-1.62	+3.15	-40
4	-0.84	-0.71	0
5	-1 15	+2.20	58
6	-1.51	-0.38	13
7	-1.40	-0.20	42
8	-1.28	-0.10	-31

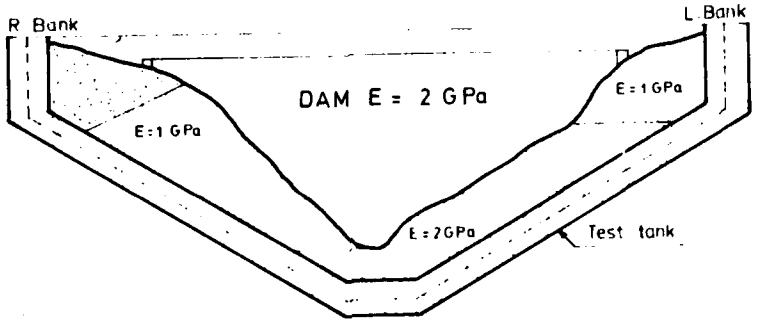
R Bank
L Bank
DAM E = 2 GPa
E=1 GPa
E=1 GPa
E=2GPa
Test tank

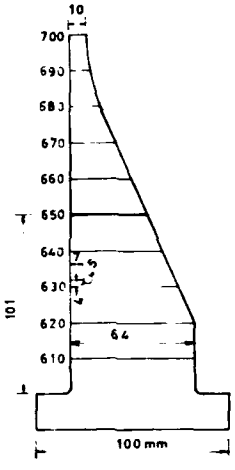

MODEL WITH
PROTOTYPE JOINT

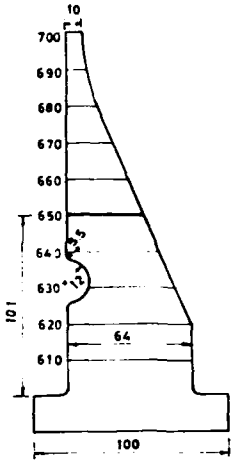

MODEL WITH
HALF CIRCULAR HOLE

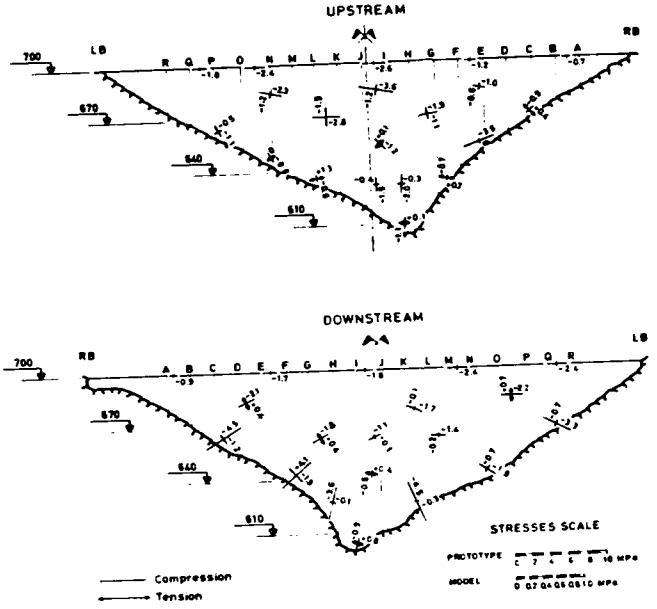
UPSTREAM
LB
RB
700
670
640
610
R Q P O N M L K J I H G F E D C B A
DOWNSTREAM
RB
LB
700
670
640
610
A B C D E F G H I J K L M N O P Q R
STRESSES SCALE
PROTOTYPE
MODEL
Compression
Tension

BETWEEN JOINTS D-G AND K-P

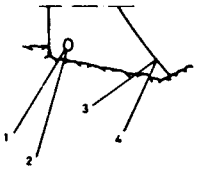

BETWEEN JOINTS G-K

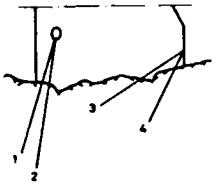

PLAN OF PRINCIPAL GROUT CURTAIN

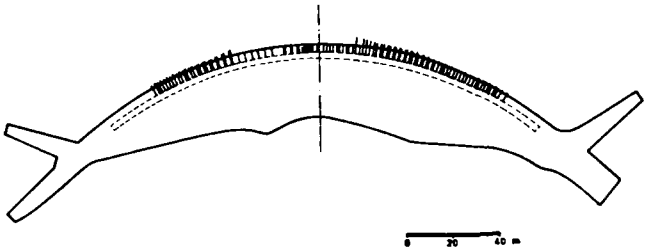

1 – Previous grout curtain (cement) – 1st phase
2 – Principal grout curtain (resine) – 2nd phase
3 – Upper consolidation (cement) – 1st phase
4 – Deeper consolidation (cement) – 1st phase

f 95

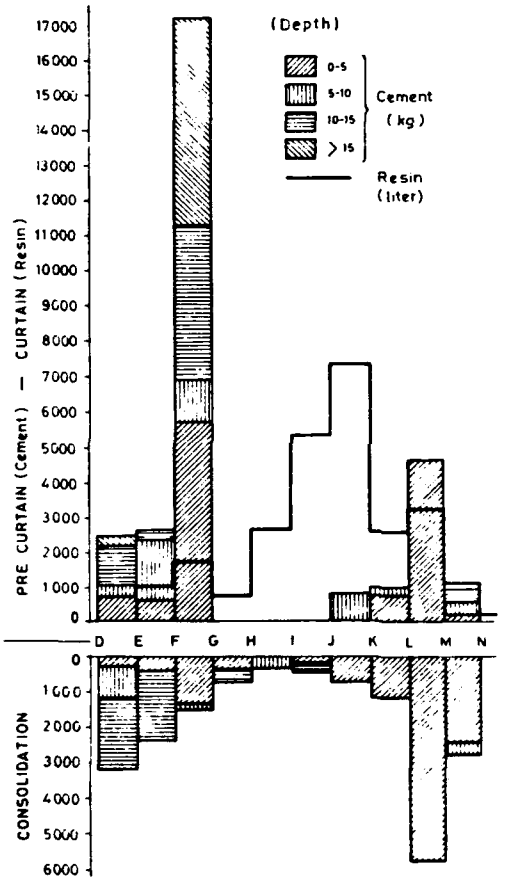
(Depth)
0-5
5-10
10-15
> 15
Cement
(kg)
Resin
(liter)
PRE CURTAIN (Cement) — CURTAIN (Resin)
17000
16000
15000
14000
13000
12000
11000
10000
9000
8000
7000
6000
5000
4000
3000
2000
1000
0
D E F G H I J K L M N
CONSOLIDATION
0
1000
2000
3000
4000
5000
6000

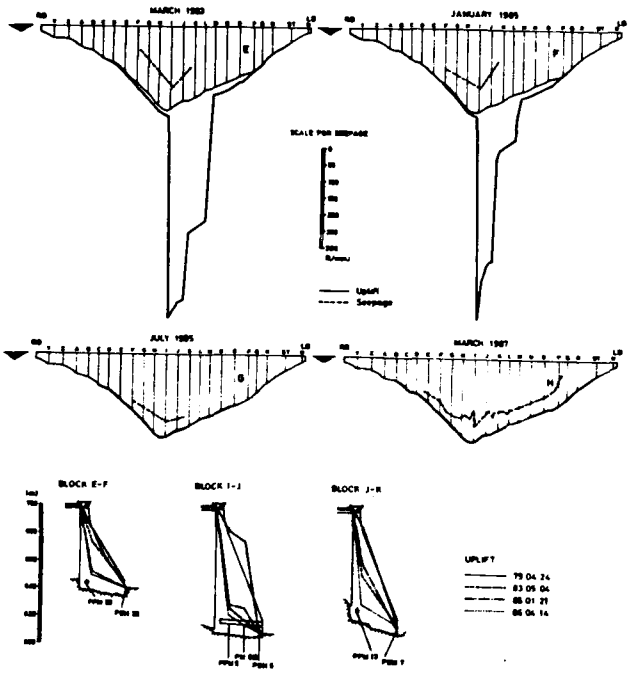
MARCH 1983
JANUARY 1985
JULY 1985
MARCH 1987
BLOCK E-F
BLOCK I-J
BLOCK J-K
UPLIFT

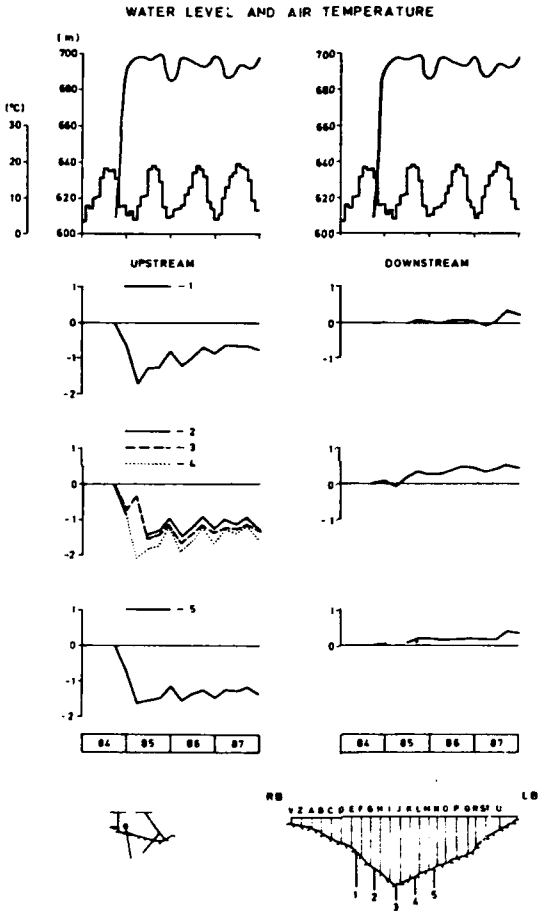
WATER LEVEL AND AIR TEMPERATURE
(m)
700
680
660
640
620
600
(°C)
30
20
10
0
UPSTREAM
DOWNSTREAM
1
2
3
4
5
84
85
86
87
RB
LB
V Z A B C D E F G H I J K L M N O P Q R S T U
1
2
3
4
5

99

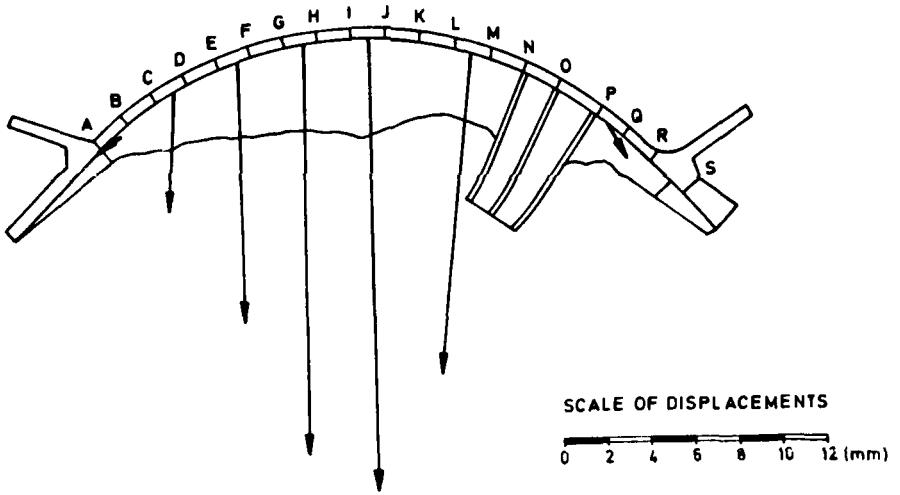
A
B
C
D
E
F
G
H
I
J
K
L
M
N
O
P
Q
R
S
SCALE OF DISPLACEMENTS
0 2 4 6 8 10 12 (mm)

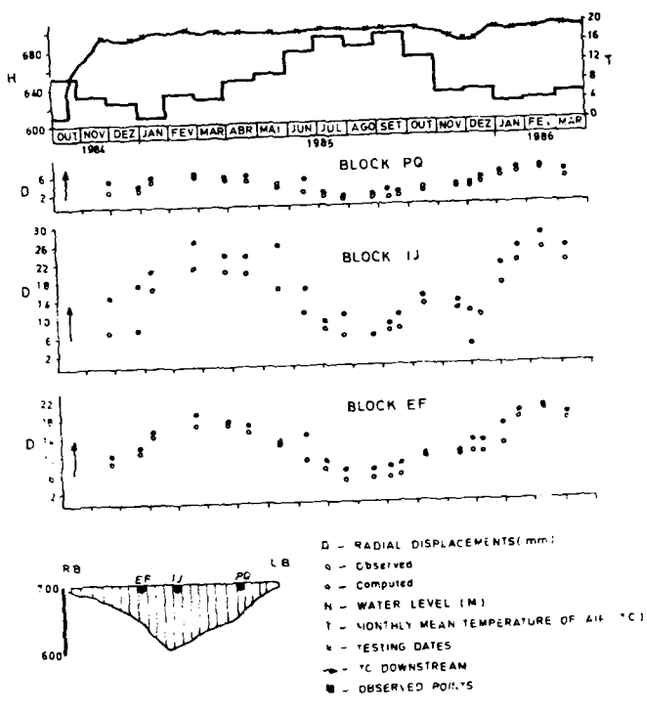
H
T
OUT NOV DEZ JAN FEV MAR ABR MAI JUN JUL AGO SET OUT NOV DEZ JAN FE. MAR
1984
1985
1986
BLOCK PQ
BLOCK IJ
BLOCK EF
D
RB
EF
IJ
PQ
LB
D - RADIAL DISPLACEMENTS(mm)
o - Observed
o - Computed
N - WATER LEVEL (M)
T - MONTHLY MEAN TEMPERATURE OF AIR °C)
- TESTING DATES
- TC DOWNSTREAM
- OBSERVED POINTS

F 101

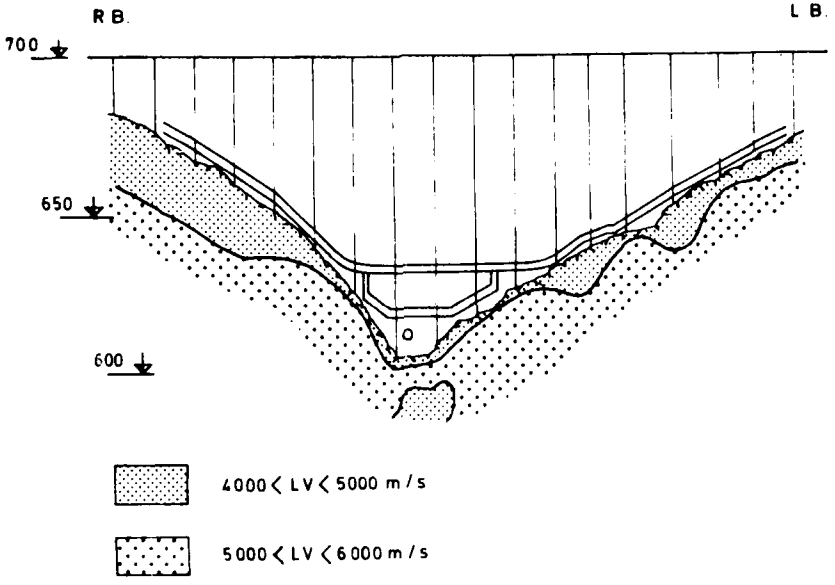

END